EFFECT OF DIFFERENT LAND USE ON INFILTRATION RATES WITHIN MINNA METROPOLITAN AREA OF SOUTHERN GUINEA SAVANNAH ZONE, NIGERIA

BY

ENTONU, Michael
MEng/SEET/2017/6983

DEPARTMENT OF AGRICULTURAL & BIORESOURCES ENGINEERING,
FEDERAL UNIVERSITY OF TECHNOLOGY,
MINNA, MINNA, NIGER STATE, NIGERIA

NOVEMBER, 2021

EFFECT OF DIFFERENT LAND USE ON INFILTRATION RATES WITHIN MINNA METROPOLITAN AREA OF SOUTHERN GUINEA SAVANNAH ZONE, NIGERIA

BY

ENTONU, Michael
MEng /SEET/2017/6983

A THESIS SUBMITTED TO THE POSTGRADUATE SCHOOL, FEDERAL UNIVERSITY OF TECHNOLOGY, MINNA, NIGERIA IN PARTIAL FULFILMENT OF THE REQUIREMENTS FOR THE AWARD OF THE DEGREE OF MASTER OF ENGINEERING (MEng) IN AGRICULTURAL & BIORESOURCES ENGINEERING (SOIL AND WATER)

NOVEMBER, 2021

ABSTRACT

This project studied the effect of urban forest types, vegetation configuration and soil properties on soil infiltration. In the study, 6 locations were considered; Undeveloped land, Farm land, Grazing land, Gardened land, Paved compound and Paved road side with 5 samples from each location in Minna City, Niger State to investigate the soil infiltration characteristics of urban soil and its influencing factors. The results showed that the steady infiltration rates of urban soil were highly variable. High variations in the final infiltration rates were observed for different vegetation patterns and compaction degrees (22.02, 17.06, 13.45). Land with shrubs and grasses had the highest infiltration rate and places with bare land had the lowest infiltration rate (7.14). In addition, the results showed that the soil infiltration rate decreased with an increase in the bulk density and with a reduction in the soil organic matter content and non-capillary porosity. The soil infiltration rate also had significantly positive relationships with the total porosity and saturated soil water content. Urban soil compaction contributed to low soil infiltration rates. Considering the effect of the land use practices on soil properties, the soils differ considerably between the six locations; that is, the undeveloped land, Farm land, Garden, Grazing land, paved compound and paved road side. The soil at the undeveloped site is a deep, well-drained soil which consist of 56% sand, 25% clay and 31% silt which makes it predominantly sandy-loam. The soil at the farm land is dominated with loamy soil with relatively high degree of homogeneity both vertically across depths and horizontally from one sample locus to the next. The soil texture at grazing land from five different samples collected showed sandy clay, silty loam, clay loam, silty loam and sandy loam, while, Paved compound and paved road side had sandy clay composition which had a high surface runoff and low infiltration (7.78, 7.45, 7.29).These results also demonstrated that the effect of soil texture on infiltration rate was probably masked by the land use practices and soil management, which agrees with the fact that water infiltration into the soil is highly sensitive to land use and soil management. Three infiltration models were applied (Horton, Kostiakov and Philip) and their performances were evaluated based on Root Mean Square Error (RMSE) and coefficient of determination (R^2). The Philip model with the least RMSE values of 0.79 cmh^{-1} and R^2 of 0.97 most closely predicted the measured infiltration. Kostiakov and Horton models provided less accurate estimates of the measured infiltration with least RMSE values of 4.63 and 5.13 and R^2 of 0.92 and 0.91, respectively. To increase the infiltration rate and water storage volume of urban soil, proper techniques to minimize and mitigate soil compaction should be used. These findings can provide useful information for urban planners about how to maximize the water volume of urban soil and decrease urban instantaneous flooding.

TABLE OF CONTENTS

CHAPTER FOUR

CHAPTER FIVE

LIST OF TABLES

LIST OF FIGURES

LIST OF PLATE

CHAPTER ONE

1.0 INTRODUCTION

1.1 Background to the Study

In the past decades, South Guinea savannah zone of Nigeria had experienced a rapid and unprecedented process of urbanization, with urban areas expanding almost exponentially outwards in many cities in parallel with infrastructural constructions, the natural movement of water into the soil is obstructed (Venter *et al*., 2019).

In developing cities, different structural constructions often represent the urbanization gradients (Zhai *et al*., 2017.) During the process of urbanization, forests and soils were significantly influenced by human activities and large areas of forests have been occupied. Meanwhile, many afforestation movements such as 'forest city' or 'eco-city' have been initiated in developed cities due to citizens' desire for a better quality of life (Lv *et al*., 2016.) Urban forest soil is affected not only by plant-soil interaction and afforestation but also by human activities such as trampling (Lasanta *et al*., 2019).

With rapid urbanization, natural vegetated soils are replaced with impervious surfaces. This land conversion could exert profound influences on hydrological processes such as inhibiting rainwater infiltration and increasing surface runoff and peak discharge rates (Jia *et al*., 2015; Zhang *et al*., 2015). Excessive runoff accompanied by low urban forest coverage could frequently cause flooding in the urban areas and pose threats to life and property (Pataki *et al*., 2011; Yao *et al*., 2015). The increase in flood risk due to short-term heavy rains has been a major concern in many cities (United Nations, 2012). Nearly all cities have set up mitigation strategies to improve the design standards of urban drainage pipe networks. However, such strategies are costly and increase the

pressure on sewage treatment plants. Therefore, effective and low-cost measures to solve waterlogging in cities need to be explored.

Although many studies on urban effect of infiltration on soils have been conducted, most of them have focused only on soil fertility (Li *et al*., 2015), heavy metal pollutants (Pan et al., 2008; Fang *et al*., 2012) and soil microorganisms (Zhao and Guo, 2010; Chen *et al*., 2012). Most previous studies in urban areas primarily used the results from rural areas to generate the runoff reduction values (Yao *et al*., 2015; Zhang *et al*., 2015). This method did not take into account the impact that the urban conditions may have on urban infiltration. In addition, urbanization has dramatically alerted the urban soil through sealing, intensive disturbance, deposition of building and daily rubbish, sedimentation of air dust, and infiltration of sewage (Zhao *et al*., 2007; Shaw *et al*., 2010). These processes damage and change the urban soil compared with the natural soil. It is important to understand scientifically the effects of urbanization on soil infiltration. Urbanization effects are typically evaluated along urban-rural gradients, which have been used in studies considering soil properties, forest soil heavy metals, polycyclic aromatic hydrocarbons and soil organic carbon Pouyat *et al*., 2008. Many results showed that soil organic matter, water-stable aggregates, cation exchange capacity, total nitrogen, total phosphorus and heavy metal concentrations (such as lead, copper, and nickel) increased from rural to urban zones (Zhang *et al*., 2003; Lu *et al*., 2009).

In the process of urbanization, soils are typically degraded by a wide range of modifications including vegetation clearing, topsoil removal, grading, and compaction. These practices significantly influence soil physical characteristics (Alaoui *et al*., 2011) and ultimately lead to the loss of critical soil-mediated ecosystem services such as storm

water mitigation (Pitt *et al*., 2008), carbon storage (Chen *et al*., 2013), and net primary productivity (Milesi *et al*., 2003). Many studies showed that soil organic amendments could help the formation of soil aggregates and improve the soil structure and therefore has a significant effect on the increasing infiltration rates (Celik *et al*., 2010; Brown and Cotton, 2011). Thus, in the process of urban green spaces management and maintenance, returning the litter to the green land, increasing the surface organic coverage or organic manure fertilizer to increase the infiltration rate should be advocated.

Compaction can be the intentional compacting of a site to increase the structural strength of the soil or it can be inadvertently caused by the use of heavy equipment and grading of lots. Soil compaction affects the physical properties of soil by increasing its strength and bulk density, decreasing its porosity, and forcing a smaller distribution of pore sizes within the soil. These changes affect the way in which air and water move through the soil and the ability of roots to grow in the soil (Scharwies, & Dinneny, 2019; Robinson, *et al.,* 2019). Changes to the way that air and water move within the soil can affect infiltration rate. A decrease in infiltration rate will result in increased runoff volume, greater flooding potential and reduced groundwater recharge within watersheds. Compaction has a significant influence on soil hydraulic properties such as soil water retention, soil water diffusivity, unsaturated hydraulic conductivity and saturated hydraulic conductivity (Galli *et al., 2021*; Sohn *et al.,* 2020). These hydraulic properties in turn govern infiltration rates. The infiltration of storm water within urban areas is an important process being promoted as part of a new storm water management strategy. This management strategy is often referred to as low impact development, which aims to reduce the volumes and peaks of runoff to predevelopment levels. Promoting infiltration is one of the primary methods for achieving this goal. The

quantification of the effect of compaction on infiltration rates is therefore, an important task.

Soil moisture controls the partitioning of rainfall into infiltration and runoff, and it controls land surface temperature through its effect on the partitioning of available energy into sensible and latent heat fluxes. It is the hydrologic state variable, together with land temperature, in models of surface water and energy balance. The state of dynamics is affected by hydrometeorological forcing of precipitation, radiation, and atmospheric evaporative demand. Furthermore, topography, land use, and soil properties across the landscape, affect soil moisture temporal evolution (Liu *et al*., 2012; Beven and Germann, 2013).

1.2 Statement of the Research Problem

Generally, with rapid urbanization, natural vegetated soils are replaced with impervious surfaces. This land conversion could exert profound influences on hydrological processes such as inhibiting rainwater infiltration and increasing surface runoff and peak discharge rates (Zipper *et al*., 2017). However, the motivation for this study is informed by the following general problems.

(i) Frequent flood event during the rainy season: urban soil characteristics especially soil physical properties, are subject to dramatic changes due to compaction by intensive human activities, which may cause frequent flood during the rainy season as a result of poor infiltration.

(ii) Poor surface runoff water quality: The prevalence of flooding is high in compacted soils and the quality of surface runoff water is reduced during flood event. The concentration of total Nitrogen, molybdate-reactive phosphorus, total

phosphors, and suspended material in urban surface runoff are significantly higher than those observed in forested or agricultural watersheds.

(iii) In urban areas, the various human activities affect the infiltration rate on the soil properties that have negative effects on the eco-environment of the city

(iv) Inconsistency in analytical approaches for estimating surface runoff and infiltration rate. The level of analytical sophistication that is required to estimate runoff and infiltration rate is somewhat inconsistent and, in most cases, the uncertainties in infiltration rates will be significant. It would not be uncommon for actual, long term infiltration rate to differ from the estimated infiltration rate by factor of 2 to 10. These differences are primarily due to uncertainties in hydraulic conductivity and hydraulic gradients.

1.3 Aim and Objectives of the Study

The aim of the study is to determine the effect of different land use on infiltration rates within Minna metropolitan area of southern guinea savannah zone, Nigeria

The objectives of this study are to:

(i) determine the water infiltration characteristics of soil under different land use

(ii) determine the sensitivity of the parameters considered

(iii) compare the performance of the three models (Horton, kostiakov and Philip models) for infiltration rate prediction.

1.4 Justification of the Study

Infiltration is one of the major components of the hydrologic cycle. It constitutes the sole source of water to sustain the growth of vegetation which is filtered by the soil which removes many contaminants through physical, chemical and biological processes,

and replenishes the ground water supply to wells, springs and streams (Shrestha *et al.*, 2018.; Gavrić *et al.*, 2019).

Infiltration is critical because it supports life on land. The ability to quantify infiltration is of great importance in watershed management. Prediction of flooding, erosion and pollutant transport all depend on the rate of runoff which is directly affected by the rate of infiltration (Ellen, 2006). Quantification of infiltration is also necessary to determine the availability of water for crop growth and to estimate the amount of additional water needed for irrigation (Ellen, 2006). Also, by understanding how infiltration rates are affected by surface conditions, measures can be taken to increase infiltration rates and reduce the erosion and flooding caused by overland flow. In order to develop improved hydrologic models, accurate methods for characterizing infiltration are required (Clark *et al.*, 2017; Sahraei *et al.*, 2020). In spite of its great importance, many water quality models still lack proper quantification of infiltration.

Information on infiltration rate is necessary in hydrologic design, irrigation, and agriculture (Sihag & Singh, 2018). It is important to have a detailed understanding of infiltration characteristics for a given land use complex. It is one of the main abstractions accounted for in the rainfall-runoff modeling. In the hydrological process, infiltration divides the water into two parts surface flow and groundwater flow. Soils of different types have different infiltration characteristics, and Infiltration rates are affected by a number of factors such as antecedent soil moisture content of soil, density and behaviour of the soil. Infiltration, therefore, has a vital role in subsurface and surface soil erosion, runoff generation, irrigation rate and hydrology.

1.5 Scope of Study

The extent of coverage of the study is limited to the Effect of Different Land Use on Infiltration Rates within Minna Metropolitan Area of Southern Guinea Savannah Zone, Nigeria.

CHAPTER TWO

2.0 LITERATURE REVIEW

2.1 Infiltration

Infiltration is the process of penetration of water into the ground surface and the intensity of this process is known as infiltration rate. The infiltration rate is expressed in term of volume of water poured per ground surface per unit of time. Soil erosion, surface runoff & ground water recharge are affected by this process. At a certain moment the maximum infiltration rate can be indicated by the infiltration capacity of soil. Infiltration of water into the soil can be determined by a simple instrument called Double ring infiltrometer. These cylinders are partially inserted into the ground and water is filled up to a margin inside the cylinder and after that the speed of penetration of water is measured with respect to the time and depth of penetration of water inside the cylinder.

Infiltration is the entrance of water originating from rainfall, snowmelt or irrigation, the soil surface into the top layer of the soil. Redistribution is the movement of water from point to point within the soil. These two processes cannot be separated because the rate of infiltration is strongly influenced by the rate of water movement within the soil below (Ellen, 2006). After each infiltration event, soil water movement continues to redistribute the water below the surface of the soil (Cheng *et al.*, 2020; Luo *et al*., 2021). Many of the same factors that control infiltration rate also have an important role

in the redistribution of water below the soil surface during and after infiltration (Ellen, 2006). Thus, an understanding of infiltration and the factors that affect it is important not only in the determination of surface runoff, but also in understanding subsurface movement and storage of water within a watershed (Qi *et al.*, 2020; Beven, 2021).

The movement of water is always from higher energy state to lower energy state and the driving force for the movement is the potential difference between energy states (Ellen, 2006). Three important forces affect the movement of water through soil. First the gravitational force, or potential difference, causes water to flow vertically downward.

This is because the gravitational potential energy level of water at a given elevation in the soil profile is higher than that of water at a lower elevation (Ellen, 2006). Also, if there is standing water on the surface, the weight of the ponded water exerts hydrostatic pressure which increases the rate of infiltration, also due to the gravitational force. Second adhesion, or the attraction of the soil matrix for water is responsible for the phenomena of adsorption and capillarity.

The matric or capillary potential refers to the energy state of the water molecules adsorbed onto the soil solids which is much reduced compared to that of bulk water (Radcliffe & Simunek, 2018; Maleksaeedi & Nuth, 2020). To a lesser extent cohesion, which describes the attraction of water molecules to each other, lowers the energy state. Together adhesive and cohesive forces produce a suction force within soil that reduces the rate of movement of water below the soil surface. The higher the soil water content the weaker the suction force and the lower the matric potential difference. Third, the attraction of ions and other solutes towards water, result in osmotic forces, that tend to reduce the energy level in the soil solution. Osmotic movement of pure water across a

semipermeable membrane into a soil solution is evidence of the lower energy state of the soil solution (Hilhorst *et al*., 2000).

2.2 Physical Processes of Infiltration

Infiltration of rainfall into pervious surfaces is controlled by three mechanisms, the maximum possible rate of entry of the water through the soil/plant surface, the rate of movement of the water through the vadose (unsaturated) zone, and the rate of drainage from the vadose zone into the saturated zone (Sprenger *et al., 2019.;* Dezső *et al.* 2019). During periods of rainfall excess, long-term infiltration is the least of these three rates, and the runoff rate after depression storage is filled to the excess of the rainfall intensity above the infiltration rate. The infiltration rate typically decreases during periods of rainfall excess (Pitt *et al.,* 2003). Storage capacity within the soil profile is recovered during periods when the drainage from the vadose zone exceeds the infiltration rate.

The surface entry rate of water may be affected by the presence of a thin layer of silts and clay particles at the surface of the soil and vegetation. These particles may cause a surface seal that would reduce a normally high infiltration rate. The movement of water through the soil depends on the characteristics of the underlying soil. Once the surface soil layer is saturated, water cannot enter soil faster than it is being drained into the vadose zone, so this transmission rate affects the infiltration rate during longer events (Pitt *et al*., 2003). The depletion of available storage capacity in the soil due to urbanization-associated compaction affects the transmission and drainage rates. The storage capacity of soils depends on the soil thickness, porosity, and the soil-water content. Many factors including soil texture, root development, soil insect and animal bore holes, structure, and presence of organic matter, affect the effective porosity of the soil.

According to (Pitt *et al.*, 2003); the infiltration of water into the surface soil is responsible for the largest abstraction (loss) of rainwater in natural areas, and the infiltration capacity of most soils allows low intensity rainfall to totally infiltrate, unless the soil voids became saturated or the underlain soil is more compact than the top layer. High intensity rainfalls generate substantial runoff because the infiltration capacity at the upper soil surface is surpassed, even though the underlain soil might still be very dry. The classical assumption is that the infiltration capacity of a soil is highest at the very beginning of a storm and decreases with time (Fernández-Pato 2018; Yang *et al.*, 2020; Beven, 2021). The soil-water content of the soil, whether it was initially dry or wet from a recent storm, will have a great effect on the infiltration capacity of certain soils (Pitt *et al.*, 2003).

Natural infiltration is significantly reduced in urban areas due to numerous factors: the decreased area of exposed soils, removal of surface soils and exposing subsurface soils, grading of soils through landscaping, and compaction of the soils during earth moving and construction operations. The decreased areas of soils are typically associated with increased runoff volumes and peak flow rates, while the effects of soil disturbance are rarely considered. Infiltration practices have long been applied in many areas to compensate for the decreased natural infiltration areas, but with limited success. Silting of the infiltration areas is usually responsible for early failures of these intended infiltration controls, although compaction from heavy traffic is also a recognized problem. More recently, "biofiltration" practices, that rely more on surface infiltration in extensively vegetated areas, are gaining in popularity and appear to be a more robust solution than conventional infiltration trenches. These biofiltration devices also allow modifications of the soil with amendments (Sileshi *et al.*, 2017).

Water moving into a soil profile displaces air, which is forced out ahead of the wetting front. If there is a barrier to the free movement of air, such as a shallow water table, or when a permeable soil is underlain by a relatively impermeable soil, the air becomes confined and the pressure becomes greater than atmospheric. Compressed air ahead of the wetting front and the counter flow of escaping air may drastically reduce infiltration rates (Glass, 2019.; Ogbuagu, 2019) found that for dry soils and for interrupted flow the main retardant to infiltration was entrapped air, while for wet soils, reduced aggregate stability and surface sealing were the main causes for reduced infiltration rates. (Le Van and Morel-Seytoux, 1972) showed that for a two-phase flow treatment of infiltration, infiltration rate after a certain time was well below the saturated hydraulic conductivity, which was considered to be a lower limit by all the previous authors. Infiltration tends to be increased for deeper water tables, since the impedance of the compressed air on infiltration is reduced and the soil profile tends to be drier compared to shallow water table conditions (Vereecken *et al*., 2019; de Moraes *et al*., 2020).

2.3 Impact of soil properties on soil infiltration

Soil water infiltration is a key process in the water cycle since it controls, inter alia, the surface water-groundwater relationship (Zhang *et al.,* 2017). The soil properties play a crucial role in this process. Many studies have demonstrated that the infiltration rate depends mainly on soil properties, such as initial moisture content, hydraulic conductivity, soil texture, porosity, swelling degree of soil colloids, organic matter content, and chemical properties (Bagarello and Sgroi, 2004; Chai *et al*., 2007; Bormann and Klaassen, 2008; Fischer *et al*., 2014). Soil bulk density is one of the most important factors that influence infiltration capacity (Yang & Zhang, 2008). The results obtained during the studies conducted by (Zhang *et al.,* 2017) at Changchun, Northeast

China showed that the soil infiltration rate decreased with increasing bulk density. For example, at a soil bulk density of 1.44 g/cm^3, the infiltration rate was lower than 5.00 cm/h. In contrast, the bulk densities of soils that had higher infiltration rates were 1.19–1.35 g/cm^3. Soil pores provide channels for water movement in the soil. If there is more connectivity between pores, the soil infiltration rate will be increased. Past studies have found that soil infiltration rates had significant positive linear correlations with the total porosity and non– capillary porosity (Yang and Zhang, 2011; Li *et al*., 2013). According to (Zhang *et al*., 2017), there were positive relationships between infiltration rates and soil total porosity and non-capillary porosity. Urban soils are frequently mixed with many gravel, coal cinders, construction waste and other artificial substances in city greening.

The existence of gravel creates a number of macropores in soil, which easily form preferential flow that is mainly influenced by gravity and not capillary pores (Zhang *et al*., 2017). Compaction is the most serious form of the physical degradation in urban areas. Compaction usually leads to increases in bulk density and decreases in porosity and formation of a crust layer that prevents water infiltration into the surface soil (Richard *et al*., 2001). According Wang *et al*. (2017) the final infiltration rate decreased with increased soil compaction. Furthermore, the final infiltration rate of non-compacted soil was significantly different from that of severely compacted soils. Specifically, the infiltration rate of non-compacted soil was 8.84 cm/h, and the infiltration rate of the severely compacted soil was 1.88 cm/h.

Generally, urban green space soils are compacted mainly by mechanical compaction in urban greening and human trampling. Compaction affects root growth of the plant and inhibits water penetration into the soil, causing waterlogging in urban areas (Yang and

Zhang, 2011). Therefore, in the process of urban greening the measures should be taken to loosen the soil and avoid compaction. In the process of urbanization, soils are typically degraded by a wide range of modifications including vegetation clearing, topsoil removal, grading, and compaction. These practices significantly influence soil physical characteristics (Alaoui *et al*., 2011) and ultimately lead to the loss of critical soil- mediated ecosystem services such as storm water mitigation (Pitt *et al*., 2008), carbon storage (Chen *et al*., 2013), and net primary productivity (Milesi *et al.,* 2003). Many studies showed that soil organic amendments could help the formation of soil aggregates and improve the soil structure and therefore has a significant effect on the increasing infiltration rates (Frankenberger, 1992; Celik *et al.,* 2010; Brown and Cotton, 2011).

In a study by Wang *et al*. (2017); there were positive relationships between soil organic matter and infiltration rate. Thus, in the process of urban green spaces management and maintenance, returning the litter to the green land, increasing the surface organic coverage or organic manure fertilizer to increase the infiltration rate should be advocated.

2.4 Impact of vegetation cover on soil infiltration

Vegetation and other ground covers such as mulches and plant residues reduce soil temperature and evaporation from the soil surface, but vegetation also loses moisture through transpiration. Vegetation increases infiltration rates by loosening soil through root growth and along with natural mulches and plant residues, intercept rain drops, which compact and damage the structure of bare soil and cause surface sealing and crusting. Living and dead plant material also add organic matter to the soil which improves soil structure and water holding capacity and provide habitat for earthworms

which further enhance the soil constitution and increase infiltration rates. Soil water content is also affected by seasonal changes in water use by plants, stage of plant growth, spacing of plants, type of vegetation, depth of roots, and extent of canopy coverage.

A steady infiltration rate, equivalent to saturated hydraulic conductivity, is one of the important indicators to evaluate soil physical characteristics and a critical component of most urban runoff models. Soil infiltration is affected by various factors such as vegetation cover, soil texture and structure, soil organic matter, antecedent water content, management system, disturbance age and landscape position (Kumar *et al*., 2012). Many previous studies have showed that there was a great difference in the soil infiltration rate of different land use and different functional urban green areas (Yang & Zhang, 2008; Wei *et al.,* 2012; Chen *et al.,* 2014). There was wide variability in soil infiltration rates among different urban forest types in our study.

Vegetation characteristics have important effects on soil infiltration capacity. In our study, the tree with shrubs and grasses had the highest values followed by tree with grasses, and tree with bare land had the lowest values. The infiltration rates in areas with shrubs and grasses were relatively higher because shrubs and grasses can loosen compacted soil and can aid in the formation of soil macropores and good soil structure (Meek *et al.,* 1989; Wu *et al*., 2016). In addition, shrubs protected the soil from compaction. Alternatively, the infiltration rate was very low in urban forests with bare land because the soil was apt to be trampled by pedestrians.

The infiltration rate of trees with sparse grasses (FFG) was higher than trees with grasses (FG) in attached forest (AF), landscape and relaxation forest (LF), possibly

because the infiltration capacity is decreased by grasses (Archer *et al*., 2002; Fischer *et al*. 2014). Thus, shrubs are better than grasses in the improvement of soil structure in urban greening (Zhang *et al.* 2017). Therefore, in order to make full use of urban green space soil for rainwater reduction, a proper vegetation configuration is needed. For example, in urban greening, more shrubs and less lawns should be promoted.

Vegetation protects the soil from raindrop splash by intercepting and absorbing the energy of the raindrops. Crusting is the drying out and hardening of the surface sealed layer. Crusting may cause immediate ponding with very low infiltration rate. A long soaking rain will tend to soften the crust so that after a time infiltration rate may increase (Ellen, 2006).

2.5 Impact of Urbanization on Soil Infiltration

Population growth and the increase of socio-economic activities experienced over the last decades has led to a pervasive urbanization global trend (Duh *et al*., 2008). Nearly half of the world's population lives in urban areas, and that percentage is expected to increase to 60% by the year 2030 (Burns *et al*. 2005). This population pressure on the environment implies changes to land use and to landscape patterns within catchments, altering the connectivity of water flows between different sub-catchments, with potential consequences for rainfall-runoff relationships, affecting local and regional water resources as well as flood hazards (Alig *et al*., 2004; Huang *et al*., 2008).

Several researchers refer that the creation of impervious surfaces, associated with the urbanization process, induces major modifications in the natural water balance and in the various phases of the hydrological cycle, such as: reduction in evapotranspiration, decrease water infiltration capacity, associated with soil compaction (Arthur-Hartranft

et al., 2003; Easton *et al*., 2007), changes in soil moisture content (Easton *et al*., 2007; Easton and Petrovic, 2008), increase of surface runoff in annual streamflow (Corbet *et al*., 1997; Semadeni-Davies *et al*., 2008; Wheater and Evans, 2009), and decrease of baseflow and groundwater recharge (Xiao & McPhearson, 2003; Llorens & Domingo, 2007; Semadeni-Davies *et al*., 2008; Wheater and Evans, 2009). These changes are reflected in higher peak runoff, larger runoff volumes, decreased lag times to peak flow and a decrease in mean residence time of streamflow (Niemczynowicz 1999; Brun & Band, 2000; Blake *et al.*, 2003; Goonetilleke *et al*., 2004; Burns *et al*., 2005; White and Greerb, 2006; Semadeni-Davies *et al*., 2008; Haase, 2009), leading potentially to increasing flood peaks. These can be particularly dramatic in small urban catchments due to flash floods risk and the associated damages to human lives and to Properties. However, despite the profusion of works, the impacts of potential land use change on storm-runoff generation and infiltration rate remain largely unknown (Ying *et al*., 2009), particularly in areas with a Mediterranean climate, and predicting urban floods continues to present difficulties.

2.6 Field Estimation of Soil Infiltration

Infiltration is the process of penetration of water into the ground surface and the intensity of this process is known as infiltration rate. The infiltration rate is expressed in term of volume of water poured per ground surface per unit of time. Soil erosion, surface runoff & ground water recharge are affected by this process (Amreeta *et al*., 2015). At a certain moment the maximum infiltration rate can be indicated by the infiltration capacity of soil. Infiltration of water into the soil can be determined by a simple instrument called Double ring infiltrometer (ASTM, 2009). As shown in Plate I, the double ring infiltrometer has two parts, one was outer ring whose diameter was 600 mm and second was inner ring whose diameter is 300 mm. The rings of infiltrometer

were driven 100 mm depth into the soil. The hammer should strike uniformly on steel plate which is placed on the top of the ring without disturbing the top soil surface. The water was filling at the same level of both rings. The profundity of water in the infiltrometer was recorded at regular interims until the steady infiltration rate was achieved. The soil sample (about100-150 gm) for calculating moisture content was collected from a site nearest to the location chosen for experimentation (Parveen, 2018).

Plate I: The Double Ring Infiltrometer having 300 mm inner diameter and 600 mm outer diameter (ASTM, 2009).

Commented [H1]:

Commented [H2R1]:

According to (Liu *et al*., 2007); the initial and final infiltration rate (cm/h) of soil was determined by the dual-ring method. The mean infiltration rate for the first 3 min was chosen as the initial infiltration rate (IIR) according to the process of soil infiltration, and then chose the average infiltration rate for 0–15 min as the average infiltration rate of the stage I (AIRSI). Likewise, the average infiltration rate of stage II (AIRSII) was for the period of 15–30 min and the average infiltration rate of stage III (AIRSIII) was for the period from 30 to 60 min. The average infiltration rate of the 0–60 min period was chosen as the overall average infiltration rate (AIR) (Wu *et al*., 2016). According to

the criteria proposed by Kohnke (1968) in (Zhang *et al*., 2017); the steady infiltration rates were categorized into seven levels: very slow ($ks \leq 0.1$ cm/h), slow ($0.1 < ks \leq 0.5$ cm/h), slow to medium ($0.5 < ks \leq 2.0$ cm/h), medium ($2.0 < ks \leq 6.3$ cm/h), medium to fast ($6.3 < ks \leq 12.7$ cm/h), fast ($12.7 < ks \leq 25.4$ cm/h) and very fast ($ks > 25.4$ cm/h).

2.7 Soil Compaction

Soil compaction is emerging as a serious problem affecting the yield of field crops leading to soil degradation worldwide. Compaction-induced soil degradation affects about 68 million hectares of land globally (Alaoui, & Diserens, 2018.; Wang, 2019). Soil compaction is the compression of soil by external forces that decrease the volume of pore space while increasing the soil density (Faloye *et al.,* 2021). It is a densification and reduction in porosity, associated with changes to the soil structure and an increase in strength and a reduction in hydraulic conductivity (Rizzon *et al.,* 2021). The extent of the soil compaction problem is a function of soil type and water content, vehicle weight, speed, ground contact pressure and number of passes, and their interactions with cropping frequency and farming practices (Larson *et al.,* 1994; Chamen *et al.,* 2003). Soil compaction occurs when soil particles are pressed together, reducing pore space between them (DeJong-Hughes, 2001).

The existence of high plough sole density layer of 5-15 cm thickness at 10-40 cm soil depth in agricultural soils was reported by (Gliński, & Lipiec, 2018) and particularly in extensively puddled soils with rice cultivation. Puddling is the process of tilling the soil at high moisture content, causing shear and compression of soil particle (Faloye, *et al* 2021). It destroys soil aggregates and peds, create plastic mud, and thus eliminates most

macropores, which transmit water, remaining macropores are filled by dispersed fine particles. Puddling also result in non-linear reduction in water flux through soil (Horn, 2021).

2.7.1 Formation of subsoil compact layer

The vast majority of soil compaction in modern agriculture is caused by vehicular traffic (Sivarajan *et al.*, 2021). The most common causes are agricultural machines such as tractors, harvesters and various other cultivation implements, as wheels travelling over moist and loose soils (Alakuku *et al.*, 2003). The degree of compaction depends on the soil strength, which is influenced by intrinsic soil properties such as texture and soil organic matter contents (Gurmu, 2019), structure of the tilled layer at wheeling (da Rosa *et al*., 2021) and its water content (Varley *et al*., 2020) and loading, which depends on axle load, tyre dimensions and velocity, as well as soil-tyre interaction (Lebert *et al.*, 1998). High axle load traffic (10 Mg axle load, 300 KPa inflation pressure) most often cause detectable differences in soil physical properties to around 50 cm depth on soils with clay content varying from 2 to 65 per cent (Arvidsson, 2001). Abebe *et al.* (1989) concluded that the surface and the subsurface soil deformation characteristics, which were taken as indicative values of soil compactibility, strongly indicate that the maximum compaction occurred during the first three passes of a loaded wheel.

Under field conditions, soil compaction is greatly influenced by the axle load and the number of tyre passes during farm operations (Canillas and Salokhe, 2001). In an experiment carried out by Raper *et al.* (1998), it was discovered that soil that was initially completely disrupted to a depth of 50 cm was re-consolidated by traffic into a soil condition similar to one that had never received a subsoiling treatment. It was also found that traffic decreased the total soil volume estimated for root growth using a 2

MPa limiting cone index value, but not the maximum rooting depth beneath the row, when an annual in-row sub-soiling practice was used. Abu-Hamdeh (2003a) found that the intensity of subsoil compaction occurring as vehicle tyre goes deeper with increasing axle load and tyre inflation pressure. The study showed that increasing tyre inflation pressure and axle load increased dry bulk density and cone penetration resistance. It has been estimated that over 30 per cent of ground area is trafficked by the tyres of heavy machinery even in genuine zero tillage systems (one pass at sowing). While under minimum tillage (2–3 passes) it is likely to exceed 60 per cent and in conventional tillage (multiple passes) it would exceed to 100 per cent ground area is trafficked by the tyres of heavy machinery during one cropping cycle (Tullberg, 1990).

Tillage and traffic using heavy machines can also induce subsoil compaction in different soil types and climatic conditions in cropped systems (Raper *et al.,* 1998; Mosaddeghi *et al.,* 2000). Ghildyal and Satyanarayana (1965) reported that the medium textured soils were more prone to compaction than that in light and heavier one. In coarse textured soils, the dominant penetration of stress was in the vertical direction, while in soil with a finer texture stress propagation was multi-directional (Ellies *et al.,* 2000). However, it was observed that in soil with a good structure, compaction due to axle load was not so deep and strong.

2.7.2 Effect of soil compaction on soil physical properties

i. One soil physical property that is always altered in response to compaction is bulk density of surface and subsurface soil. It has been reported by several researchers that compaction increases bulk density by disrupting soil aggregates or by compression of soil aggregates forming restrictive layer and thus decreases soil volume by compressing the soil particles (Shah, *et al*., 2017; Kumar, *et al*.,

2018). da Silva *et al.*, 1997 investigated the effects of tillage, wheel traffic, soil texture and organic matter content on dry bulk density and relative bulk density as an index of compactness. The dry bulk density was strongly affected by tillage, wheel traffic, soil texture and organic matter content. The results reveal that intensity of tillage and wheel traffic increases bulk density while addition of organic matter decreases bulk density of soil. Verbist *et al.*, 2007 reported significantly higher penetration resistances between 20 and 40 cm depth, a significantly higher soil bulk density and a per cent decrease in drainage pore space over the surface or top layer.

ii. Soil strength or penetration resistance (PR) is another property affected by compaction. Bulk density is the function of total porosity of soil but penetration resistance is the interplay of many factors or soil properties such as bulk density, water content, soil texture, soil structure and clay mineralogy, etc. Soil strength is used as a measure of soil compaction because it reflects the resistance offered by soil to root penetration (Hamza and Anderson, 2003). Zhang *et al.*, (2006) investigated the relationships between soil water content and penetration resistance (PR), the comparison of soil compaction induced by small power tractor and the medium power tractor, the effect of tractor weight on compaction, the effect of number of tractors passes and tillage on penetration resistance, and the effect of compaction on crop yields, etc. The small powered tillage system created a more compacted plow layer over the medium powered tillage due to increased passes required with this system. Small four-wheeled tractors showed a significantly higher PR over medium power tractor in the surface soil and subsoil. The penetration resistance was significantly and negatively correlated with soil water content at time of penetration resistance

measurement (Zhang *et al.* 2006). After trafficking in a wheat field, the highest penetration resistance was found in the depth interval of 5 to 14 cm. The results of the study further reported that crop yield decreased with increasing numbers of tractor passes. Similar results were also reported by Balbuena *et al.,* (2000), who found that 10 passes significantly affect soil properties of the surface layer to 50 cm depth than that in the 1-pass and no-traffic control treatments. At high soil moisture content, the difference in soil resistance between compacted soil (with traffic) and un-compacted soil (no traffic) was low and usually less than that the value that limits root growth (>2 MPa). However, as soils get drier, soil compaction in the surface layer becomes discernible (Silva *et al.,* 2000). Reichert *et al.,* (2004) reported that penetration resistance for 6-10 cm layer was greater than that in 2 MPa for no tillage, from 30 days after beans seeding until the end of the beans cycle.

iii. Soil compaction considerably affects the soil permeability. Soil infiltration is directly proportional to the stability of soil structure (Rabot, *et al*., 2018; Tang, *et al*., 2019), pore size, volume and structure (Patel and Singh, 1981; Ankeny *et al.,* 1990; Badalıkova and Hruby, 2006). Radford *et al.* (2000) determined the changes in various soil properties immediately after the application of a known compaction load (10 and 2 Mg load on the front and rear axles, respectively) to a wet vertosol and found that compaction was mostly restricted to the top 20 cm of the soil where it decreases the number of pores per unit area in each of the three pore size ranges at soil surface and up to 10 cm depth. Ankeny *et al.,* 1995 found that wheel traffic reduced ponded water infiltration rates, but the impacts varied with soil type. On a silty clay loam, Ankeny *et al.,* 1990 found that wheel traffic reduced unsaturated water infiltration rates, but the reduction was greater in

chisel-ploughed soil than that in no-tilled soil. Abo-Abda and Hussain 1990 reported 13-42 per cent reduction in infiltration of sandy soil due to compaction while, Agrawal 1991 attributed reduction in infiltration and percolation losses of water and nutrients due to reduction in water transmitting pores. Tarawally *et al.,* 2004 measured pore size distribution in a Rhodic Ferralsol in western Cuba to study the effects of three levels of soil compaction on soil moisture retention parameters. The study concluded that highest levels of soil compaction were caused at the soil water states corresponding to the field saturation and field capacity treatments. The negative effects of soil compaction on soil hydro-physical properties, denoted by an increased volume of <0.5μm pores at the detriment of the 50–0.5 and >50 μm pore size fractions, followed the similar trend. Marsili *et al.,* 1998 evaluated the change in physical properties of an arable clay soil following passage of rubber and metal-tracked tractors for ploughing on clay soil in centre-south and insular Italy in lucerne. The decrease in macroporosity was greater in treatments involving the rubber-tracked tractor (from 10.6% to 4.0%) than for the metal tracked tractor (from 10.6% to 7.3%).

iv. Hydraulic conductivity decreased and the lowest values were found after one and four passes of the rubber-tracked tractor (1.5 and 0.08 mm h-1, respectively). Kayombo *et al.,* 1991 showed that an increase in axle load from 4 to 8 Mg reduced water infiltration rates upto 35 per cent. Similarly, on a sandy loam soil, water infiltration decreased linearly with the increase in the number of passes (0, 5, 10, 15, and 20) of a tractor of 5 Mg by weight (Ohu *et al.,* 1993). Due to reduction in infiltration rates, Singh *et al.,* 1980 reported improved water use efficiency in rice under highly permeable soils due to reduction in percolation losses as a result of subsoil compaction. On a silt loam, Blanco-

Canqui *et al.,* 2004 reported that wheel traffic reduced saturated hydraulic conductivity by about three times and increased bulk density by 6 per cent, averaged across various tillage systems. Canarache *et al.,* 1984 reported 1-3 per cent (w/w) decrease in water content in 0-20 cm soil layer with 30 tractor wheel passes over zero wheel passes in several soils of Romania. A traffic pan of 1.81 Mg m-3 density at a depth of 15-25 cm depth reduced water recharge by 2-3 cm in 180 cm soil profile (Sur *et al.,* 1980). This resulted in surface soil layer remain wet longer at each irrigation in plots with compacted subsoil layer than that in uncompacted subsoil layer. Ghildyal and Satyanarayana (1965) reported decrease in hydraulic conductivity, non-capillary pores and void ratios of sand, sandy loam, sandy clay loam and clay soils with increase in bulk density due to compaction treatments. It had been reported that hydraulic conductivity was directly related to the macropore space while micropores increased at the expense of macropores on compaction. Hydraulic conductivity underneath permanent tracks in a controlled traffic system spreaded laterally into the subsoil (Kirchhof *et al.,* 2000). Soil compaction increased bulk density and strength of the soil and thus affected the conductivity, permeability and diffusivity of water and air (Greenland 1977).

Higher bulk density of subsoil has several folds reduced the saturated hydraulic conductivity and greater penetration resistance at given water content than that in layers above or below this subsoil layer (Sur *et al.,* 1980). It also resulted in decreased profile water storage by 2-3 cm when bulk density of subsoil layer exceeds 1.8 Mg m-3 from 1.55 Mg m-3 in sandy loam soil. The properties of subsoil layer vary with soil texture, water content, type and amount of clay and organic matter content (Singh 1986).

Schwen *et al.,* (2011) in a study to measured water infiltration under different compaction levels to characterize the effects of compaction on the soil's porosity and its associated water-conducting properties. The study further concluded that compaction reduced saturated hydraulic conductivity due to distortion of structural flow paths, connectivity and hydraulic effectiveness of many macropores. Compaction rearranged the pore space, resulting in more water-conducting mesopores. Ishaq *et al.,* (2001) conducted a field experiment at Pakistan during 1997–1998 and 1998–1999 on a sandy clay loam soil to study subsoil compaction effects on soil physical properties and crop yield of sorghum. They observed that penetration resistance increased and total porosity and air-filled porosity decreased significantly due to subsoil compaction.

Assouline (2006) modelled the relationship between soil bulk density and the water retention curve and reported that increase in the soil bulk density during compaction may influence many aspects of the soil- plant-water relations. Simulation results showed a decrease in the fraction of larger pores and a resulting decrease in water retention at high capillary heads, as well as an increase in smaller pores and the related increase in water retention at relatively low capillary heads was observed. Quiroga *et al.,* (1999) found resistance to penetration and susceptibility to compaction to be inversely related to organic matter content and therefore higher under continuous cultivation. Hydraulic conductivity was lower in cultivated soils, especially in fine textured soils. The results showed that in sandy to loam soils, an increase of about 5 g kg-1 organic matter was required to achieve a 0.06 Mg m-3 decrease in bulk density at the optimum proctor moisture content. The results also indicate that the loss of

organic matter in the cultivated soils makes them more susceptible to compaction, which not only has adverse mechanical effects on plants growth, development and yield but also gives rise to a considerable reduction in hydraulic conductivity. Sur *et al.,* (1980) reported that the saturated hydraulic conductivity of compact layer at 15-20 cm depth in rice soil was only half to that of saturated hydraulic conductivity in uncompacted soil. This hard layer formed with in as little as in a period of three years on sandy loam soil (Sharma and De Datta 1986).

v. Assouline *et al.,* (1997) concluded that soil compaction behavior was not only a function of soil texture, but it was also observed to be affected by pH, CEC, clay particle thickness, and by the presence of organic matter, iron oxides, and free aluminum hydroxides, which determine the nature of the resulting cohesive forces between the soil constituents. The results indicated that damages resulting from compaction, following 30 yr of intensive cultivation, were greater in the Palotina soil over the Cascavel soil. Lipiec and Stepniewski (1995) analyzed that soil compaction resulting from vehicular traffic or tillage systems, affects transformations and uptake of nutrients due to changes in soil hydraulic, aeration, and diffusive properties, as well as by its effect on root growth and configuration. Nutrient uptake was reduced by soil compaction. One of the dominant factors affecting soil compaction levels is soil moisture content; with change in compaction level the soil moisture content changes. Under moderate compaction an increase in nutrient inflow rate per unit length or surface of the roots alleviates a reduction in total nutrient uptake.

2.7.3 Effect of soil compaction on infiltration and percolation

Soil compaction causes a decrease in large pores (called macropores), resulting in a much lower water infiltration rate into soil, as well as a decrease in saturated hydraulic conductivity. Saturated hydraulic conductivity is the movement of water through soil when the soil is totally saturated with water (Lipiec and Stepniewski, 2005) unsaturated hydraulic conductivity is the movement of water in soil that is not saturated. Unsaturated hydraulic conductivity sometimes increases due to compaction and it is important when water has to move to roots. Thus, compacted soils are sometimes not as drought sensitive as uncompacted soil assuming the root system is of equal size in both cases, which is usually not the case (Douglas and Crawford, 1993).

2.8 Slope and Rainfall Intensity

Slope also affects infiltration rate. A decrease in water infiltration rate was observed with increase in the slope steepness for grass covered slopes (Haggard *et al*., 2005; Huat *et al*., 2006). According to Haggard *et al*. (2005), the slope may have the greatest effect on surface runoff production and infiltration rate when the soil is close to saturation. On the other hand, there is evidence that on bare sloping land infiltration rates are higher than on bare flat land (Poesen, 1984). This effect is most likely due to reduced seal development on sloping land, as greater runoff velocities maintain a larger proportion of sediment particles in a suspended state resulting in more open pore structure (Römkens *et al*., 1985) as reported in Ellen, 2006.

Rainfall intensity is the instantaneous rainfall rate, and for a uniform storm or rainfall simulation may be obtained by dividing the depth of rainfall by the duration of rainfall. For non-ponded conditions, the maximal rate of infiltration called the infiltration capacity by Horton (1940) or infiltrability by Hillel (1971), equals or exceeds the

rainfall intensity and the rainfall intensity provides the upper limit for the infiltration rate. The infiltration rate, therefore equals the rainfall rate until the time of ponding. If the rate of where θ rainfall is less than the saturated hydraulic conductivity for the soil, infiltration may continue indefinitely at the rainfall rate without the occurrence of ponding. In this case the water content of the soil does not reach saturation, but approaches a limiting value, which depends on the rainfall intensity. For a given rainfall intensity, R, the soil profile approaches a uniform water content θ_{LL} is the water content for which the hydraulic conductivity, K, is equal to the rainfall rate, R; K (θ_L) = R. Since unsaturated hydraulic conductivity increases with increasing water content, the higher the rainfall intensity, the higher the value of θ_L (Skaggs and Khaleel, 1982).

When the rainfall intensity exceeds the ability of the soil to absorb water, infiltration proceeds at the infiltration capacity. At the time of ponding, the infiltration capacity can no longer keep pace with the rainfall intensity and depression storage fills up and then overflows as runoff. If the rainfall has a higher intensity, depression storage will fill faster and time of runoff will occur sooner, after the time of ponding. The rate of infiltration (f) after time of ponding, however, will not depend on rainfall intensity (R) for f less than R except to the degree that more intense rainfall may cause greater raindrop splash and greater surface sealing. Raindrop splash is the splashing of soil particles (and water) into the air when bombarded by raindrops. This damages the surface soil structure and causes soil detachment and surface sealing which occurs when enough soil particles that splash into the air, land in pore openings, and block them from infiltrating water. Much of the decrease in infiltration rate seen in unprotected soils is attributed to surface sealing (Shirmohammadi, 1984).

2.9 Physical Basis of Equations /Richards Equation

A French hydraulic engineer, H. Darcy established in 1856, that the specific flow rate through porous media is proportional to the hydraulic gradient (Kirkham and Powers, 1972).

$$q_z = -K(h)\frac{\partial H}{\partial Z} \quad (2.1)$$

where, H = h + z = total hydraulic head; (L), h = pressure head; (L), z = vertical distance from the datum plane where H = 0; (L), $\frac{\partial H}{\partial Z}$ = hydraulic gradient in the z (vertical) direction, K(h) = hydraulic conductivity which depends on properties of both the fluid and the porous medium; (Lt^{-1}), and q_z = specific flow rate ($q=\frac{Q}{A}$) in the z (vertical) direction; (Lt^{-1}). *Q* = volumetric flow rate; (L^3t^{-1}). *A* = area of surface subjected to rainfall or ponding; (L^2).

Darcy's equation is the basis for describing the movement of water through soil. Hydraulic conductivity is a function of the soil water content, and soil water content is a function of pressure head (Kirkham and Powers, 1972). A variation of the Darcy equation that applies only to horizontal flow is given by Kirkham and Powers (1972).

$$q = -\frac{K}{\rho g}\left(\frac{P_2 - P_1}{L}\right) \quad (2.2)$$

The relationship between soil water content (θ) and capillary pressure head (*h*) is a soil property called the soil water retention curve (*h*(θ)). The function *h*(θ) is not a unique function and depends not only on the water content, but also on whether the soil is wetting or drying. In other words, the soil water retention curve exhibits hysteresis.

Richards (1931) derived two equations that are considered to be governing equations of infiltration, because they describe the relationships between the soil properties on which

infiltration depends, and are based on Darcy's law and conservation of mass. The soil properties that characterize infiltration are hydraulic conductivity $K(h)$ (Lt^{-1}), diffusivity $D(\theta)$ ($L^2 t^{-1}$), and water holding capacity $C(h)$ (L^{-1}). For layered soils these properties must be known for each layer, and for anisotropic soils the properties must be known as a function of flow direction (Skaggs and Khaleel, 1982). Anisotropic soils have different physical properties along different axes. The derivation of the Richards' equation from Darcy's law and the law of conservation of mass is instructive in understanding the infiltration process, as well as in understanding many of the other equations used to approximate infiltration.

Conservation of mass requires that the change in water content with respect to time is equal to the change in specific flow rate:

$$\frac{\partial \theta}{\partial t} = \nabla . q \tag{2.3}$$

Assuming change in flow rate is occurring only in the z direction:

$$\frac{\partial \theta}{\partial t} = - \frac{\partial}{\partial z} (q_z) \tag{2.4}$$

Substituting Equation 2.1 into Equation 2.4:

$$\frac{\partial \theta}{\partial t} = \frac{\partial}{\partial Z} (K(h) \frac{\partial H}{\partial Z}) \tag{2.5}$$

Substituting for H in terms of h and z:

$$\frac{\partial \theta}{\partial t} = \frac{\partial}{\partial z} (K(h) \frac{\partial h}{\partial z}) + \frac{\partial K(h)}{\partial z} \frac{\partial z}{\partial z} \tag{2.6}$$

Using the chain rule, one may state:

$$\frac{\partial \theta}{\partial t} = \frac{d\theta}{dh} \frac{\partial h}{\partial t} \tag{2.7}$$

And the water holding capacity, *C(h)*, is equal to $\partial\theta/\partial h$, which is the slope of the soil-water retention curve.

By substitution:

$$C(h)\frac{\partial h}{\partial t} = \frac{\partial}{\partial Z}\left(K(h)\frac{\partial h}{\partial z}\right) + \frac{\partial K(h)}{\partial z} \quad (2.8)$$

This is the h-based Richards equation, which may be used for unsaturated or saturated conditions. The θ-based equation,

$$\frac{\partial \theta}{\partial t} = \frac{\partial}{\partial Z}\left(D(\theta)\frac{\partial \theta}{\partial Z}\right) + \frac{\partial K(\theta)}{\partial Z} \quad (2.9)$$

cannot be used to model flow in soils at or near saturation, because dθ tends to zero and D(θ) becomes infinite. The θ based equation also fails in cases of layered profiles, since in cases where abrupt transitions occur between layers, θ is not continuous (Hillel, 1998). Equation 2.9 is the same as Equation 2.8, where

$$D(\theta) = K(h)\frac{dh}{d\theta} \quad (2.10)$$

and $\frac{dh}{d\theta}$ approaches infinity, when moisture content approaches saturation such that $d\theta$ approaches zero. For completely unsaturated flow the θ-based equation is advantageous because changes in both θ and $D(\theta)$ are typically an order of magnitude less than corresponding changes in h and C for the h-based equation. As a result, round-off errors in numerical solutions of the θ-based equation are less significant than for the h-based equation (Skaggs and Khaleel, 1982). The numerical solution of the Richards equation for a given set the hydrologist to use the physical properties governing movement of water and air through soils to precisely quantify vertical percolation of water subject to a variety of conditions. These predictions are of initial and boundary conditions, allows critical for assessment of groundwater recharge and in the analysis of contaminant movement through soil (Skaggs and Khaleel, 1982).

However, the numerical solution of the Richards equation requires numerous measurements to be made to adequately describe variations in soil properties that occur both vertically in the soil profile and from point to point in the field (Skaggs and

Khaleel, 1982), and therefore infiltration models with simplified data requirements are desirable for practical use.

2.10 Approximate Models

Several equations that simplify the concepts involved in the infiltration process have been developed for field applications. Approximate models such as those of Philip and Green and Ampt apply the physical principles governing infiltration for simplified boundary and initial conditions. They imply ponded surface conditions from time zero on (Hillel, 1998), and are based on assumptions of uniform movement of water from the surface down through deep homogenous soil with a well define wetting front; assumptions that are more valid for sandy soils than for clay soils (Haverkamp *et al*., 1987). These assumptions reduce the amount of physical soil data needed from that of numerical solutions, but also limits their applicability under changing initial and boundary conditions (Haverkamp *et al.,* 1987). Equations that are physically based approximations use parameters that can be obtained from soil water properties and do not require measured infiltration data. Thus, they should be able to produce estimates at lower cost than empirical equations. Other equations are partially or entirely empirical and parameters must be obtained from measured infiltration data or roughly estimated by other means. Empirical equations such as those of Kostiakov and Horton are less restrictive as to mode of water application because they do not require the assumptions regarding soil surface and soil profile conditions that the physically based equations require (Hillel, 1998). Where soils are heterogeneous, and factors such as macropore flow and entrapped air complicate the infiltration process, empirical equations may potentially provide more accurate predictions, as long as they are used under similar conditions to those under which they were developed. This is because their initial parameters are determined based on actual field-measured infiltration data (Skaggs and

Khaleel, 1982; Rawls et al. 1993). One characteristic of infiltration that all the equations predict is an initially rapid decrease in rate with time for ponded surfaces (Skaggs and Khaleel, 1982).

2.10.1 Kostiakov equation

Kostiakov (1932) and independently Lewis (1938) proposed a simple empirical infiltration equation based on curve fitting from field data. It relates infiltration to time as a power function:

$$f_p = K_k\, t^{-\alpha} \qquad (2.11)$$

where, f_p = infiltration capacity [Lt^{-1}], t = time after infiltration starts [t], and K_k [L] and α [unitless] are constants that depend on the soil and initial conditions. The parameters, K_k and α must be evaluated from measured infiltration data, since they have no physical interpretation. The equation describes the measured infiltration curve and given the same soil and same initial water condition, allows prediction of an infiltration curve using the same constants developed for those conditions. Criddle et al. (1956) used the logarithmic form of the equation

$$\log f_p = \log K_k - \alpha \log t \qquad (2.12)$$

to determine the parameter values for K_k and α by plotting log f_p against log t, which results in a straight line if the Kostiakov equation is applicable to the data. The intercept of the equation (infiltration rate at time t = 1) is log K_k and the slope is -α. The higher the value of -α, the steeper the slope and the greater the rate of decline of infiltration. The greater the value of K_k, the greater the initial infiltration value (Naeth, 1991). The Kostiakov equation is widely used because of its simplicity, ease of determining the two constants from measured infiltration data and reasonable fit to infiltration data for many

soils over short time periods (Clemmens, 1983). The major flaws of this equation are that it predicts that the infiltration capacity is infinite at t equals zero and approaches zero for long times, while actual infiltration rates approach a steady value (Philip,1957a; Haverkamp et al., 1987; Naeth, 1991). Also, it cannot be adjusted for different field conditions known to have profound effects on infiltration, such as soil water content (Philip, 1957a). Mezencev (1948) proposed a modification to Kostiakov's equation by adding a constant to the equation that represents the final infiltration rate reached when the soil becomes saturated after prolonged infiltration.

$$f_p = K_k t^{-\alpha} + f_c \qquad (2.13)$$

Israelson and Hanson (1967) also developed the modified Kostiakov equation and applied it for estimation of irrigation infiltration. Mbagwu (1993) recommended the modified Kostiakov equation for routine modeling of the infiltration process on soils with rapid water intake rates. The Kostiakov and modified Kostiakov equations tend to be the preferred models used for irrigation infiltration, probably because it is less restrictive as to the mode of water application than some other models. The SIRMOD model (Walker, 1998) simulates the hydraulics of surface irrigation (border, basin and furrow) at the field level and employs the modified Kostiakov infiltration equation to represent infiltration characteristics.

Ghosh (1980, 1983) obtained better results with the Kostiakov equation than the Philip model for fields with wide spatial variability in the infiltration data. Clemmens (1983) found that the Kostiakov equation provided significantly better predictions than the theoretical equations of Philip and GA for border irrigation infiltration data. Naeth (1991) found that the Kostiakov equation fit double ring infiltrometer data very well for all three ecosystems that he studied. Naeth (1988) also found that the Kostiakov

equation was sensitive to changes in infiltration capacity brought about through different grazing treatments. However, Gifford (1976) found that the Kostiakov equation did not fit infiltrometer data collected from semi-arid rangelands in Australia and the United States. Gifford (1978) determined that the coefficients in the Kostiakov equation were more closely related to vegetation factors than to soil factors from infiltrometer data run with soils pre-wet to field capacity prior to the infiltration test.

Ghosh (1985) challenged the commonly accepted view that the value of the α term in the Kostiakov equation lies between zero and one, and proved mathematically that the value of α can be greater than unity. Mbagwu (1990) however, found empirically that the value of α was consistently less than one. Fok (1986) showed that the K_k and α terms of the Kostiakov equation do have physical meaning even though several authors have described it as purely empirical. Mbagwu (1994) found that the two soil properties with greatest influence over the K_k term are the effective porosity and bulk density. Bulk density which correlated inversely with the K_k explained 43% of the variability, effective porosity which is exponentially related to K_k explained 78% of the variability in this parameter. Mbagwu (1994) found a critical effective porosity threshold of 15 – 20 %, below which the value for was drastically reduced. He also found the saturated hydraulic conductivity to be linearly correlated with the Kostiakov's K_k ($r = 0.9823$, $p \leq 0.001$). These three relationships to these physical soil properties he found to be the same for the Kostiakov K_k as they are for the Philip's transmissivity term, C_a. Moreover, Mbagwu (1994) related Kostiakov K_k to Philip's C_a by the equation:

$$K_k = 24.22\ C_a - 0.83 \qquad (2.14)$$

which has correlation coefficient (r) of 0.9735, $p \leq 0.001$. Thus, the very positive relationship between the two parameters and the similarity of the physical properties that exert influence over them, suggest that the time coefficient K_k in Kostiakov's model

has the same physical significance as the Philip's C_a. Both parameters depict the ability of soils to transmit water under ponded infiltration (Mbagwu, 1994). Ghosh (1985) proved mathematically that the Philip's transmissivity term and the Kostiakov's K_k represent similar soil physical properties. Mbagwu (1994) did not find the α term in Kostiakov's model to be significantly correlated with any measured soil properties and concluded that α appears to be less influenced by physical properties than other parameters.

2.10.2 Horton equation

The Horton model of infiltration (Horton, 1939, 1940) is one of the best-known models in hydrology. Horton recognized that infiltration capacity (f_p) decreased with time until it approached a minimum constant rate (f_c). He attributed this decrease in infiltration primarily to factors operating at the soil surface rather than to flow processes within the soil (Xu, 2003). Beven (2004) discovered, upon making a study of Horton's archived scientific papers, that Horton's perceptual model of infiltration processes was far more sophisticated and complete than normally presented in hydrological texts. Furthermore, his understanding of the surface controls on infiltration continue to have relevance today (Beven, 2004).

Horton defines an exhaustion process as one in which the rate of work performed is proportional to the work remaining to be performed. He related the infiltration rate to the rate of work performed and the change in infiltration capacity from f_p to f_c as the work remaining to be performed, with β as the proportionality factor (Horton, 1940).

Horton (1939, 1940) derived his equation for infiltration, which describes a pattern of exponential decay of infiltration rate from this basic relationship.

$$\frac{-df_p}{dt} = \beta(f_p - f_c) \quad (2.15)$$

He divided both sides of equation 2.15 by $f_p - f_c$ and multiplied both sides by dt to yield

$$\frac{df_p}{f_p - f_c} = \beta dt \quad (2.16)$$

next he integrated equation 2.16 to obtain

$$\text{In}\,(f_p - f_c) = -\beta t + \text{const} \quad (2.17)$$

when t = 0, $f_p = f_o$, therefore const must equal ln $(f_o - f_c)$. Therefore,

$$\text{In}\frac{f_p - f_c}{f_o - f_c} = \beta t \quad (2.18)$$

Alternatively

$$\frac{f_p - f_c}{f_o - f_c} = e^{-\beta t} \quad (2.19)$$

The final form of the Horton equation is obtained when both sides of equation 2.18 are multiplied by the denominator on the left-hand side followed by addition of f_c to both sides.

$$f_p = f_c + (f_o - f_c)\, e^{-\beta t} \quad (2.20)$$

where, f_p = the infiltration capacity or potential infiltration rate; (Lt^{-1}), f_c = the final constant infiltration rate; (Lt^{-1}), f_o = the infiltration capacity at t = 0; (Lt^{-1}), β = a soil parameter (t^{-1}) that controls the rate of decrease of infiltration and must depend on initial water content, θ_i ($L^3 L^{-3}$) and application rate, R; (Lt^{-1}). t = time after start of infiltration.

The parameters, f_c, β, and f_o must be evaluated from measured infiltration data. Subtracting f_c from both sides of equation (2.20) and then taking the natural log of each side gives the following equation for a straight line.

$$\ln (f_p - f_c) = \ln (f_o - f_c) - \beta t \quad (2.21)$$

When experimental value f_c is subtracted from experimental values for *f* and the natural log of the resulting values are plotted as a function of time, β can be determined from the slope of the line and f_o can be determined from the intercept. Other methods for finding parameters include a least squares method (Blake *et.al*., 1968).

Horton's equation has advantages over the Kostiakov equation. First, at t equals 0, the infiltration capacity is not infinite but takes on the finite value f_o. Also, as t approaches infinity, the infiltration capacity approaches a nonzero constant minimum value of f_c (Horton, 1940; Hillel, 1998). Horton's equation has been widely used because it generally provides a good fit to data. Although the Horton equation is empirical in that β, f_c and f_o must be calculated from experimental data, rather than measured in the laboratory, it does reflect the laws and basic equations of soil physics (Chow *et al*., 1988). However, the Horton equation is cumbersome in practice since it contains three constants that must be evaluated experimentally (Hillel, 1998). A further limitation is that it is applicable only when rainfall intensity exceeds f_c (Rawls *et al*., 1993). Horton's approach has also been criticized because he neglects the role of capillary potential gradients in the decline of infiltration capacity over time and attributes control almost entirely to surface conditions (Bevin, 2004). Another criticism of the Horton model is that it assumes that hydraulic conductivity is independent of the soil water content (Novotny and Olem, 1994).

2.10.3 Holtan equation

Holtan (1961) described an empirical equation based on a storage concept. The equation was developed at the USDA hydrograph laboratory of the Agicultural Research Service in order to provide a means by which infiltration could be estimated using information

that was generally available or could be readily obtained for major soils of the nation (Holtan, 1967). The premise of the equation is that the factors with greatest influence over infiltration rate are soil water storage, surface connected porosity, and the effect of plant root paths (Rawls et al., 1993). After several modifications, the final form of the equation is written as (Holtan and Lopez, 1971):

$$f_p = GIaSA^{1.4} + f_c \quad (2.22)$$

where, f_p = infiltration capacity at given time; [Lt^{-1}], *SA* = available storage in the surface layer, "A" horizon at given time; [L], *GI* = growth index of crop in percent of maturity *a* = an index of surface connected porosity ((in. $hr.^{-1}$ per $(in.)^{1.4}$ of storage). This is a function of surface conditions and density of plant roots. f_c = the constant or steady state infiltration rate and in Holtan equation is estimated from the soil hydrologic group; [Lt^{-1}].

SA is computed from:

$$SA = (\theta_s — \theta_i)\, d \quad (2.23)$$

where, θ_s = saturated water content of the soil; [$L^3 L^{-3}$], θ_i= actual volumetric water content of the soil; [$L^3 L^{-3}$] and *d* = depth of the surface layer; [*L*].

The Holtan equation is relatively easy to use. The hydrologic soil group can be obtained from the SCS National Engineering Handbook (1964). Estimates for parameters f_c and *a* are provided in table 2.1 and Table 2.2. A serious obstacle with the Holtan Equation is the determination of the control depth on which to base *SA*. Holtan and Creitz (1967) recommended using the depth to the plow layer or to the first impeding layer or depth of A horizon provided in SCS soil survey. However, Huggins and Monke (1966) found that the effective control depth varied depending on both the surface condition and the

farming practices used for seedbed preparation. Smith (1976) argued that infiltration curves are physically much more closely related to moisture gradients and hydraulic conductivity than to soil porosity and that therefore the Holtan equation could not be expected to adequately describe the infiltration process. However, recent studies have been conducted that show a strong relationship between infiltration rate and soil porosity (Messing *et al*., 2005; Kozak and Ahuja, 2005).

Novotny and Olem, (1994) wrote that although Holtan's model is more complex than Horton's, it appears to be less physically based, since it relates infiltration rate to the total water content in an arbitrarily chosen control layer and to the advancement of the wetting front in the unsaturated soil zone. Also, since the Holtan equation does not directly reference time, *f*(*t*) is difficult to develop. Since infiltration rate is a function of the available water storage, the infiltration equation must be accompanied by a simultaneous solution of the storage equation:

$$SA_t = (SA_{t-1} - F_{t-1} + f_c \Delta t) \quad (2.24)$$

where, SA_t = available storage at time t; [L], SA_{t-1} = available storage at time t; SA_{t-1} available storage at previous time step; (L), (L), F_{t-1} = cumulative infiltration at previous time step; (L), and f_c= final constant infiltration rate (or drainage rate); (L^{-1}). Δt = elapsed time.

Table 2.1: Estimates by Hydrology Group for the final infiltration rate, f_c in the Holtan Equation (Musgrave, 1955)

Hydrological soil group	**f_c (in./hr.)**
A	0.45 – 0.30
B	0.30 – 0.15
C	0.15 – 0.05
D	0.05 – 0.05

Table 2.2: Estimates of vegetative parameter "a" in the Holtan infiltration equation (Frere, *et al*., 1975)

Land use or cover	Basal area rating	
	Poor condition	**Good condition**
Fallows	0.1	0.3
Row crops	0.1	0.2
Small grains	0.2	0.3
Hay (legumes)	0.2	0.4
Hay (sod)	0.4	0.6
Pasture (Bunch grass)	0.2	0.4
Temporary pasture (sod)	0.2	0.6
Permanent pasture (sod)	0.8	1.0
Woods & forests	0.8	1.0

* Adjustments needed for "weeds" and "grazing" & for fallow land only, poor condition means "after row crop", and good condition means "after sod".

2.10.4 Philip equation

Philip (1957a) developed an infinite-series solution to solve the non-linear partial differential Richards' equation (Richards, 1931), which describes transient fluid flow in a porous medium for both vertical and horizontal infiltration. Philip's rapidly converging series solves the flow equation for a homogeneous deep soil with uniform initial water content under ponded conditions. For cumulative infiltration the general form of the Philip infiltration model is expressed in powers of the square-root of time, t, as in equation (2.25);

$$F = St^{1/2} + C_{a1}t + C_{a2}t^{3/2} + \ldots \quad (2.25)$$

where, F = cumulative infiltration; [L] S = sorptivity; [$Lt^{-1/2}$], a function of initial and final soil water content, θ_i and θ_n Ca1, C_{a2} = constants that depend on both soil properties and on θ_i and θ_n. Philip (1957b) defined sorptivity (S) as the measurable physical quantity that expresses the capacity of a porous medium for capillary uptake and release of a liquid. White and Perroux (1987) referred to sorptivity as an integral property of the soil hydraulic diffusivity. S is constant provided the water content at the inflow end is constant (Jury *et al*., 1991).

The time derivative of F is the infiltration rate, f ; [Lt^{-1}] which is

$$f = St^{-1/2} + C_{a1} + 3/2C_{a2}t^{1/2} + \ldots \quad (2.26)$$

For horizontal infiltration (i.e. no gravity driven flow), all terms are zero except for the first term on the right side of equations (2.25) and (2.26) and the equations apply to all times greater than zero (Sullivan et al., 1996). For vertical infiltration, 2.25 and 2.26 apply only for a short time when the matric-potential gradient is much greater than the gravity-potential gradient (Sullivan et al., 1996). All terms beyond the first two terms on the right-hand side of equations 2.25 and 2.26 are considered to be negligible (Jury *et al*., 1991).

Philip (1957b) proposed that by truncating his series solution for infiltration from a ponded surface after the first two terms, a concise infiltration rate equation could be obtained which would be useful for small times. The resulting equation is,

$$f = S/2\ t^{-1/2} + C_a \quad (2.27)$$

where, f = infiltration rate; (Lt^{-1}); S = sorptivity; ($Lt^{-1/2}$). t = time after start of infiltration; (t), C_a = rate constant; (Lt^{-1}).

The form of Philips truncated equation is very similar to that of Kostiakov. In fact, the modified Kostiakov equation with α equal to 0.5 is essentially the same equation. The parameters *S* and C_a are dependant on the soil and the initial water content and can be evaluated numerically using procedures provided by Philip if the properties of diffusivity and pressure head as a function of soil water content are known. Philips (1957b) and Talsma (1969) showed that the value of the rate constant, C_a, that results from using Philip's method is approximately $K_s/3$. However, the equation predicts values of infiltration rate that are too low for long time periods, because this approximation is not physically consistent; as t approaches infinity.

A shortcoming of the Philip infiltration model is that the assumptions for which the equation is applicable are rarely found in the field on a large scale. Soil types vary both spatially and with depth, as does vegetation and surface conditions. Although parameter values can be obtained by making point measurements in the field, variability limits the worth of test results for application to larger areas such as watersheds (Sullivan, 1996). Whisler and Bouwer (1970) found that determining the values of the parameters S and C_a for the Philip equation from physical soil properties was very time consuming and yielded results that were not in agreement with the experimental curve. They were able to obtain close agreement with experimental values when they determined parameter values by curve fitting, but lost the physical significance of the parameters by using this method. Smiles and Knight (1976) suggested that the appropriateness of infiltration data to the 2-parameter Philip equation can be determined by plotting $Ft^{-½}$ as a function of $t^{½}$. When equation (2.24) is truncated after the first two terms and both sides are divided through by $t^{½}$, an equation for a straight line is obtained

$$Ft^{-1/2} = S + C_a t^{1/2} \quad (2.28)$$

The linearity of this curve for early times indicates that equation 2.26 is appropriate for describing the infiltration process and the values for S and A can be determined from the y-intercept and slope of the line respectively. When used in this manner, the equation is empirical rather than physically based, although it is derived from physical theory. Philip's model was adapted for constant intensity rainfall by Luce and Cundy (1992) to determine rainfall excess and time of ponding for solution of the kinematic wave overland flow equation. They included depression storage between time of ponding and time of initiation of runoff. The time at which depression storage of depth, h_n is filled is expressed as:

$$h_n = \int_{t_p}^{t_n} R - f(t)dt \quad (2.29)$$

where, R = rainfall intensity t_p= time of ponding, t_n = time of runoff initiation and

$$f(t) = S[t - (t_p - t_s))^{-1/2} + C_a \quad (2.30)$$

where, $t_p - t_s$ is a time correction factor, with t_p equaling time of ponding and t_s representing the time when f(t) = R under continuously ponded conditions.

Combining equations (2.29) and (2.30) and integrating gives:

$$h_n = (R - C_a)(t_n - t_p) - 2S(t_n - t_p + t_s)^{1/2} + 2St_s^{1/2} \quad (2.31)$$

The time runoff begins, t_n can be determined by numerically evaluating this equation.

2.10.5 Green-Ampt equation

Green and Ampt (GA) proposed in 1911 an approximate model that directly applies Darcy's law. The original equation was derived for infiltration from a ponded surface into a deep homogeneous soil with uniform initial water content. The GA model has been found to apply best to infiltration into uniform, initially dry, coarse textured soils which exhibit a sharply defined wetting front as depicted in Figure 2.2 (Hillel and Gardner, 1970). This pattern is often called a piston displacement profile or plug flow. The transmission zone is a region of nearly constant water content above the wetting front, which lengthens as infiltration proceeds. The wetting front is characterized by a constant matric suction, regardless of time or position and is a plane of separation between the uniformly wetted infiltrated zone and the as-yet totally un-infiltrated zone (Hillel, 1998). These assumptions simplify the flow equation so that it can be solved analytically. Although measured infiltration data are not required to make predictions using the GA equation, Green and Ampt (1911) recommended that soil physical properties should be measured the field, so that undisturbed field conditions are reflected in the resulting values.

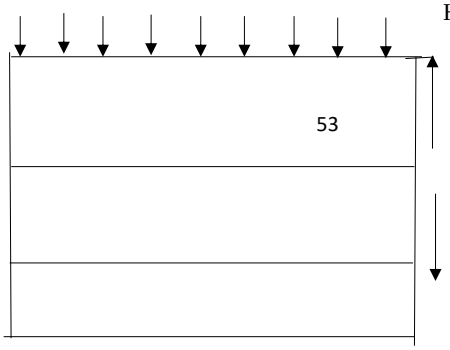

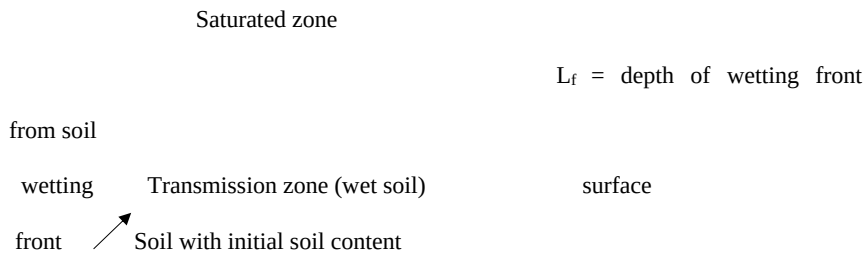

Figure 2.2: water entry assumption, transmission zone and sharply defined wetting front (Green and Ampt, 1911)

The following form of the GA equation was derived from direct application of Darcy's Law:

$$f = \frac{K_{fs}(H_o + S_f + L_f)}{L_f} \quad (2.32)$$

where, f = infiltration rate; (Lt^{-1}), K_{fs} = hydraulic conductivity of the transmission zone; (Lt^{-1}), H_o = the depth of water ponded on the surface; (L), S_f = the effective suction at the wetting front; (L) and L_f = the distance from the surface to the wetting front; (L).

Bouwer (1966, 1969) showed that the hydraulic conductivity parameter, as it appears in Equation 2.21, is not the conductivity at full saturated value, because of air entrapped in the soil pores, but is instead the conductivity at residual air saturation. This has also been called 'resaturated hydraulic conductivity' (Whisler and Bouwer, 1970). He described measurement of K_{fs} in the field by air-entry permeametry. When field measurements are not feasible, Bouwer (1966) suggested that, where $K_{sf} = 0.5K_s$, K_s is the laboratory value for saturated hydraulic conductivity.

Expressing the cumulative infiltration, F (L) as:

$$F = (\theta_s - \theta_i)L_f = M_i L_f \quad (2.33)$$

and assuming very shallow depth of ponding so that $H_o \approx 0$, equation (2.31) may be rewritten as,

$$f = K_{fs} + \frac{K_{fs}+M_i+S_f}{F} \quad (2.34)$$

where, M_i is the moisture deficit, or the difference between saturated and initial volumetric water contents. Although Green and Ampt assumed total saturation behind the wetting front, Philip (1954) observed that this was not a necessary requirement. He assumed that θ_s was constant, but not necessarily equal to the total porosity. Similarly, K_{fs} is expected to be slightly less than the saturated hydraulic conductivity. When f = df/dt is substituted into equation |2.34|, integration with the condition that F= 0 at t = 0, yields:

$$K_{fs}t = F - M_i S_f \ln\left(1 + \frac{F}{M_i S_f}\right) \quad (2.35)$$

This form of the equation relates infiltration volume to time from start of infiltration, which is convenient for some applications.

In spite of the many assumptions under which the GA equation was originally developed, it has been adapted for use under a much wider variety of conditions. The GA equation produced reasonably good predictions for non-uniform soil profiles that become denser with depth (Childs and Bybordi, 1969), for profiles where hydraulic conductivity decreases with depth (Bouwer, 1969) or increases with depth (Bouwer, 1976), and for soils with partially sealed surfaces (Hillel and Gardner, 1970). Bouwer (1969) described a tabular procedure for calculating the GA relationship between cumulative infiltration and time for soils with non-uniform initial water contents and hydraulic conductivities. He showed that the soil profile could be split into layers, each with its own water content, moisture deficit, and hydraulic conductivity from which the GA approach could be used to calculate cumulative infiltration and time intervals

(Bouwer, 1969, 1976). Bouwer (1969) calculated an effective hydraulic conductivity for each depth using the harmonic mean of the hydraulic conductivities for the entire profile above that depth.

CHAPTER THREE

3.0 MATERIALS AND METHOD

3.1 Study Area

Niger state lies in the Southern Guinea Savannah ecological zone of Nigeria, it is the largest state in the country between latitude $8^0$10'N and $11^0$3'N and longitude $3^0$20'E and $7^0$30'E. Niger state has two distinct seasons, which are the rainfall and dry seasons. The rainy season usually starts in the southern part of the state as from early April and

ends in late October and some rare cases first half of November. The dry season starts mostly as from mid-November and ends in March of the following year. (Ehounou *et al., 2019*) stated that the average annual rainfall, temperature, and relative humidity of Niger state are 1,312 mm, 27.3^{o}c and 50.2%, respectively. The most common type of soil in Niger State is the alluvial soils because of its floodplain characteristic. The soil is known to have good water holding capacity (Ibrahim, 2021). Figure 3.1 shows extracted map of the study location from Niger State, Nigeria.

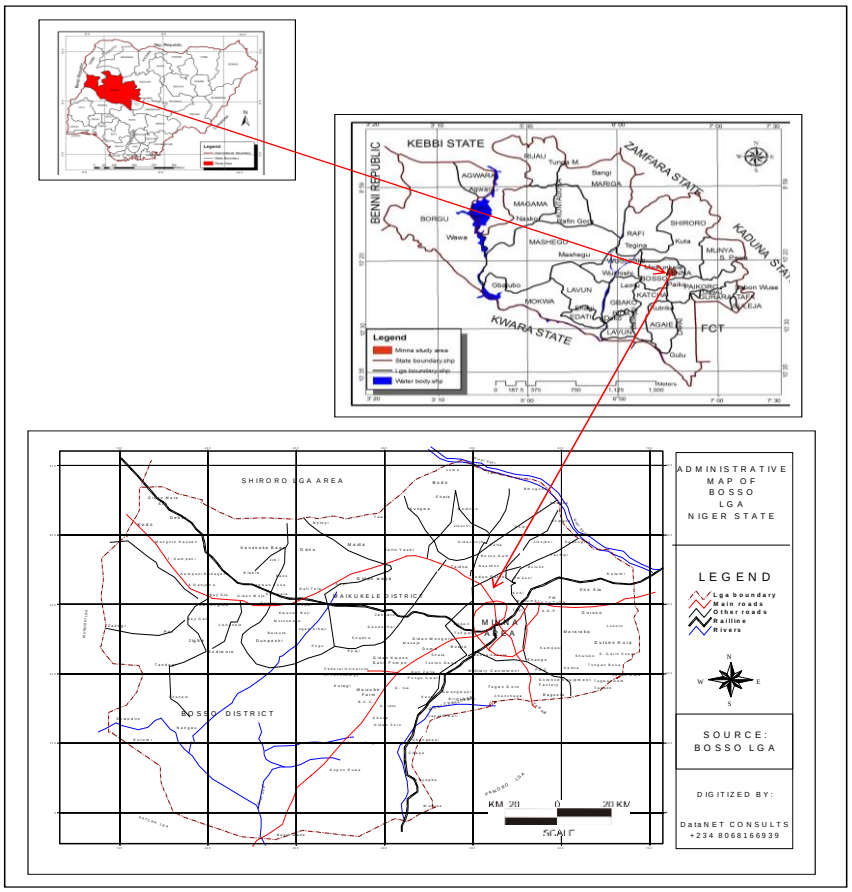

Figure 3.1: Extracted Map of the Study Location from Niger State, Nigeria (Abubakar, 2019)

3.2 Soil Sampling

Soil samples was collected from six (6) different locations, at each site, five soil samples were collected from each of three depths: 0-15 cm, 15-30 cm and 30-45 cm which was use in the determination of initial moisture content, soil bulk density, and a first run of saturated hydraulic conductivity measurements. The initial moisture content was determined using the gravimetric method. In order to avoid making holes in the grass-covered plots, soil was sampled from the area immediately adjacent to the plots.

Below each sample, a shovel will be used to lower the hole to the next sampling level and a tape measure will be used to measure the depth until the final depth is obtained. Samples were retained in rings, wrapped in thin perforated plastic or foil, taped with duct tape, labeled, and stored in the shade. Sites were divided into 5 roughly equal segments and samples were obtained from one hole in each segment. An attempt was made to choose ground that appeared to have been undisturbed for some time. Auger was employed to obtain larger samples and it was sent to the soil lab for texturing.

The sample locations were undeveloped land, Farm land, Garden, Grazing land, paved compound and paved road side.

3.3 Method

3.4 Development of Infiltration Rate

The infiltration rate was determined using a double ring infiltrometer. It consists of thin metal cylinder with inner diameter of 300mm and 600mm outer diameter, and this cylinder was driven into ground and 10-12cm of the cylinder was above the ground level. And water was poured from the top and we noted the volume of water added to the ring to find the Incremental Infiltration velocity. We also took note of the infiltrated water depth for 5,10,20, 30, 40, 50, 60, 70, 80, 90, 100, 110, 120, 130, 140, 150, 160, 170, and 180 mins until we get the constant infiltration depth. A graduated jar was used to add water and scale was used to measure the depth of water infiltrated.

The quantity of water added to the inner ring, to maintain the liquid level constant was the measure of the depth of water that infiltrates the soil. The depth of water infiltrated during time intervals was convinced as an incremental infiltration velocity, here it was expressed in centimeter per hour (cm/hr). The maximum-steady state or mean

incremental infiltration velocity, depends on the purpose of the test is equivalent to the infiltration rate.

3.4.1 Soil property analysis

Soil physical and chemical properties were determined according to standard methods (Jat *et al*., 2018). The following physical parameters were determined;

I. The antecedent soil water content (AWC)
II. Bulk Density (BD)
III. Hydraulic Conductivity

(i) The Antecedent soil Water Content (AWC)

The gravimetric method as described by Gardner (1986) was employed to establish initial soil water content for both sites. Wet samples were weighed, dry in force-draft oven at 104^{o}C to remove all water from controlled sample until the weight does not vary more than 0.01% without changing its physical or chemical characteristics of the soil samples for 24-48 hours, and then weigh again. Gravimetric soil water content was then determined by equation (3.1).

$$\theta_m = \frac{mass\ wet\ soil - mass\ dry\ soil}{mass\ dry\ soil} = \frac{m_w}{m_s} \quad (3.1)$$

(ii) Bulk density (BD)

To convert to volumetric soil water content, the bulk density of the soil was obtained. The length and diameter of the soil rings was measured and the volume was calculated by equation 3.2

$$V = \frac{\pi d^2}{4} L \quad (3.2)$$

where, V is the volume of soil water content, d is the diameter of the soil rings and L is the length of the soil rings.

Therefore, bulk density can be calculated accordingly as in equation |3.3|

$$\rho_b = \frac{m_s}{m_v} = \frac{mass\ of\ dry\ soil}{volume\ of\ soil} \quad (3.3)$$

Volumetric water content was estimated using equation 3.4

$$\frac{v_w}{v_s} = \frac{m_w}{m_s} \times \frac{m_s}{v_s} \times \frac{v_w}{m_w} \quad (3.4a)$$

where, V_w = volume water (cm^3), V_s = volume of dry soil (cm^3), m_w = mass of water (g) and m_s = mass of dry soil (g).

$$\theta_i = \theta_m \times \frac{\rho_b}{\rho_w} \quad (3.4b)$$

Alternatively,

where,

$\theta_i = \frac{v_w}{v_s}$ (Volumetric water content, $cm^3\ cm^{-3}$)

$\theta_m = \frac{m_w}{m_s}$ (Gravimetric water content, $g\ g^{-1}$)

$\rho_b = \frac{m_s}{v_s}$ (Bulk density of soil , $g\ cm^{-3}$)

$\rho_w = \frac{v_w}{m_w}$ (Density of water, $g\ cm^{-3}$)

(iii) Hydraulic conductivity

Falling head method was employed to determine saturated hydraulic conductivity. The soil sample was first saturated under a specific head condition, the water was then allowed to flow through the soil without adding any water, so the pressure head will decline as the water passes through the specimen (Liu, 2001). The initial head (h_i) and the final head (h_f) was evaluated as the head drops from h_i to h_f in a time Δt, the hydraulic conductivity was calculated by the equation:

$$K_s = (\frac{L}{\Delta t}) \ln (\frac{h_f}{h_i}) \quad (3.5)$$

3.4.2 Determination of infiltration equations parameter

3.4.2.1 *Kostiakov equation model for the estimation of infiltration characteristics*

For the Kostiakov equation, the base values for the two empirical constants a and b will be determined by using equation (3.6)

$$f_p = a\, t^{-b} \quad (3.6)$$

where, f_p = infiltration capacity (Lt^{-1}), t = time after infiltration starts (t), and a (L) and b (unitless) are constants that depend on the soil and initial conditions. The parameters, a and b must be evaluated from measured infiltration data, since they have no physical interpretation.

Log f_p would therefore be plotted against log t and finding the slope and y-intercept of the resulting straight line. The intercept of the equation (infiltration rate at time t = 1) is log a and the slope is -b. Infiltration is directly proportional to a, but is inversely related to b

3.4.2.2 *Horton infiltration model for the estimation of infiltration characteristics*

The Horton equation (1940) is one of the most popular empirical models simulating infiltration of water into soils (Philips, 1957). The infiltration equation is a three-parameter equation and equation (3.7) were employed:

$$f = f_c + (f_o - f_c)\, e^{-kt} \quad (3.7)$$

Where, f = infiltration rate at time t, mm hr^{-1}; f_o = initial infiltration rate, mm hr^{-1}; f_c = final infiltration rate, mm hr^{-1}; k = rate constant in dimension of time, t (t^{-1}).

The field measured infiltration rates versus elapsed time will be plotted so that the infiltration rate at any time f_o and f_c can be estimated from the curve that would be

represented as the intercept on the y-axis and the value of the steady-state (final) infiltration rates respectively. In other words, the initial infiltration (f_o) is equal to f at time zero (Verma, 1982). Since infiltration rate for all the measurement will be taken from a starting time of 1 minute, a logarithmic trend line will be used in the regression of infiltration rate against time to determine the intercept (f_o) at time zero. The procedure will be repeated for all 10 measurement points.

Equation 3.7a can be linearised as:

$$f - f_c = (f_o - f_c)\, e^{-kt} \tag{3.7a}$$

Taking the natural logarithm of both sides,

$$\ln(f - f_c) = \ln(f_o - f_c) - kt \tag{3.7b}$$

$$\ln(f - f_c) / \ln(f_o - f_c) = - kt \tag{3.7c}$$

$$\ln\left(\frac{f - fc}{fo - fc}\right) = - kt \tag{3.7d}$$

Let the expression in parenthesis in Equation 3.10d be represented by y, therefore;

$$\ln y = - kt \tag{3.7e}$$

This can easily be taken back to its non-linear form given by:

$$y = e^{-kt} \tag{3.7f}$$

To solve for the equation, *f* will be taken as the measured infiltration rate at any given time t.

Computing the values of the initial (f_o) and final steady-state infiltration (f_c) in the left hand-side of (Equation 3.10d) and solving resulted in the natural logarithm of y (Equation 3.10e) which was plotted against elapsed time to give a straight line on the semi-logarithm scale. Because (Equation 3.10d) gives a semi-logarithmic expression, another way is plotting directly into exponential regression of *y* against time as a non-linear least sum of squares technique. In this study however, the estimates of *k* will be

obtained as the slope from the best fit regression line. The estimates obtained in linear plot of the natural logarithm of *y* and time will be the same as that obtained directly in the exponential plot of y against time (Eqs. 3.10e and 3.10f). It shows that the exponential function represents the data fit for the Horton infiltration equation (Turner, 2006). Knowing *k*, the new infiltration rate will be calculated in (Equation 3.10a). Infiltration rate will be calculated for each point and later compare to actual field measurements using linear regressions from Microsoft office Excel 2010.

3.4.2.3 ***Philip infiltration model for the estimation of infiltration characteristics***

For cumulative infiltration, the general form of the Philip infiltration model is expressed in powers of the square-root of time, t, as in equation 3.8;

$$F = St^{1/2} + C_{a1}t + C_{a2}t^{3/2} + \ldots \; n \qquad (3.8a)$$

The time derivative of F is the infiltration rate, f ; $|Lt^{-1}|$ shall be calculated using the equation 3.8b

$$f = St^{-1/2} + C_{a1} + 3/2C_{a2}t^{1/2} + \ldots \; n \qquad (3.8b)$$

where, F = cumulative infiltration; |L|; S = sorptivity; ($Lt^{-1/2}$), a function of initial and final soil water content, θ_i and θ_n Ca1, C_{a2} = constants that depend on both soil properties and on θ_i and θ_n. Philip (1957b) defined sorptivity (S) as the measurable physical quantity that expresses the capacity of a porous medium for capillary uptake and release of a liquid.

In the Philip equation, the parameter C_a will be estimated to be k_s, $2k_s/3$, $k_s/2$ and $k_s/3$

.

3.4.2.6 ***Statistical performance for the developed model***

The performance of the various model was evaluated by means of error statistics criteria such as

(i) Root mean square error:

$$RMSE=\sqrt{\frac{\sum_{i=1}^{n}(Q_i-\widehat{Q_i})^2}{n}} \quad (3.9a)$$

where, Q_i is the measured discharge and $\hat{Q}$ is the simulated discharge, n is the number of observations (instants).

(ii) Coefficient of determination

$$R^2 = 1-\frac{SSE}{SSy} \quad (3.9b)$$

where, SSE = $\sum_{i=1}^{n}(Q_i-\widehat{Q_i})^2$, SSy = $\sum_{i=1}^{n}(Q_i-\overline{Q_o})^2$

where, $\bar{Q}$ is the arithmetic mean of the observed Q.

(iii) Standard deviation and coefficient of variation

Standard deviation is a quantity expressing by how much the members differ from the mean value for the group

$$\sigma = \sqrt{\frac{\sum_{i=1}^{n}(Q_i-\mu)^2}{n}} \quad (3.9c)$$

The coefficient of variation can be used to compare variability. It is the ratio of the standard deviation to the mean (average)

$$CV = \frac{\sigma}{\mu} \quad (3.9d)$$

where, cv is the coefficient of variation, μ is the mean, and σ is the standard deviation

3.5 Data Analysis

The values of soil property were averaged for the three samples from each plot. Pearson correlation coefficients was employed to detect relationships between soil properties and infiltration variables. One-way analysis of variance (ANOVA; $P < 0.05$) was used to compare the differences between means.

CHAPTER FOUR

4.0 RESULT AND DISCUSSION

4.1 Comparison of Sites

4.1.1 Soil textural classification

Soil analyses for the five land use practices are presented in Table 4.1. The soil properties presented in the table are particle-size fractions (sand, silt, clay and loam), bulk density, saturated hydraulic conductivity and available water content. Considering the effect of the land use practices on soil properties (Table 4.1), the soils differ considerably between the six locations; that is, the undeveloped land, Farm land, Garden, Grazing land, paved compound and paved road side. The soil at the undeveloped site is a deep (i.e., it can provide more water and nutrients to the plants), well-drained, soil which consist of 56% sand, 25% clay and 31% silt. The soil at the f arm land is dominated with loamy soil with relatively high degree of homogeneity both vertically across depths and horizontally from one sample locus to the next. The soil texture at grazing land from five different samples collected showed sandy clay, silty loam, clay loam, silty loam and sandy loam, respectively. Paved compound and paved road side are sandy clay because the soil was replaced during construction work to increase the bulk density of the soil and reduce infiltration rate. These results also demonstrate that the effect of soil texture on infiltration rate was probably masked by the land use practices and soil management, which agrees with the fact that water infiltration into the soil is highly sensitive to land use and soil management, as also observed by (Bai, *et al*., 2020.; dos Santos, *et al*., 2018).

Table 4.1: Soil properties analysis

Study Location	% Clay	% Sand	% Silt	soil texture	bulk density (g/cm^3)	moisture content	hydraulic conductivity (cm/hr)
Undeveloped (Fallow)							
I	18	56	38	Sandy loam	1.47	0.11	3.07E-01
II	9	83	74	Loamy sand	1.62	0.08	3.10E+00
III	41	44	3	Clay	1.32	0.11	5.81E-03
IV	14	53	39	Sandy loam	1.5	0.12	4.66E-01
V	42	42	0	Clay	1.31	0.11	4.08E-03
Farm Land							
I	24	39	15	Loam	1.39	0.13	7.56E-02
II	15	68	53	Sandy loam	1.52	0.09	5.75E-01
III	30	43	13	Clay loam	1.36	0.12	2.24E-02
IV	22	43	21	Loam	1.41	0.13	7.20E-02
V	29	43	14	Clay loam	1.37	0.12	2.15E-02
Garden (Vegetative)							
I	33	37	4	Clay loam	1.34	0.013	1.86E-02
II	26	38	12	Loamy	1.38	0.13	3.83E-02
III	11	34	23	Silty loam	1.50	0.16	7.25E-01
IV	37	33	4	Clay loam	1.31	0.13	5.79E-03
V	30	49	19	sandyclayloam	1.38	0.11	2.09E-02
Grazing Land							
I	39	52	13	sandy clay	1.34	0.1	1.18E-02
II	8	38	30	Silty loam	1.55	0.16	1.62E+00
III	22	55	33	sandyclayloam	1.43	0.11	1.08E-01
IV	18	30	12	Silty loam	1.42	0.16	1.10E-01
V	17	57	40	Sandy loam	1.48	0.11	2.63E-01
Paved Compound							
I	23	62	39	sandy clay	1.64	0.09	1.33E-01
II	34	45	11	Sandyclayloam	1.55	0.11	1.33E-02
III	20	63	43	sandy loam	1.46	0.1	1.86E-01
IV	38	46	8	sandy clay	1.53	0.11	6.77E-03
V	48	48	0	sandy clay	1.50	0.1	2.82E-03
Paved Road Side							
I	49	47	2	sandy clay	1.60	0.1	4.69E-03
II	50	46	4	sandy clay	1.69	0.1	2.97E-03
III	38	56	18	sandy clay	1.55	0.09	1.01E-02
IV	39	53	14	sandy clay	1.64	0.09	7.01E-03
V	38	60	22	sandy clay	1.56	0.08	9.09E-03

4.1.2 Bulk density measurement

Bulk density was measured after saturated hydraulic conductivity and soil water retention measurements, resulting in slightly lower bulk densities than would have been obtained by measuring bulk density of separate samples, because a small amount of soil was unavoidably lost during these procedures. Undeveloped plot bulk density values varied very little with depth (1.31-1.62 g/cm^3), aside from a slightly less dense surface layer, due to plant roots, and other organic matter, and a denser plow pan layer at approximately 18-20 cm. The similarity of bulk density values across depth at this site is not surprising, since the soil is relatively homogeneous with the majority of the layers being sandy loam. The values for bulk density measured from this site are 1.47g/cm^3, 1.62g/cm^3, 1.32g/cm^3, 1.5g/cm^3 and 1.31g/cm^3 as presented in Figure 4.1 which corresponded to the values for sandy loam (1.7 g/cm^3) and sandy clay loam (1.6 g/cm^3) in a diagram by Ellen (2006). Recalling that the bulk density measurements were low due to soil loss during other laboratory procedures performed on the soil samples, sandy loam is more plausible at this site.

The bulk density values of the Farm land (1.36-1.52 g/cm^3) also varied very little with depth and it is predominated by loamy soil (mixed sandy and clayey loam) and the soil shows less homogeneity, with the surface layer having considerably lower average bulk density of 1.41 g/cm^3 due to more plant roots and worm holes in that layer. This is inconformity with (Mutonyi, & Muturi, 2021) findings for Upper Marlboro and Poplar Hill sites. Density increases with depth until a plow pan is reached (1.52 g/cm^3) at approximately 25-30 cm depth and then decreases due to high clay content in the deeper layers. The bulk density values of the garden area also varied very slightly with depth (1.31-1.5 g/cm^3) which is predominately loamy soil, while the grazing land bulk density varied very little with depth (1.34-1.55 g/cm^3) and it is predominated by mixed silty loam and sandy clay due to land degradation and desertification which is similar to the

work of Dada *et al*., 2017. Paved compound and paved road site are dominated by sandy clays with varied bulk density of (1.3-1.46 g/cm^3) and (1.3-1.35 g/cm^3), respectively. This is similar to the findings of (Natarajan *et al*., 2020).

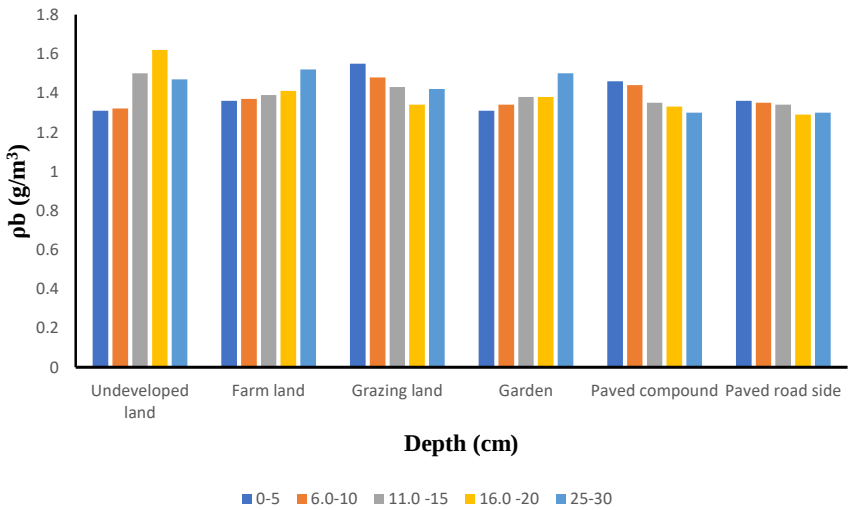

Figure 4.1: Average bulk densities of the five study locations as a function of depth.

4.1.3 Hydraulic conductivity (Ks)

Hydraulic conductivity values of Undeveloped land, Farm land and Garden in Figure 4.2 shows a clear decreasing trend with increasing depth. The surface layers have significantly higher Ks of 3.10 cm/hr, 0.575 cm/hr and 0.725 cm/hr for Undeveloped land, Farm land and Garden study areas, respectively. This may be due to the presence of plant roots, worm holes and plant debris which cause increased aeration and looser packing of soil, along with some preferential flow as water finds channels through the soil instead of moving uniformly through the column. This is similar to the findings of (Bimbraw, 2021). With increased depth, higher clay content results in much slower movement of water as very few and thiny pores in clay provide strong resistance to flow. Figure 4.2 also indicated that the hydraulic conductivity values of grazing land,

paved compound and Paved road side fluctuate but gradually increases as depth increases with the lowest hydraulic conductivities at the surface of 0.018 cm/hr, 0.00677 cm/hr and 0.00297 cm/hr, respectively. The lower values at the surface are due to soil compaction, degradation and clayey content.

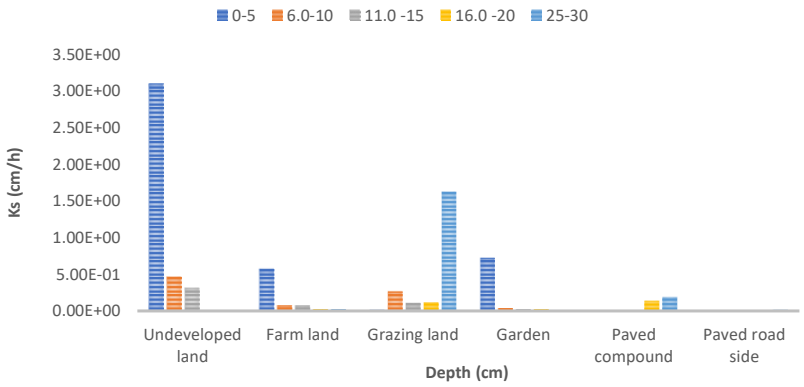

Figure 4.2: Hydraulic Conductivity (Ks) for the various study locations

4.1.4 Moisture content

Seasonal and climatic conditions along with soil attributes were seen to have significant impact on initial water content at all the sites. Infiltration rate test was carried out during the month of January, 2020 when the soils were extraordinarily dry and very hard. The undeveloped and Farm land surfaces because of exposure to the sun and wind, had scanty vegetation for protection. This was the driest layer prior to wetting. This is in conformity with the study carried out by Ellen (2006) for Poplar Hill site. Each subsequent depth was moister than the previous layer with the deepest layer having a water content of only 0.12 and 0.13 (cm^3/cm^3), respectively. The soils at these sites are well-drained, sandy loam soil that does not hold as much water as clay, or clay-loam soil. Though the Farm land holds more water than the undeveloped land due to presence of clay soil. The moisture content of paved compound and paved road side ranging from

0.08 to 0.11 cm^3/ cm^3. The surface layers of the two sites had lesser water content than the other depths. The limited surface water content is probably due to hard surface and compaction processes that had taken place over time. Both of these factors affect water-holding capacity of the surface soil. Clay content increased with depth and consequently, the deeper layers the greater water-holding capacity. Aside from the damp surface layer, there was a definite trend from lower water at lesser depth to higher water at greater depth. The surface layer of a Garden had higher water content than the other depths ($0.16cm^3/cm^3$). The higher surface water content is probably due to the vegetation and plant residue cover, as well as the greater amount of organic matter in the surface layer. These factors are known to increase the water-holding capacity of the surface soil as observed in the works of Bimbraw (2021). Figure 4.3 below shows the presence of water moisture content in the upper layer of the soils.

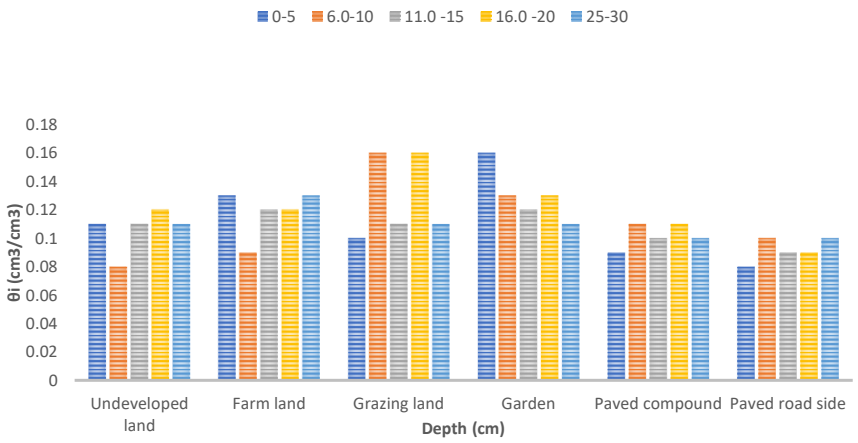

Figure 4.3: Average Moisture Content for various Study Area

4.2 Compacted Urban Soils Effects on Infiltration Rates

Infiltration rate was carried on two different compacted soil at different locations within five sampled points to examine runoff losses from paved compound and paved road side in urban areas. Table 4.2 shows the infiltration rates at urban compacted soil and the result indicated that urban soil compaction contributed to low soil infiltration rates. This is due to the soil infiltration rate decrease with an increase in the bulk density, a reduction in the soil organic matter content and non-capillary porosity. The soil infiltration rate also had significantly positive relationships with the total porosity and saturated soil water content. This is an evidenced that infiltration rate decreased with increased soil compaction (Table 4.2). It also proved that infiltration rate of non-compacted soil was significantly different from that of severely compacted soils.

4.3 Infiltration Curves

The infiltration rate curve obtained from the infiltrometer at undeveloped land was of a fairly steep slope. The initial infiltration rates of the five different sample points were equal to the infiltration rates of about (44.88 cm h^{-1}, 46.89 cm h^{-1}, 42.88 cm h^{-1}, 40.88 cm h^{-1} and 43.89 cm h^{-1}), and then decreased in a logarithmic fashion to approach an asymptote representing a final constant infiltration rates of approximately (12.6 cm h^{-1}, 14.16 cm h^{-1}, 10.26 cm h^{-1}, 8.35 cm h^{-1} and 13.16 cm h^{-1}), respectively. Figure 4.4 shows the infiltration rate curve produced for the Undeveloped site. In an undeveloped land, the rate was initially very high due the nature of the soil; that is sandy loamy. The infiltration behaviour may be attributed to an initial hydraulic conductivity which gradually gave way to decreased conductivity as the soil water content and pore connectivity decreased.

Table 4.2: Compacted urban soils infiltration rate

LOCATIONS		Infiltration Rate																		
	(Min)	**05**	**10**	**20**	**30**	**40**	**50**	**60**	**70**	**80**	**90**	**100**	**110**	**120**	**130**	**140**	**150**	**160**	**170**	**180**
Paved Road Side	I	22.02	17.06	15.90	13.60	13.45	12.95	12.77	11.97	11.89	11.78	11.06	10.96	10.86	10.67	10.04	9.76	9.54	9.15	9.14
	II	20.02	15.06	13.09	13.6	12.45	11.95	10.77	9.97	9.89	9.78	9.06	8.96	8.86	8.67	7.94	7.76	7.54	7.15	7.14
	III	23.06	18.44	16.54	14.32	13.55	12.67	11.96	11.77	11.23	10.87	10.56	10.02	9.79	9.67	9.09	8.89	8.67	8.55	8.19
	IV	22.79	17.05	16.77	15.02	14.55	13.07	12.96	12.76	12.05	11.77	11.46	11.02	10.79	10.67	10.09	9.88	9.78	9.45	9.29
	V	17.79	15.05	14.77	13.02	12.55	11.07	10.96	10.76	10.05	9.77	9.46	9.02	8.79	8.67	8.09	7.88	7.78	7.45	7.29
Paved compound	I	25.98	23.06	21.54	19.76	17.68	15.46	15.06	14.79	14.52	14.03	13.79	13.54	12.86	12.76	11.79	11.67	10.88	10.67	10.23
	II	23.98	21.06	19.54	17.76	15.68	13.46	11.06	10.79	10.52	10.03	9.79	9.54	8.86	8.76	8.55	8.07	7.88	7.67	7.23
	III	26.88	24.16	22.55	20.66	18.78	16.56	16.26	15.99	15.62	15.03	14.89	14.44	13.96	13.76	12.79	12.67	11.88	11.67	10.12
	IV	24.78	22.04	20.54	18.76	16.58	14.56	14.06	13.89	13.42	13.03	12.89	12.55	10.96	10.77	9.78	9.68	8.89	8.68	8.22
	V	25.88	21.06	20.54	18.76	17.68	16.46	16.06	15.79	15.52	15.03	14.79	14.54	13.86	13.76	12.79	11.67	10.88	10.67	9.23

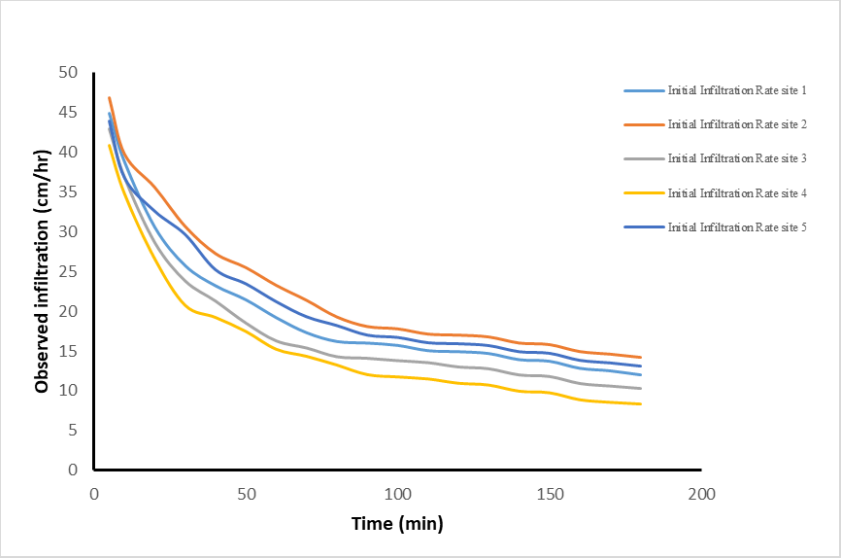

Figure 4.4: Infiltration rate curve for Undeveloped land

The initial infiltration rates of Farm land for five different sample points obtained from the rainfall simulation are 75.75 cm h^{-1}, 73.76 cm h^{-1}, 76.76 cm h^{-1}, 74.76 cm h^{-1}, and 75.75 cm h^{-1} and then decreased in a logarithmic fashion to approach an asymptote representing a final constant infiltration rates of approximately 26.05 cm h^{-1}, 27.25 cm h^{-1}, 27.26 cm h^{-1}, 25.36 cm h^{-1} and 24.05 cm h^{-1}, respectively. The infiltration curve in figure 4.5 indicated that there is a slight difference between the initial infiltration values as well as the difference between the final values. This infiltration behavior may be attributed to an initially increase conductivity due to presence of vegetation cover and sandy conditions, which then gradually gave way to decreased conductivity as the soil water content decreases and pore connectivity decreased. The infiltration curve for the various points on the farmland are presented in figure.4.5 below;

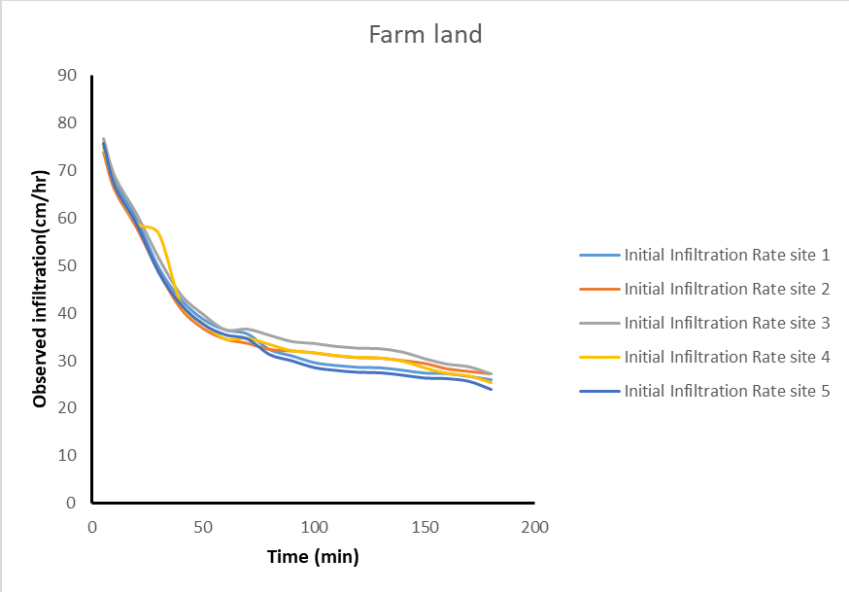

Figure 4.5: Infiltration rate cure for various locations on the Farm land

Figure 4.6 below described the infiltration curve of Gardened area with a slightly steep slope. The following initial average infiltration rates were obtained for each of the plots 20.77 cm h^{-1}, 21.97 cm h^{-1}, 19.89 cm h^{-1}, 22.67 cm h^{-1}, and 18.87 cm h^{-1} and with the final values of 7.87 cm h^{-1}, 7.77 cm h^{-1}, 6.97 cm h^{-1}, 8.12 cm h^{-1}, and 6.47 cm h^{-1}, respectively. This infiltration rate behavior may be attributed to an initially high hydraulic conductivity due to sandy clay loam conditions, which then gradually gave way to decreased conductivity due to clayey content. The infiltration results also showed that gardened area low bulk density, high hydraulic conductivity and low moisture content and these could explain the observed high infiltration rate at the garden area. This rate of infiltration could be observed with areas where there is high organic matter content which are known to decay after garden seasons are over. As observed in the works of Bimbraw (2021), most

garden areas where the studies were carried out, it was observed that after the cropping season, waste materials of the crops such as the leaves, stems were left to decay. The decay materials further mixed up with soil to form loamy type of soil which enhances the movement of water through the soil profile. This is an evident in the rate of infiltration in the study area, this process was observed by the studies carried out by Lai and Doren (1990) for water infiltration for two soils in Ohio. In this study, it was identified that the presence of decaying plant materials improved aeration system of the soil which also improved the water circulation process in the soil.

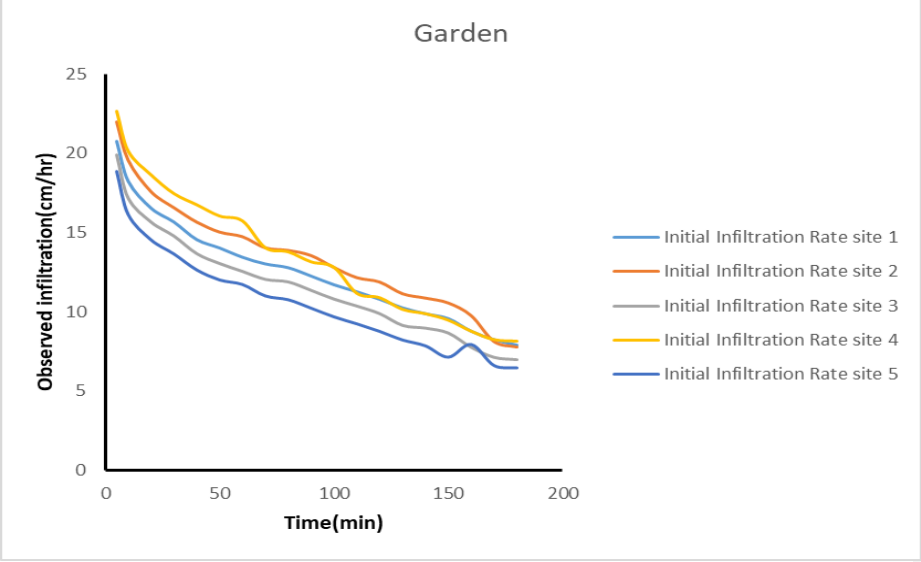

Figure 4.6: Infiltration rate curve for gardened area

Infiltration curves of Grazing land had initial infiltration values of 15.78 cm h^{-1}, 13.88 cm h^{-1}, 17.68 cm h^{-1}, 14.75 cm h^{-1}, and 16.58 cm h^{-1}, as shown in figure 4.7. Grazing land experienced degradation of soil physical attributes in the soil surface zone especially soil

structure and structure-moderated soil properties e.g., bulk density, hydraulic conductivity, and moisture content. The rate of soil infiltration was very low in grazing land due to soil compaction as a result of trampling, resulting in higher "bulk density which reduces soil pore space and restricts water and oxygen movement and decreases in plant cover which allow for soil erosion and rapid evaporation of soil moisture. Pore spaces are smaller in tightly packed soil, reducing the amount of water and oxygen that would normally collect in these pores and making it more susceptible to erosion. This is similar to the work carried by Dada *et al.* (2018). When they determined the soil density and hydraulic conductivity over a track path of cattle herds in Abeokaita, Ogun State.

The differences in bulk density between the grazing land may be influencing the soil moisture trends that were found in this study. The greater bulk density in grazing land was a likely contributor to this because compacted soil encourages water run-off, not infiltration (Houlbrooke *et al.* 2011). Studies by Zhao *et al.* (2011). Studies by Zhao *et al*. (2011) and Herbin *et al*. (2011) have also found greater bulk density measurement to be correlated with lower soil moisture. Other contributing factors to grazing land relatively low soil moisture includes its coarse soil and its high levels of bare ground, along with a lack of an insulating litter layer. The coarser soil found in grazing land indicates erosion. The lighter particles of silts and clay are easily washed or blown away through erosion, leaving the heavier particles of sand behind (Pei *et al*., 2008). The high levels of bare, exposed ground in grazing land supports the possibility that erosion was occurring in grazing land.

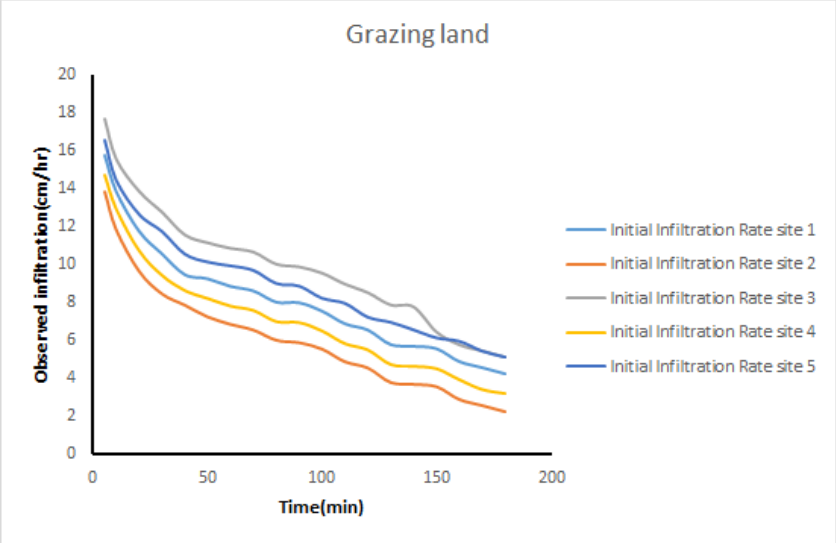

Figure 4.7: Infiltration rate curve for grazing land area

Infiltration rate curves of paved road side had initial infiltration values of 22.02 cm h^{-1}, 20.02 cm h^{-1}, 23.06 cm h^{-1}, 22.79 cm h^{-1}, and 17.79 cm h^{-1}, as shown in figure 4.8. It was deduced from the infiltration test that paved road side has poor water movement process because of the impermeable pavement, which means practically a high enough compaction degree and a low air space. The soil compaction which has reduced the void spaces led to poorer water movement in the soil zone. The rate of movement of water in the sandy area was observed to be slower compared to the findings of Dada *et al*. (2018). This is because of the machine compaction carried during the road construction.

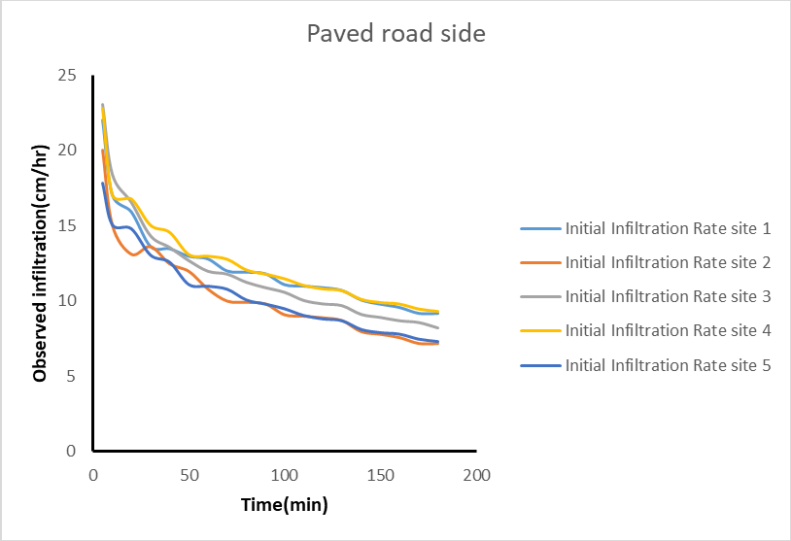

Figure 4.8: Paved road side infiltration curve

The initial infiltration values of paved compound are (25.98 cm h^{-1}, 23.98 cm h^{-1}, 26.88 cm h^{-1}, 24.78 cm h^{-1}, and 25.88 cm h^{-1} as presented in figure 4.9 below: Paved compound experienced low infiltration rate due to low hydraulic conductivity, high bulk density, soil compaction and degradation. (Burch *et al.* 1987) reported that bare soils, exhibit lower infiltration capacities and less macroporosity. These results also demonstrate that the effect of soil texture on infiltration rate was probably masked by the land use practices and soil management, which agrees with the fact that water infiltration into the soil is highly sensitive to land use and soil management. This is inconformity with the findings of Lal and van Doren (1990).

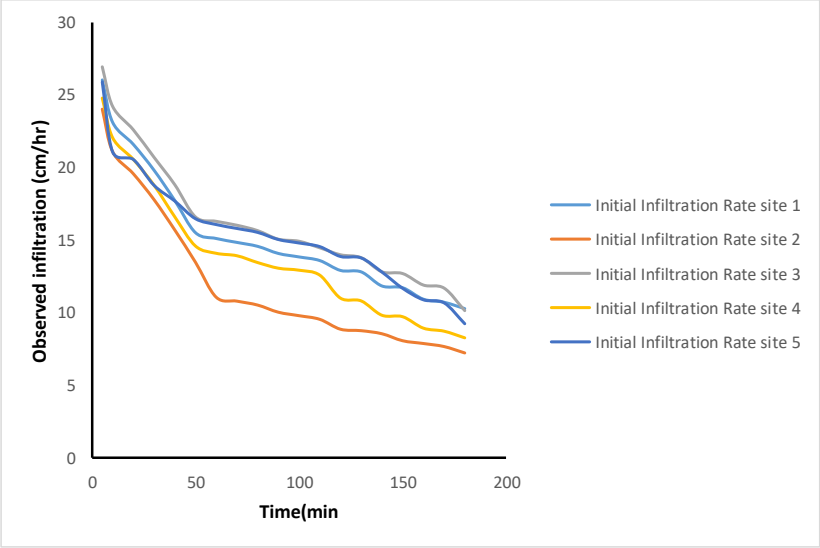

Figure 4.9: Paved compound infiltration curve

4.4 Sensitivity Analysis Results

The base values for parameters for each equation are shown in Table 4.3. Many infiltration models have been developed to predict infiltration rate as a function of time and physical or empirical parameters, for a different type of soils. Each of these models is suitable to certain conditions. The parameters feed these models have uncertainties. These uncertainties become important depending on the sensitivity (accuracy) of them to the rate of infiltration. The sensitivity of the parameters involved in the Horton, Philip and Kostiakov equations were compared, using typical physical or empirical parameters for soil under consideration. This was done in conformity with the finding of Khasraei, *et al.* (2021). Sensitivity analysis in table 4.3 was used to determinate how "sensitive" the predictions of a model is to change in the values of the parameters involved. The sensitivity analysis permits studying the uncertainties or incomplete knowledge that are associated and

the relative importance of them (Pathmanathan, *et al.* 2019). Some of these parameters are very difficult to be measured or calculated. In these cases, the sensitivity analysis allows determining the level of parameters' accuracy necessaries to make the model valid and useful.

Table 4.3 also shows the constant representing the rate of decrease in the infiltration rate is the most sensitive parameter for short times, followed by the initial infiltration capacity. The final capacity is more sensitive for long times. Therefore, f_o and β sensitivities decrease increasing time and fc sensitivity increases increasing time. This result is in conformity with the study by Khasraei, *et al*. (2021). It shows that Philip's equation is not very sensitive to changes in C_a (Philip constant that depends soil property), being even less at short times. Nevertheless, it is very sensitive to changes in S, especially in short times.

Table 4.3: A description of the sensitivities of parameters for each equation and their trends over time

MODELS	STUDY LOCATIONS	Equation (fb)	Constant	Base value I	II	III	IV	V
Horton	Undeveloped land	fb=fc +(fo -fc)e^-bt	b, fo, fc	3, 44.88, 12.06	3,46.89,14.16	3, 42.88, 10.26	3, 40.88, 8.35	3, 43.89, 13.16
	Farm Land	fb=fc +(fo -fc)e^-bt	b, fo, fc	3, 75.75, 26.05	3,73.76,27.25	3, 76.76, 27.26	3, 74.76, 25.36	3, 75.75, 24.05
	Garden	fb=fc +(fo -fc)e^-bt	b, fo, fc	3, 20.77, 7.87	3, 21.97,7.77	3, 19.87, 6.97	3, 22.67, 8.123,	3, 18.87, 6.47
	Grazing Land	fb=fc +(fo -fc)e^-bt	b, fo, fc	3, 25.98, 10.23	3, 23.98,7.23	3, 26.88, 10.12	3, 24.78, 8.22	3, 25.88, 9.23
	Paved Compound	fb=fc +(fo -fc)e^-bt	b, fo, fc	3, 25.98, 10.23	3, 23.98 7.23	3, 26.88, 10.12	3, 24.78, 8.22	3, 25.88, 9.23
	Paved Road Side	fb=fc +(fo -fc)e^-bt	b, fo, fc	3, 22.02, 9.14	3, 20.02,7.14	3, 23.06, 8.19	3, 22.79, 9.29	3, 17.79,7.29
Philip	Undeveloped	fb = S/2t^-1/2 + Ca	Ca	6.54	9.19	4.49	2.75	8.61
	Farm Land	fb = S/2t^-1/2 + Ca	Ca	16.56	18.34	19.71	17.85	15.23
	Garden	fb = S/2t^-1/2 + Ca	Ca	7.87	8.61	6.93	7.95	6.08
	Grazing Land	fb = S/2t^-1/2 + Ca	Ca	3.83	2.02	5.43	2.84	4.83
	Paved Compound	fb = S/2t^-1/2 + Ca	Ca	9.04	5.06	9.98	7.38	9.99
	Paved Road Side	fb = S/2t^-1/2 + Ca	Ca	7.71	5.86	6.36	7.82	6.45
Kostiakov	Undeveloped	fb = at^-b	a, b	15.87, 0.65	18.34, 0.68	13.87, 0.62	11.83, 0.57	11.83, 0.57
	Farm Land	fb = at^-b	a, b	32.32, 0.71	33.03, 0.74	33.77, 0.73	31.93, 0.71	30.54, 0.69
	Garden	fb = at^-b	a, b	10.00, 0.75	10.21, 0.73	9.04, 0.73	10.56, 0.72	8.38, 0.72
	Grazing Land	fb = at^-b	a, b	5.92, 0.65	3.77, 0.50	7.14, 0.67	4.87, 0.59	6.88, 0.69
	Paved Compound	fb = at^-b	a, b	12.64, 0.75	9.58, 0.67	12.85, 0.74	10.79, 0.70	11.91, 0.74
	Paved Road Side	fb = at^-b	a, b	10.76, 0.79	8.78, 0.75	10.07, 0.74	11.01, 0.79	8.87, 0.77

4.5 Performance Analysis of the Infiltration Models

A series of graphics illustrating the time history of the prediction of infiltration rate is showed in order to describe how accurate the predictions are related to changes in specifics parameters involved in the models.

4.5.1 Horton sensitivity analysis

The Horton Equation shows greatest sensitivity to the parameters f_c, f_o and β as can be seen in Figures 4.0 to 4.14 by the highest condition numbers for that parameter. It shows that the infiltration rate's sensitivity to change in fc increases over time. It shows the time history of the prediction of infiltration rate using the Horton`s equation. The parameters used to calculate the infiltration rate sensitivity on Horton`s equation was the initial infiltration capacity, the final capacity and the constant representing the rate of decrease in the infiltration rate. The Horton infiltration rate's sensitivity to change in f_o decreases over time, opposite to the trend followed for the f_c parameter. This is in conformity with the work of Estefania (2015) for infiltration sensitivity analysis.

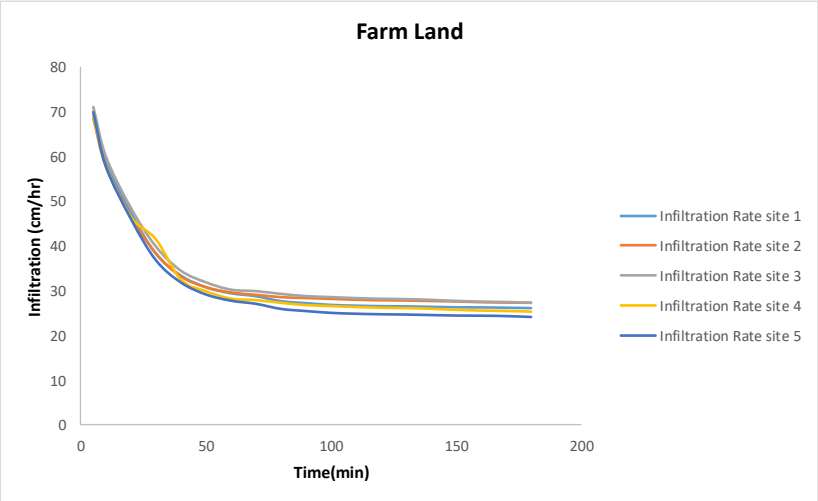

Figure 4.10: Farm Land infiltration rate sensitivity to f_o, f_c, and β

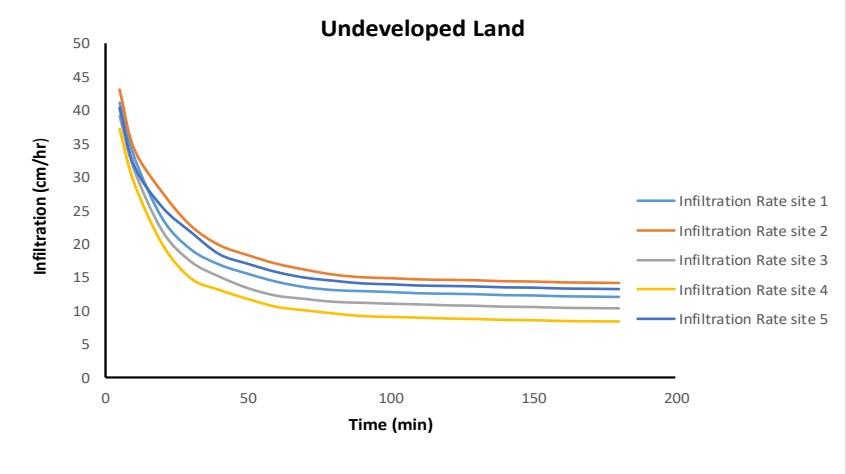

Figure 4.11: Undeveloped Land infiltration rate sensitivity to f_o, f_c, and β

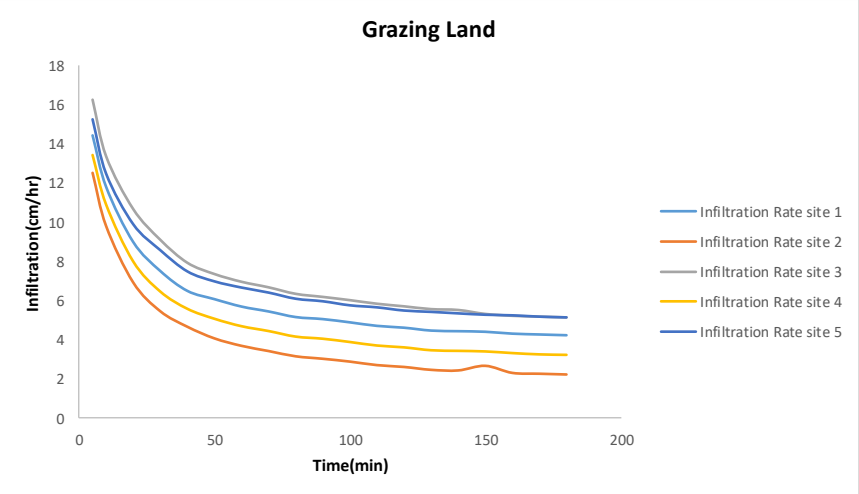

Figure 4.12: Grazing Land infiltration rate sensitivity to f_o, f_c, and β

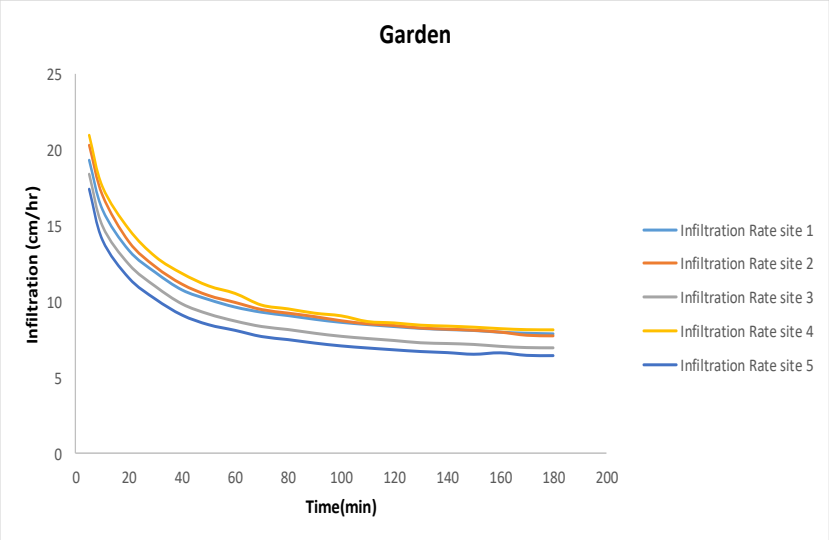

Figure 4.13: Garden infiltration rate sensitivity to f_o, f_c, and β

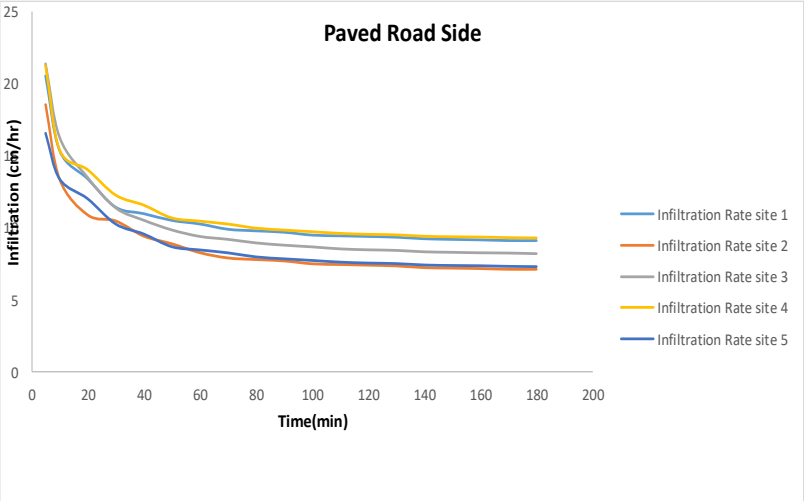

Figure 4.14: Paved road side infiltration rate sensitivity to f_o, f_c, and β

The Figures 4.10 to 4.14 above illustrates the prediction of infiltration rate at increasing time varying the initial infiltration capacity which means that infiltration rate increases increasing the initial infiltration capacity. It also demonstrates the prediction of

infiltration rate at increasing time varying the final capacity. The various figures demonstrate the prediction of infiltration rate at increasing time varying the constant representing the rate of decrease in the infiltration rate, and it illustrates that infiltration rate decreases increasing the constant representing the rate of decrease in the infiltration rate.

4.6 Philip Sensitivity Analysis

It shows the time history of the prediction of infiltration rate using Philip`s equation. The parameters used to calculate the infiltration rate sensitivity on Philip`s equation was the constant rate of infiltration and the soil sorptivity as showed in Figures 4.15 to 4.20. The Philip equation shows much greater sensitivity to changes in sorptivity by the considerably larger condition numbers for that parameter. It also shows an initially high sensitivity of infiltration rate to change in sorptivity decreases over time.

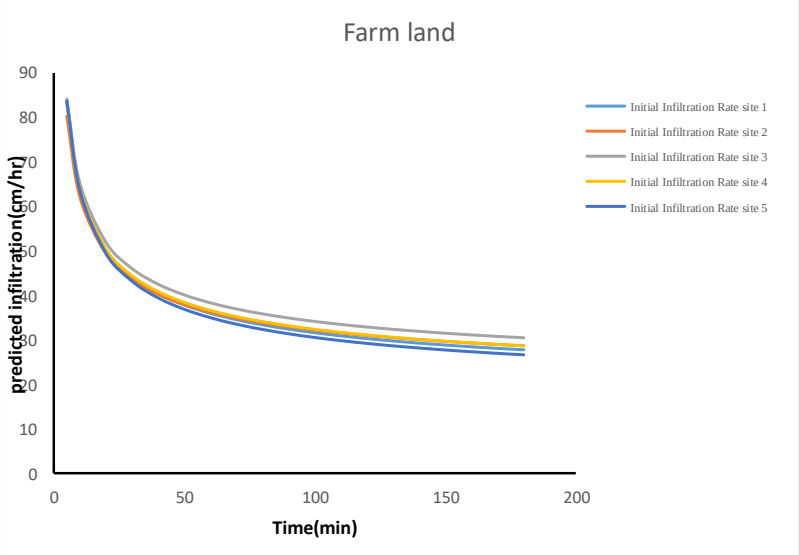

Figure 4.15: Farm Land infiltration rate shows Philip Infiltration Sensitivity to Changes in the Value of Parameter C_a

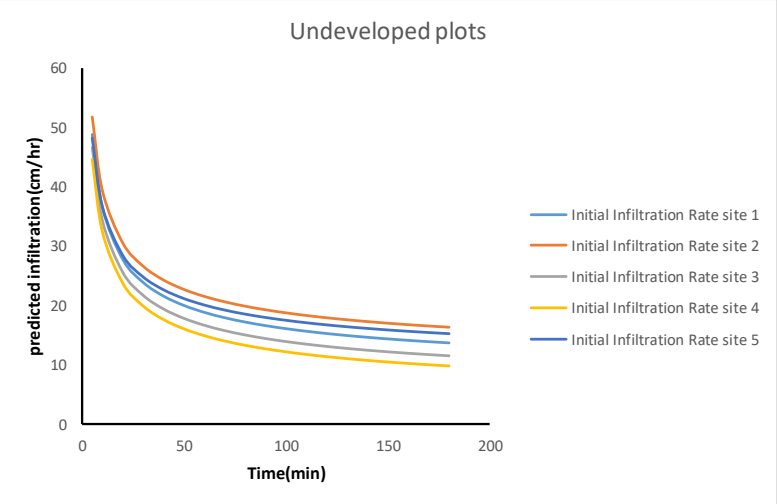

Figure 4.16: Undeveloped Land infiltration rate shows Philip Infiltration Sensitivity to Changes in the value of Parameter C_a

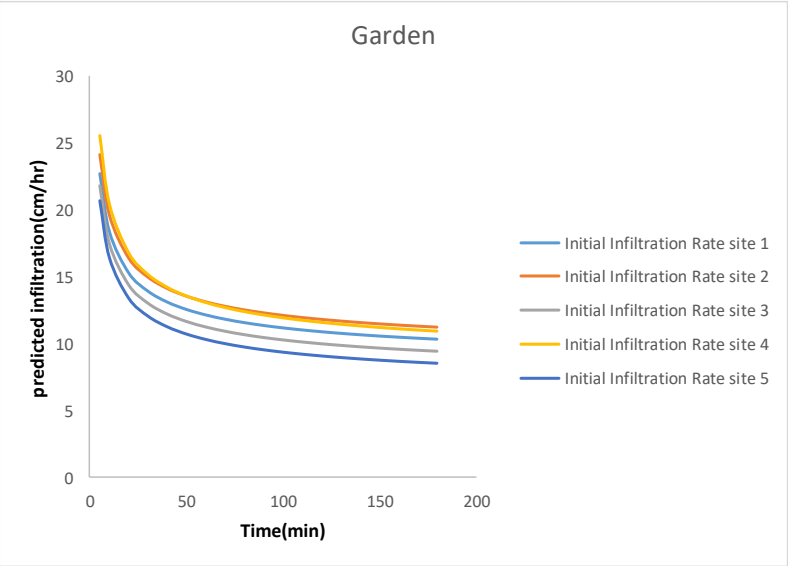

Figure 4.17: Garden infiltration rate shows Philip Infiltration Sensitivity to Changes in the value of Parameter C_a

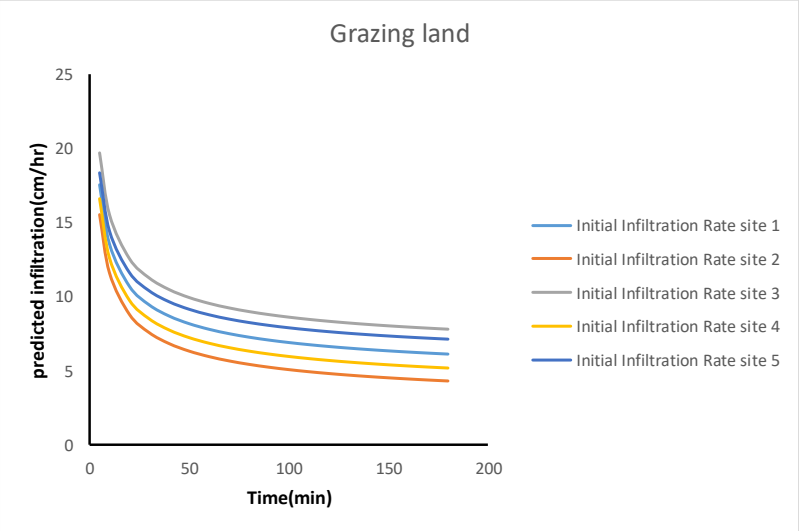

Figure 4.18: Grazing land infiltration rate shows Philip Infiltration Sensitivity to Changes in the value of Parameter C_a

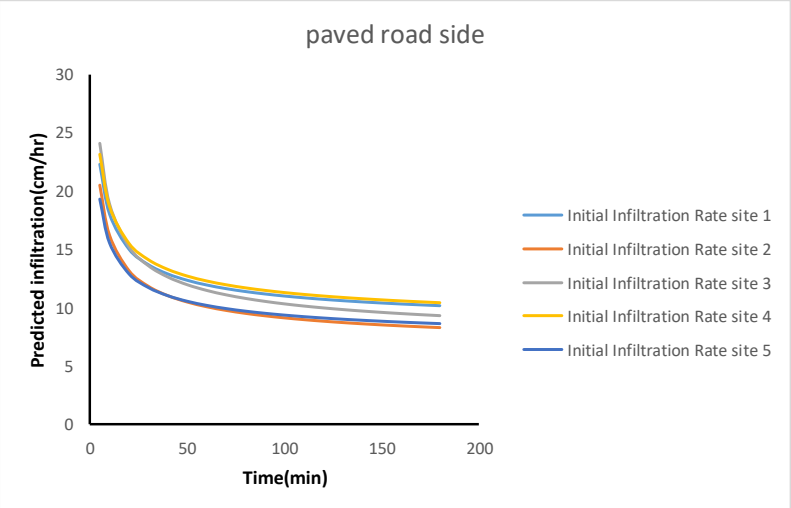

Figure 4.19: Paved road side infiltration rate shows Philip Infiltration Sensitivity to Changes in the value of Parameter C_a

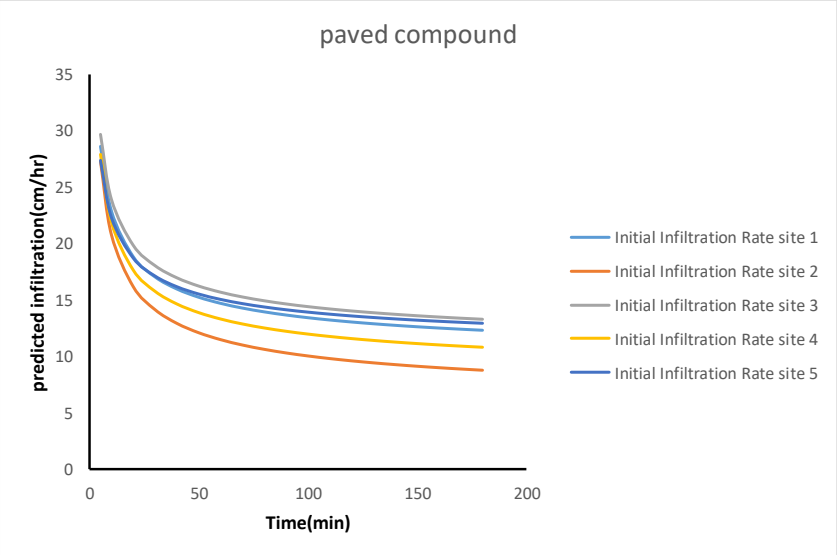

Figure 4.20: Paved Compound infiltration rate shows Philip Infiltration Sensitivity to Changes in the value of Parameter C_a

Figures 4.15 to 4.20 illustrates the prediction of infiltration rate at increasing time varying the constant rate of infiltration. This shows that infiltration rate increases increasing the constant rate of infiltration. It also demonstrates the prediction of infiltration rate at increasing time varying the soil sorptivity, and it illustrated that infiltration rate increases increasing the soil sorptivity.

4.7 Kostiakov Sensitivity Analysis

The Kostiakov infiltration rate is directly proportional to the parameter (a). Therefore, has condition number equal to 1 for all changes in constant a. The parameters used to calculate the infiltration rate sensitivity on Kostiakov`s equation were the empirical constants “a and b”. The infiltration rate has a more complex relationship with the parameter α which is shown in Figure 4.21 to 4.25. It illustrates the prediction of infiltration rate at increasing time varying the empirical constant a. This implies that infiltration rate increases increasing the empirical constant a. It demonstrates the

prediction of infiltration rate at increasing time varying the empirical constant b, and the implication is that infiltration rate decreases with increasing empirical constant b.

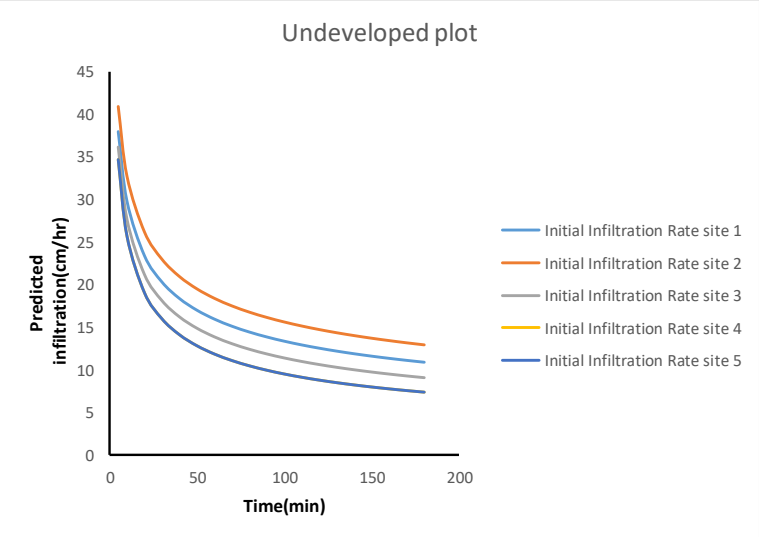

Figure 4.21: Undeveloped land infiltration rate shows Kostiakov Infiltration Sensitivity to the Change in value of the Parameter b

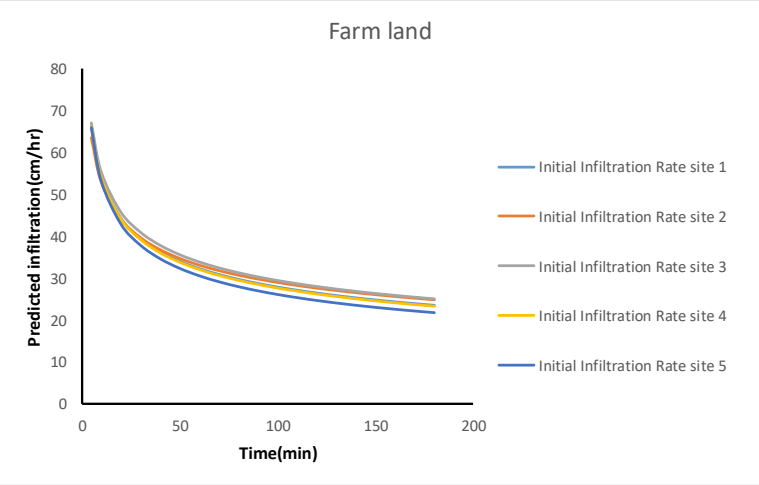

Figure 4.22: Farm land infiltration rate shows Kostiakov Infiltration Sensitivity to the Change in Value of the Parameter b

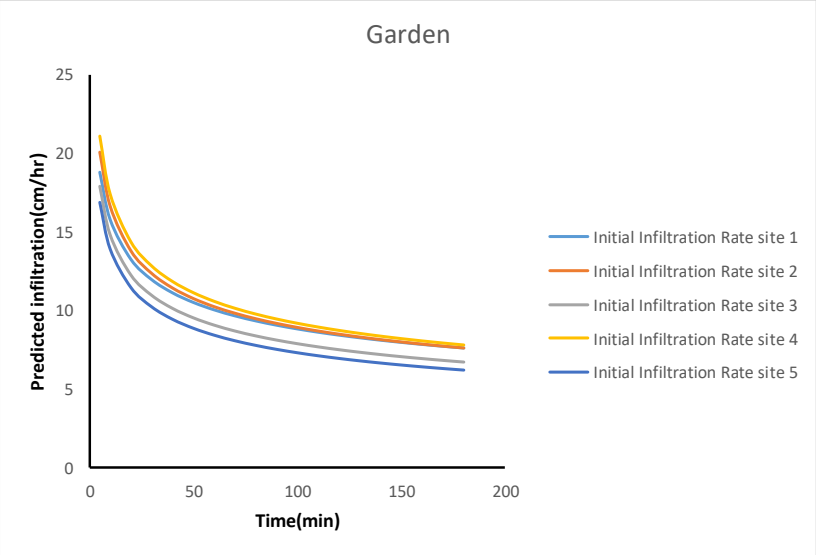

Figure 4.23: Garden infiltration rate shows Kostiakov Infiltration Sensitivity to the Change in value of the Parameter b

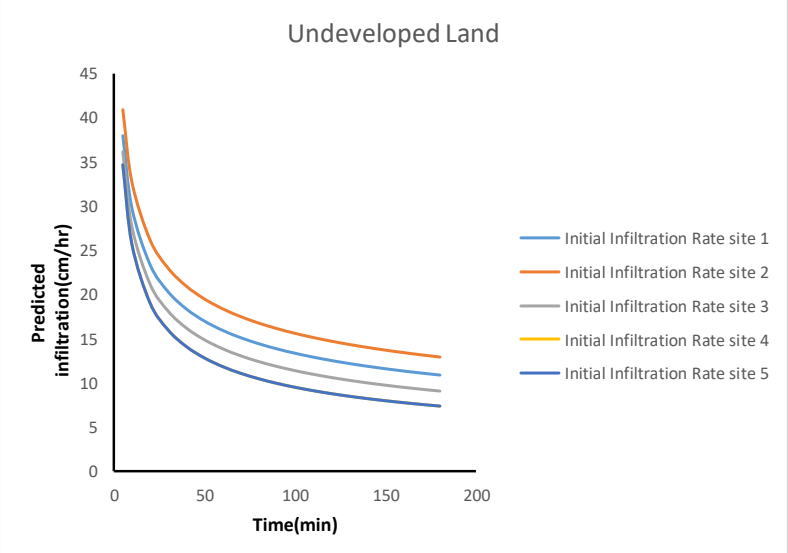

Figure 4.24: Undeveloped land infiltration rate shows Kostiakov Infiltration Sensitivity to the Change in value of the Parameter b

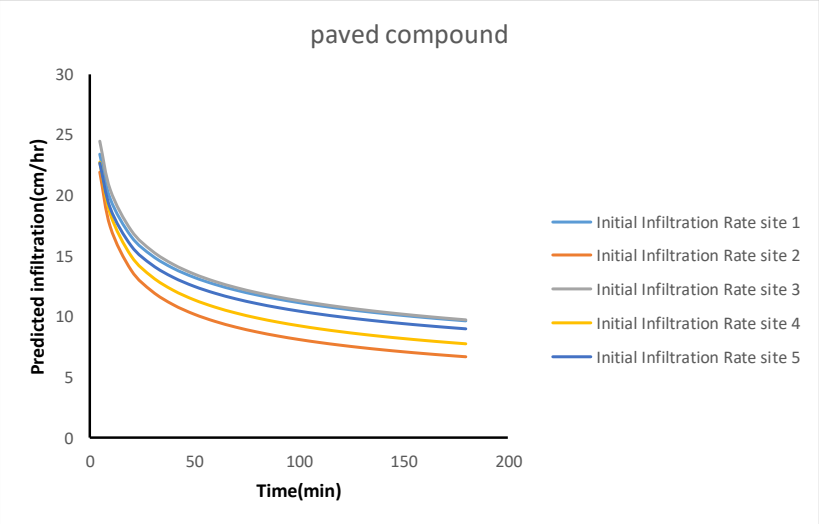

Figure 4.25: Paved Compound infiltration rate shows Kostiakov Infiltration Sensitivity to the change in value of the Parameter α

4.8 Evaluation of Equations

The Philip model with the least Root Mean Square Error (RMSE) value of 2.73 most closely predicted the measured infiltration. Kostiakov and Horton models provided less accurate estimates of the measured infiltration with least RMSE values of 7.13 and 7.00, respectively. This result is in conformity with the work of Faloye *et al*. (2021). The higher final constant infiltration rate for the earlier rainfall simulation that was used to obtain the parameter values for the simulation of interest, resulted in the greater divergence of these models from the values calculated for the observed runoff data. These results demonstrate the lack of flexibility in the Horton and Kostiakov models and hence, the need to be cautious when using one plot to calibrate another, since the plots must be very similar in order for the predictions made from the infiltration data from the first plot to accurately predict infiltration on the second. This is not any different from the findings of Turner (2006) for Popular Hill site study area where he discovered that Green- Ampt (GA) and Philip equations are the more versatile equations,

since they were applicable both in situations where rainfall rate was insufficient and sufficient and they do not rely on earlier infiltration data which may have been obtained under different field conditions. Figure 4.26 (a-k) showed the model predicted infiltration rates plotted versus the observed infiltration rates to obtain R^2 values.

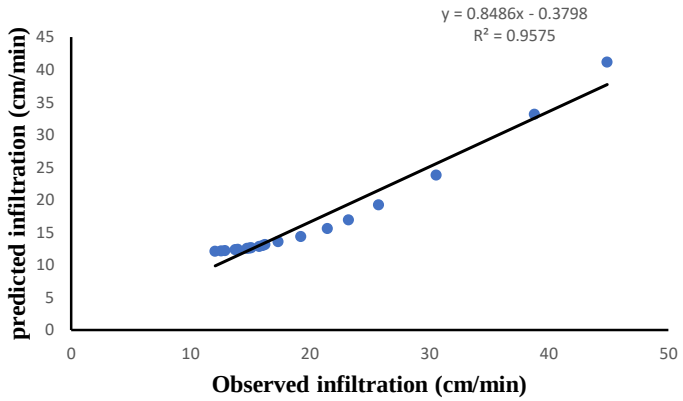

Figure 4.26a: Horton scattered plot for undeveloped land

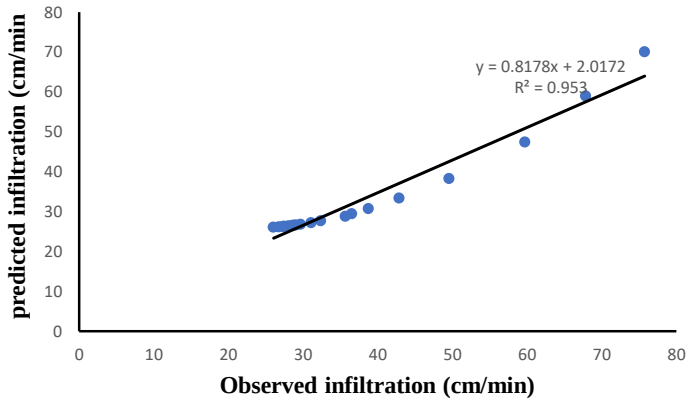

Figure 4.26b: Horton scattered plot for Farm land

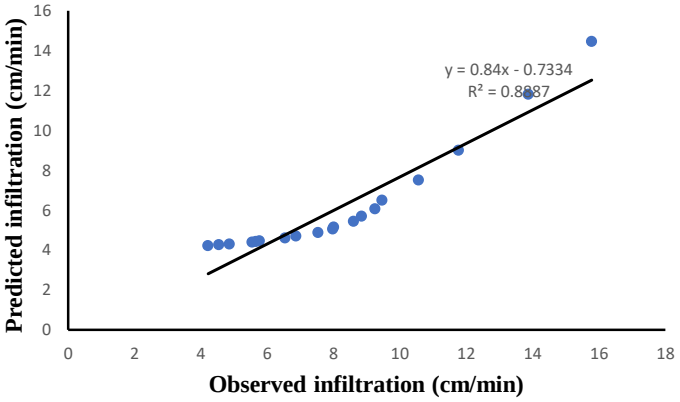

Figure 4.26c: Horton scattered plot for Grazing Land

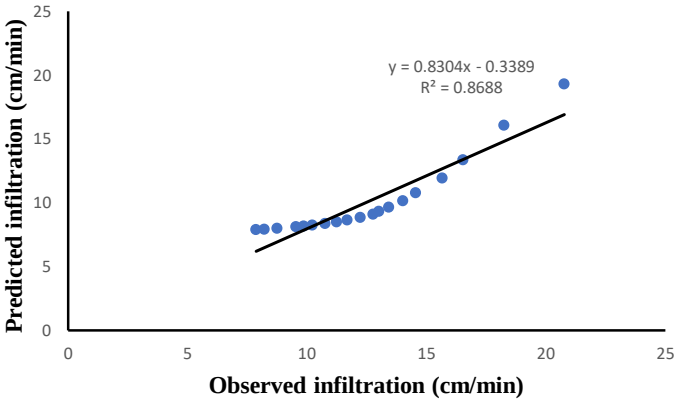

Figure 4.26d: Horton scattered plot for Garden

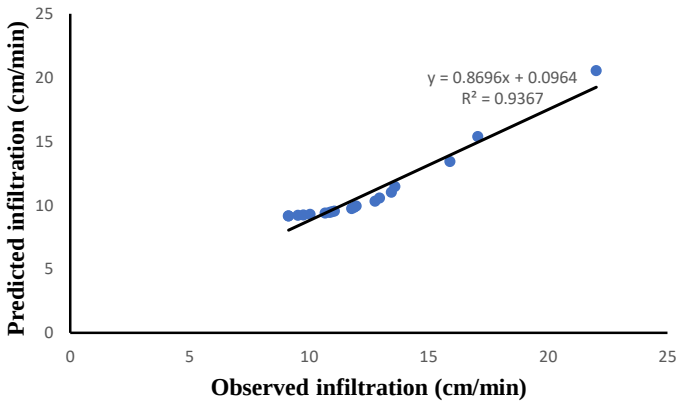

Figure 4.26e: Horton scattered plot for paved road side

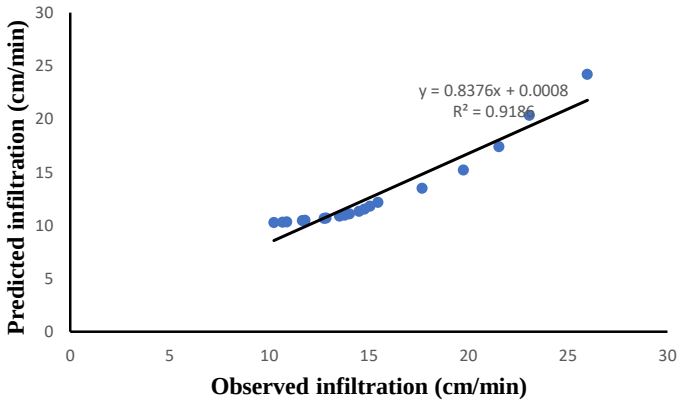

Figure 4.26f: Horton scattered plot for Farm land

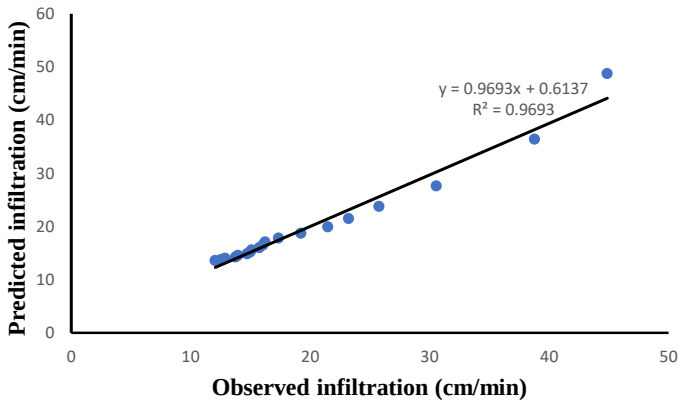

Figure 4.26g: Philip equation scattered plot for Undeveloped Land

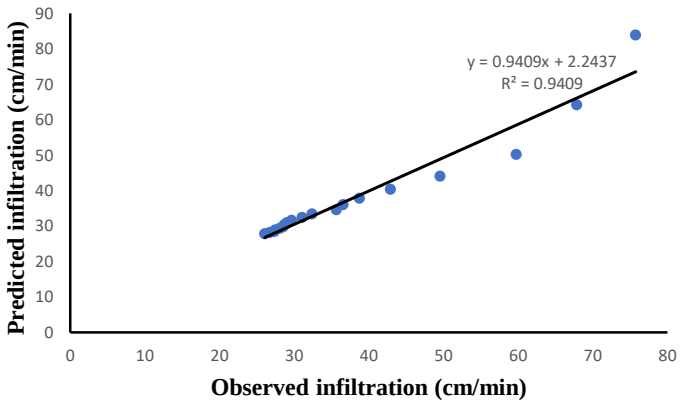

Figure 4.26h: Philip equation scattered plot for Farm Land

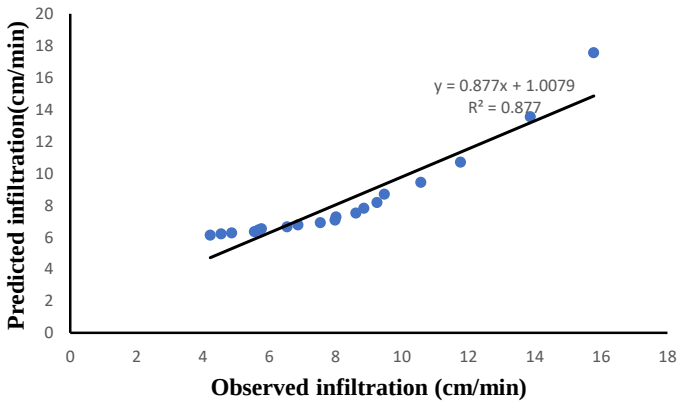

Figure 4.26i: Philip equation scattered plot for Grazing Land

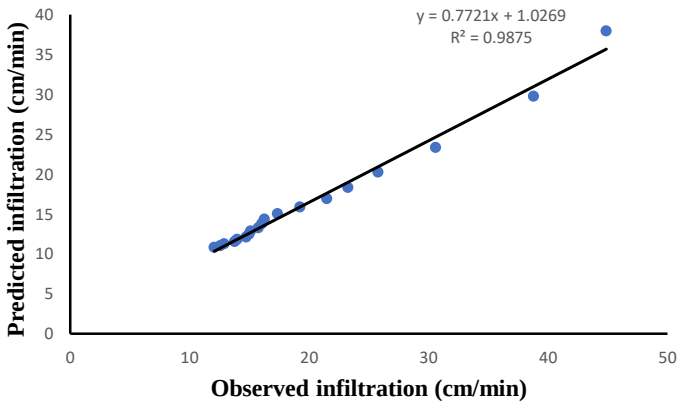

Figure 4.26j: Kostiakov equation scattered plot for Undeveloped Land

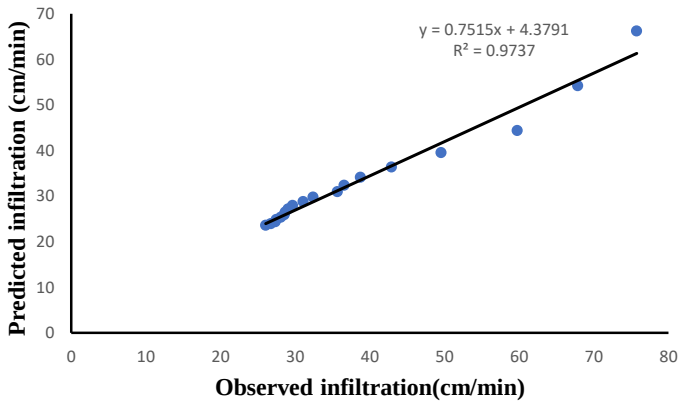

Figure 4.26k: Kostiakov equation scattered plot for Farm Land

The scattered plots above showed the predictive or correlational relationship between the variables. The observed infiltration is the independent variables while predicted infiltration is the dependent variables. The added trend line indicates the mathematically best fit to the data. This also provides additional signal as to how strong the relationship between the two variables is, and to determine the presence of outlier points.

According to table 4.4, the R^2 values indicate the degree to which data variations (i.e., the difference between the observed data and predicted data) are explained by each model. RMSE shows the amount of divergence of the model values from the observed values. If the model curve closely parallels the observation curve coefficient of determination (R^2) will be close to 1, but the RMSE may not be very low. A model that has a low RMSE will also have a high R^2, but it may not be as high an R^2 as a model with a higher RMSE, but that is more parallel, diverging by about the same amount from all observed values. Horton has a high R^2, but is off, probably because of the value for fc, the final constant infiltration rate that was obtained from an adjacent site. Kostiakov, although having the highest RMSE still

has a high R^2 as well. This result was in conformity with findings by Turner (2006) for Poplar Hill and Upper Marlboro site for comparison of infiltration equations Maryland.

Table 4.4: Shows model goodness of fit for all three (3) models including RMSE and R^2 values.

Models	Study locations	R^2					X^2					RMSE					P-value
		I	II	III	IV	V	I	II	III	IV	V	I	II	III	IV	V	
Horton	Undeveloped land	0.96	0.94	0.96	0.96	0.94	17.03	19.31	17.35	21.28	18.22	14.83	16.45	14.05	14.33	15.53	0.00
	Farm Land	0.95	0.96	0.96	0.95	0.95	19.22	14.42	22.24	24.98	24.00	21.37	19.31	25.08	25.57	24.18	0.58
	Garden	0.87	0.84	0.87	0.84	0.88	14.66	23.31	16.21	19.08	13.79	10.80	13.86	10.75	12.31	9.52	0.17
	Grazing Land	0.89	0.89	0.85	0.89	0.88	16.93	26.34	23.15	20.47	14.93	8.91	8.86	11.37	8.88	9.01	0.00
	Paved Compound	0.92	0.93	0.91	0.90	0.87	11.39	12.57	17.96	18.18	23.14	10.80	9.75	14.00	12.46	15.06	0.03
	Paved Road Side	0.94	0.92	0.94	0.93	0.91	5.13	7.31	7.35	5.72	6.96	6.60	7.00	7.69	6.99	6.91	0.09
Philip	Undeveloped land	0.97	0.93	0.97	0.97	0.93	1.72	4.03	1.69	1.89	3.64	5.19	8.44	4.69	4.81	7.30	0.00
	Farm Land	0.94	0.95	0.94	0.91	0.95	4.52	3.22	3.82	6.70	4.43	10.96	8.24	9.08	11.27	10.68	0.60
	Garden	0.84	0.81	0.84	0.78	0.86	2.81	3.75	3.17	5.38	2.78	5.07	5.72	5.20	7.65	4.70	0.05
	Grazing Land	0.88	0.88	0.81	0.88	0.86	2.82	4.03	4.20	3.32	2.73	4.15	4.10	5.33	4.20	4.34	0.00
	Paved Compound	0.89	0.88	0.88	0.86	0.84	2.29	3.68	2.63	3.99	3.16	4.68	5.30	5.10	6.46	5.89	0.01
	Paved Road Side	0.96	0.92	0.96	0.94	0.88	0.62	1.39	0.79	0.94	1.63	2.33	2.97	2.73	2.98	3.61	0.14
Kostiakov	Undeveloped land	0.99	0.97	0.98	0.98	0.95	15.48	17.42	16.09	19.10	119.74	15.37	16.80	14.64	14.91	37.23	0.00
	Farm Land	0.97	0.97	0.97	0.95	0.97	18.54	15.45	21.97	26.24	22.97	22.07	20.04	25.75	26.24	24.91	0.57
	Garden	0.91	0.88	0.90	0.86	0.92	13.56	22.31	15.12	18.33	12.70	10.84	13.89	10.79	12.33	9.57	0.17
	Grazing Land	0.92	0.88	0.86	0.90	0.92	15.83	25.89	22.34	19.56	13.85	8.97	8.86	11.39	8.92	9.06	0.00
	Paved Compound	0.95	0.93	0.94	0.92	0.90	10.47	12.52	16.93	17.08	22.04	10.91	9.90	14.09	12.54	15.12	0.03
	Paved Road Side	0.98	0.96	0.99	0.97	0.95	4.63	6.61	6.34	5.15	6.24	6.73	7.13	7.83	7.12	6.97	0.09

CHAPTER FIVE

5.0 CONCLUSION AND RECOMMENDATIONS

5.1 Conclusion

Based on the results obtained, the following conclusions were drawn

That Philip equation was a better predictor of the rate of infiltration of water into the soils for the various locations. The R^2 values of Philip equation when compared with others was relatively high which indicated its' high relevance in the area of soil-water relationship for the various study locations. The RMSE values further enhanced the applicability of Philip equation for the study area as it shows the amount of divergence of the modelled values from the observed values.

Urban compacted soils have low infiltration rate and high runoff. This is due to the fact that the soil infiltration rate decreased with an increase in the bulk density and with a reduction in the soil organic matter content and non-capillary porosity.

Philip equation analysis shows much greater sensitivity to changes in sorptivity by the considerably larger condition numbers compare to Horton and kostiakov equations analysis. While Horton equation shows greatest sensitivity to the infiltration parameters f_c, $f_{o,}$ and β.

5.2 Recommendations

Thus, resulting from the conclusions drawn, the following recommendations are provided namely: -

1. Philip models perform best and it is more versatile equation, since it can perform better both in situations where rainfall rate was insufficient and sufficient and it does not rely earlier infiltration data which may have been obtained under different field conditions.

2. Philip equation is also recommended to be applicable in an area with dry soil conditions and sandy soils with high saturated hydraulic conductivity values for effective and accurate prediction of infiltration.
3. For the purposes of determining potential infiltration rates, soils could be classified as either compacted or non-compacted. This classification of the compaction of a soil could have a significant effect on hydrological modeling.

5.3 Contribution to Knowledge

The thesis evaluated the Effect of Different Land-use on infiltration rate within Minna, Niger State. Six different locations (Undeveloped Land, Farm Land, Grazing Land, Gardened Land, Paved Compound and Paved Road Side) were considered.

The result revealed that there was high variations in the final infiltration rate for the six locations due to different vegetation patterns and degree of compaction.

The soil properties of the six different land-use scenarios considered were also analyzed and it was discovered that they were sandy-loam, loamy soil, clay-loam, silt-loam and sandy-clay for undeveloped land, farm land, gardened land, grazing land, paved compound and paved road side respectively.

In addition, three infiltration models (Horton, Kostiakov and Philip) were employed to predict the measured infiltration rate for future references, it was discovered from the result that for Minna metropolitan, Philip model is most suitable for infiltration prediction with the least error values (RMSE) of 0.79 and with highest coefficient of determination (R^2) of 97.

Therefore, these findings can provide useful information to Minna Urban planners on how to maximize urban water volume so as to minimize runoff and reduce instantaneous flooding.

REFERENCES

Abebe, A.T., Tanaka, T. & Yamazaki, M. (1989). Soil compaction by multiple passes of a rigid wheel relevant for optimization of traffic. *Journal of Terramechanics*, 26: 139-48.

Abo-Abda, B. & Hussain, A.G. (1990). Impact of machinery compaction and tillage system on infiltration rate of sandy soils. *Arid Soil Research and Rehabilitation* 4: 157-62.

Abu-Hamdeh, N. H. (2003a). Compaction and subsoiling effects on corn growth and soil bulk density. *Soil Science Society of America Journal* 67 (12) 13-19.

Abubakar, U. B. (2019). *Mapping Groundwater Potentials of Bosso and Environs, Niger State, Nigeria* (Doctoral Dissertation).

Adachi, T. (1990). Effect of rice soil puddling on water percolation. *Transaction of International Congress Soil Science 14th*, Kyoto, Japan (14) 6-51.

Agrawal, R.P. (1991). Water and nutrient management in sandy soils by compaction. *Soil and Tillage Research* (19) 121-130.

Alaoui, A. & Diserens, E. (2018). Mapping soil compaction–A review. *Current opinion in environmental science & health*, (5) 60-66.

Amreeta, C., Vinay, B., Patra, K. C. & Mrunmayee, M. S. (2015). Standard Test for Determination of Infiltration Rate of Soil Using Double Ring Infiltrometer

Alakkuku, L., Weisskopf, P., Chamen, W.C.T., Tijink, F.G.J., Van der Linden, J.P., Pires, S., Sommer, C. & Spoor, G. (2003). Prevention strategies for field traffic-induced subsoil compaction: a review Part 1. Machine-soil interactions. *Soil and Tillage Research*, 73(1), 45-60.

Alaoui, A., Lipiec, J. & Gerke, H.H. (2011). A review of the changes in the soil pore system due to soil deformation: a hydrodynamic perspective. *Soil and Tillage Research*, 115–116: 1–15. doi: 10.1016/j.still.2011.06.002

Alig, R.J., Kline, J.D. & Lichtenstein, M. (2004). Urbanization on the US landscape: looking ahead in the 21st century. Landscape and Urban Planning, (69) 219–234.

Ankeny, M.D., Kaspar, T.C. & Horton, R. (1990). Characterization of tillage and traffic effect on unconfined infiltration measurements. *Soil Science Society of America Journal*, 54(8), 37-40.

Arthur-Hartranft, S.T., Carlson, T.N. & Clarke, K.C. (2003). Satellite and ground-based microclimate and hydrologic analyses coupled with a regional urban growth model. Remote Sens. Environ., 86, 385-400.

Arvidsson, J. (2001). Subsoil compaction caused by heavy sugarbeet harvesters in Southern Sweden. I. Soil physical properties and crop yield in six field experiments. *Soil and Tillage Research*, 60:67-78.

ASTM D3383 (2009). Standard test method for infiltration rate of soils in field using double–ring infiltrometer, West Conshohocken, PA. 2009.

Assouline, S., Tavares-Filho, J. & Tessier, D. (1997). Effect of compaction on soil physical and hydraulic properties: experimental results and modeling. *Soil Science Society of America Journal*, 61(3), 90-98.

Badalıkova, B. & Hruby, J. (2006). Influence of minimum soil tillage on development of soil structure. In: Soil management for sustainability. *Advances in Geoecology*, 38(4), 30-35.

Bagarello, V. & Sgroi, A, (2004). Using the single-ring infiltrometer method to detect temporal changes in surface soil field– saturated hydraulic conductivity. *Soil and Tillage Research*, 76(1), 13–24. doi: 10.1016/j.still.2003.08.008

Bai, X., Jia, X., Jia, Y. & Hu, W. (2020). Modeling long-term soil water dynamics in response to land-use change in a semi-arid area. *Journal of Hydrology*, *585*, 124824.

Balbuena, R.H., Terminiello, A.M., Claverie, J.A., Casado, J.P. & Marlats, R. (2000). Soil compaction by forestry harvester operation. Evolution of physical properties. *Revista Brasileira de Engenharia Agrícola e Ambiental*, 4(4), 53-59.

Beven, K. J. & Germann, P. (2013). Macropores and water flow in soils revisited, Water Resour. Res., 49, 3071–3092, doi:10.1002/wrcr.20156, 2013.

Beven, K. (2021). The era of infiltration. *Hydrology and Earth System Sciences*, *25*(2), 851-866.

Bevin, K. J. (2004). Robert E. Horton's perceptual model of infiltration processes. Hydrological Processes 18: 3447-3460.

Bimbraw, A. S. (2021). *Established and Emerging Practices for Soil and Crop Productivity*. CRC Press.

Blake, W.H., Walsh, R.P.D., Barnsley, M.J., Palmer, G., Dyrynda, P. & James, J.G. (2003). Heavy metal concentrations during storm events in a rehabilitated industrialized catchment. Hydrol. Processes, 17, 1923-1939.

Blake, G. J. (1968). Infiltration at the Puketurua experimental basin. *Journal of Hydrology*, 7(1), 38-46.

Blanco-Canqui, H., Gantzer, C.J., Anderson, S.H. & Alberts, E.E. (2004). Tillage and crop influences on soil properties for an Epiaqualf. *Soil Science Society of America Journal*, 68(5), 67-76.

Bormann, H. & Klaassen, K. (2008). Seasonal and land use dependent variability of soil hydraulic and soil hydrological properties of two Northern German soils. *Geoderma*, 145(3–4), 295–302.doi: 10.1016/j.geoderma.2008.03.017

Bouwer, H. (1966). Rapid field measurement of air-entry value and hydraulic conductivity of soil as significant parameters in flow system analysis. *Water Resources Research*, 2:729-738.

Bouwer, H. (1969). Infiltration of water into nonuniform soil. *Journal of Irrigation and Drainage Division, ASCE* 95(IR4): 451-462.

Bouwer, H. (1976). Infiltration into increasingly permeable soils. *Journal of Irrigation and Drainage Division, ASCE* 102(IR1): 127-136.

Brown, S. & Cotton, M. (2011). Changes in soil properties and carbon content following compost application: results of on-farm sampling. *Compost Science & Utilization*, 19(1), 87–96. doi:10.1080/1065657x.2011.10736983

Bruand, A. & Cousin, I. (1995). Variation of textural porosity of a clay-loam soil during compaction. *European Journal of Soil Science*, 46(3), 377–385. doi: 10.1111/j.1365-2389.1995. tb01334.x

Brun, S.E. & Band, L. E. (2000). Simulating runoff behaviour in an urbanizing watershed Computers. Environ. Urban Systems, 24, 5-22.

Burns, D., Vitvar, T., McDonnell, J., Hassett, J., Duncan, J. & Kendall, C. (2005). Effects of suburban development on runoff generation in the Croton River basin, New York, USA. *Journal of Hydrology,* 311,266-281.

Canarache, A., Trandafirescu, T., Colibas, I., Colibas, M., Horobeanu I, Patru, V. & Simota, H. (1984). Effect of induced compaction by wheel traffic on soil physical properties and yield of maize in Romania. *Soil and Tillage Research,* 4: 199-213.

Canillas, E.C. & Salokhe, V.M. (2001). Regression analysis of some factors influencing soil compaction. *Soil and Tillage Research,* 61 167-78.

Celik, I., Gunal, H. & Budak, M. (2010). Effects of long-term organic and mineral fertilizers on bulk density and penetration resistance in semi-arid Mediterranean soil conditions. *Geoderma*, 160(2), 236–243. doi: 10.1016/j.geoderma.2010. 09.028

Chaudhary, M.R., Khera, R. & Singh, C.J. (1991). Tillage and irrigation effects on root growth, soil water depletion and yield of wheat following rice. *Journal of Agricultural Science Cambridge*, 116: 9-16.

Chai, Y., Wang, E. & Chen, X, (2007). Water storage capacity and permeability of undisturbed typical black soil. *Journal of Soil and Water Conservation*, 21(3): 158–161.

Chamen, T., Alakukku, L., Pires, S., Sommer, C., Spoor, G., Tijink, F. & Weisskoff, P. (2003). Prevention strategies for field traffic induced subsoil compaction: a review. Part 2. Equipment and field practices. *Soil and Tillage Research,* 73(1), 61-74.

Chen, S., Wang, X. & Lu, F. (2012). Research on forest microbial community function variations in urban and suburban forests. *Chinese Journal of Soil Science,* 43(3), 614–620.

Chen, Y. J., Day, S. D. & Wick, A. F. (2013). Changes in soil carbon pools and microbial biomass from urban land development and subsequent post-development soil rehabilitation. *Soil Biology and Biochemistry*, 66: 38–44. doi: 10.1016/j.soilbio. 2013.06.022

Chen, Y. J., Day, S. D. & Wick, A. F. (2014). Influence of urban land development and subsequent soil rehabilitation on soil aggregates, carbon, and hydraulic conductivity. *Science of the Total Environment*, 494–495: 329–336. doi: 10.1016/j.scitotenv.2014.06.099

Chow, V. T., Maidment, D. R. & Mays, L. W. (1988). *Applied Hydrology*. New York, NY.: McGraw-Hill.

Cheng, Y., Yang, W., Zhan, H., Jiang, Q., Shi, M. & Wang, Y. (2020). On the Origin of Deep Soil Water Infiltration in the Arid Sandy Region of China. *Water*, 12(9), 24-29.

Clark, M. P., Bierkens, M. F., Samaniego, L., Woods, R. A., Uijlenhoet, R., Bennett, K. E., ... & Peters-Lidard, C. D. (2017). The evolution of process-based hydrologic models: historical challenges and the collective quest for physical realism. *Hydrology and Earth System Sciences*, 21(7), 3427-3440.

Clemmens, A. J. (1983). Infiltration equations for border irrigation models. P266-274. In: *Advances in infiltration. Proc. Nat. Conf. on Advances in Infiltration.* Dec. 12-13. Chicago, Ill. ASAE Pub. 11-83. St. Joseph, Mo.

Corbetts, C., Wahlb, M., Portera, E., Edwards, D. & Moised, C. (1997). Nonpoint source runoff modeling. A comparison of a forested watershed and an urban watershed on the South Carolina coast. *Journal of Experimental Marine Biology and Ecology*, 213, 133-149.

Criddle, D. W., Davis, S., Pair, C. H. & Shockley, D. G. (1956). Methods for evaluating irrigation systems. USDA Soil Conservation Service. U. S. Government Printing Office.

da Rosa, D. P., Reichert, J. M., Lima, E. M. & da Rosa, V. T. (2021). Chiselling and wheeling on sandy loam long-term no-tillage soil: compressibility and load bearing capacity. *Soil Research*.

Da Silva, A.P., Kay, B.D. & Perfect, E. (1997). Management versus inherent soil properties effects on bulk density and relative compaction. *Soil and Tillage Research* 44 81-93.

DeJong-Hughes, J.M., Swan, J.B., Moncrief, J.F. Voorhees, W.B. (2001). Soil Compaction: Causes, Effects and Control (Revision). University of Minnesota Extension Service BU-3115-E.

Dezső, J., Czigány, S., Nagy, G., Pirkhoffer, E., Słowik, M. & Lóczy, D. (2019). Monitoring soil moisture dynamics in multilayered Fluvisols. *Bulletin of Geography. Physical Geography Series*, 16(1), 131-146.

de Moraes, M. T., Debiasi, H., Franchini, J. C., Mastroberti, A. A., Levien, R., Leitner, D. & Schnepf, A. (2020). Soil compaction impacts soybean root growth in an Oxisol from subtropical Brazil. *Soil and Tillage Research*, *200*, 104611.

dos Santos, K. F., Barbosa, F. T., Bertol, I., de Souza Werner, R., Wolschick, N. H. & Mota, J. M. (2018). Study of soil physical properties and water infiltration rates in different types of land use. *Semina: Ciências Agrárias*, 39(1), 87-98.

Duh, J., Shandas, V., Chang, H. & George, L. (2008). Rates of urbanisation and the resiliency of air and water quality. Science of the total environment, 400:238-256.

Easton, Z.M., Gérard-Marchant, P., Walter, M.T., Petrovic, A.M. & Steenhuis, T.S. (2007b). Hydrologic assessment of an urban variable source. Water Resources Research, 43, 3432-3450.

Ehounou, J. N., Kouamé, B., Tahi, M. G., Kassin, E. K., Kotaix, J. A. A., Dékoula, C. S., ... & Soro, N. (2019). Global Warming Influence on Major Seasonal and Intra-seasonal Rainfall Indicators for Sustainable Cocoa Production in West-central Côte d'Ivoire. *Journal of Experimental Agriculture International*, 1-10.

Ellen, R. T. (2006). Comparison of Infiltration Equations and their Field Validation with Rainfall Simulation

Ellies, S. A., Smith, R.R., JoseDorner, F.J. & Proschle, T.A. (2000). Effect of moisture and transit frequency on stress distribution on different soils. *Agro Suro* 28:60-68.

Fang, X., Tang, Z. & Tian, D. T. (2012). Distribution and ecological risk assessment of 7 heavy metals in urban forest soils in Changsha city. Acta Ecologica Sinica, 32(23): 7596– 7606.

Faloye, O. T., Ajayi, A. E., Zink, A., Fleige, H., Dörner, J. & Horn, R. (2021). Effective stress and pore water dynamics in unsaturated soils: Influence of soil compaction history and soil properties. *Soil and Tillage Research*, *211*, 104997.

Fernández-Pato, J., Gracia, J. L. & García-Navarro, P. (2018). A fractional-order infiltration model to improve the simulation of rainfall/runoff in combination with a 2D shallow water model. *Journal of Hydroinformatics*, 20(4), 898-916.

Fischer, C., Roscher, C. & Jensen, B. (2014). How do earthworms, soil texture and plant composition affect infiltration along an experimental plant diversity gradient in grassland? *PLoS One*, 9(2): e98987. doi: 10.1371/journal.pone.0098987

Flowers, M.D. & Lal, R. (1998). Axle load and tillage effects on soil physical properties and soybean grain yield on a mollic ochraqualf in northwest Ohio. *Soil and Tillage Research*, 48: 21-35.

Fok, Y. S. (1986). Derivation of Lewis-Kostiakov intake equation, *Journal of Irrigation and Drainage Engineering*. 112: 164-171.

Frere, M. H., Onstad, C. A. & Holtan, H. N. (1975). ACTMO, an agricultural chemical transport model. ARS-H-3, USDA-ARS.

Gardner, W. (1986). Water Content p. 493-544. In A. Klute (ed.) *Methods of Soil Analysis. Part 1*, 2nd ed. Soil Science Society of America, Madison, WI.

Galli, A., Peruzzi, C., Beltrame, L., Cislaghi, A. & Masseroni, D. (2021). Evaluating the infiltration capacity of degraded vs. rehabilitated urban greenspaces: lessons learnt from a real-world Italian case study. *Science of the Total Environment*, 14(7), 6-12.

Gavrić, S., Leonhardt, G., Marsalek, J. & Viklander, M. (2019). Processes improving urban stormwater quality in grass swales and filter strips: A review of research findings. *Science of the Total Environment*, 669, 431-447.

Ghildyal, B.P. & Satyanarayana, T. (1965). Effect of compaction on the physical properties of four different soils in India. *Journal of the Indian Society of Soil Science*, 13(1), 49-55.

Gifford, G. F. (1976). Applicability of some infiltration formulae to rangeland infiltrometer data. *J. Hydrol.* 28: 1-11.

Gifford, G. F. (1978). Use of infiltration coefficients as an aid in defining hydrologic impacts of range management schemes. *J. Range Manage.* 31: 115-117.

Ghosh, R. K. (1980). Modeling infiltration. *Soil Science* 130: 297-302.

Ghosh, R. K. (1983). A note on the infiltration equation. *Soil Science* 136: 333-338.

Ghosh, R. K. (1985). A note on Lewis-Kostiakov's infiltration equation. *Soil Science*, 139: 193-196.

Glass, B. (2019). *Examining Hydrogeological Processes in Freezing Soils using Remote Geophysical and Numerical Techniques* (Master's thesis, University of Waterloo).

Gliński, J. & Lipiec, J. (2018). *Soil physical conditions and plant roots*. CRC press.

Goonetilleke, A., Thomas, E., Ginn, S. & Gilbert, D. (2005). Understanding the role of land use in urban stormwater quality management. *Journal of Environmental Management*, 74, 31–42.

Green, W. H. & Ampt, G. (1911). Studies of Soil Physics, Part 1. The flow of air and water through soils. *Journal of Agricultural Science* 4: 1-24.

Greenland, D.J. (1977). Soil damage by intensive arable cultivation: temporary or permanent? *Philosophical Transactions of the Royal Society B: Biological Sciences* 281: 193-208.

Guerif, J. (1984). The influence of water-content gradient and structure anisotropy on soil compressibility. *Journal of Agricultural Engineering Research*, 29(3), 67-74.

Gurmu, G. (2019). Soil organic matter and its role in soil health and crop productivity improvement. *Forest Ecology and Management*, *7*(7), 475-483.

Haase D. (2009). Effects of urbanisation on the water balance – A long-term trajectory. Environ. Impact. Asses. Rev., doi: 10.1016/j.eiar.2009.01.002.

Haggard, B.E., Moore, P.A. & Brye, K.R. (2005). Effect of Slope on Runoff from a Small Variable-Slope Box. *Journal of Environmental Hydrology*. 13: paper 25. Available: HTTP://HYDROWEB.COM.

Hamza, M.A. & Anderson, W.K. (2003). Responses of soil properties and grain yields to deep ripping and gypsum application in a compacted loamy sand soil contrasted with a sandy clay loam soil in Western Australia. *Australian Journal of Agricultural Research*, 54(2), 73-82.

Harris, W.L. (1971). The soil compaction process. In: *Compaction of Agricultural Soils*, edited by Barnes KK *et al.,* American Society Agricultural Engineers, St. Joseph, MI 9–44.

Haverkamp, R., Rendon, L. & Vachaud, G. (1987). Infiltration equations and their applicability for predictive use. P. 142-152. In Yu- SI Fok (ed.) *Infiltration Development and Application.* Honolulu, Hawaii.

Hettiaratchi DRP (1987). A critical state soil mechanics model for agricultural soils. *Soil and Use Management* 3 94-105.

Hillel, D. (1998). *Environmental Soil Physics*. Academic Press. San Diego, CA.

Hillel, D. and W. R. Gardner. (1970). Transient infiltration into crust topped profiles. *Soil Science* 109: 69-76.

Hillel, D. (1971). *Soil and Water: Physical Principals and Processes*. Academic Press, New York, NY.

Hilhorst, M. A., Dirksen, C., Kampers, F. W. H. & Feddes, R. A. (2001). Dielectric relaxation of bound water versus soil matric pressure. *Soil Science Society of America Journal*. 65: 311-314

Holtan, (1961). A concept for infiltration estimates in watershed engineering. USDA, Agricultural Research Service Publication 41-51.

Holtan, H. N. & Creitz, N. R. (1967). Influence of soils, vegetation and geomorphology on elements of the flood hydrograph. Symposium on floods and their computation, Leningrad, Russia.

Holtan, H. N. & Lopez, N. C. (1971). USDAHL-70 model of watershed hydrology. *USDA-ARS Tech. Bull. No. 1435*, Agricultural Research Station, Beltsville, Md..

Horn, R. F. (2021). Soils in agricultural engineering: Effect of land, use management systems on mechanical soil processes. *Hydrogeology, chemical weathering, and soil formation*, 187-199.

Horn, R., Trautner, H., Wuttke, M. & Baumgart, T. (1994). Soil physical properties related to soil structure. *Soil and Tillage Research*, 35 23-36.

Horton, R., Ankeny, M. D. & Allmaras, A. A. (1994). Effects of compaction on soil hydraulic properties.Pp.479-500.In: Soil compaction in crop production. Elsevier Science B.V., Amsterdam, Netherlands

Horton, R. E. (1939). Analysis of runoff plot experiments with varying infiltration capacity. *Transactions of the American Geophysicists.* Union, Part IV: 693-694.

Horton, R. E. (1940). An approach towards a physical interpretation of infiltration capacity. *Soil Science Society of America*, 5: 399-417.

Huang, H., Cheng, S., Wen, J. & Lee, J. (2008). Effect of growing watershed imperviousness on hydrograph parameters and peak discharge. Hydrological Processes, 22, 2075–2085.

Huang, X., Huang, X. & Chen, C. (2009). The characteristic, mechanism and regulation of urban spatial expansion of Changchun. *Areal Research and Development*, 28(5), 68–72.

Huat, B. B. K., Ali, F. H. J. & Low, T. H. (2006). Water infiltration characteristics of unsaturated soil slope and its effect on suction and stability *Geotechnical and Geological Engineering*, 24: 1293–1306.

Huggins, L. F. & Monke, E. J. (1966). The mathematical simulation of the hydrology of small watersheds. Lafayette, Indiana: TR1 Perdue Water Resources Research Center

Ibrahim, J. S. (2021). *Impact of Tungan-Kawo Irrigation Scheme on Rice Production in Wushishi Local Government Area, Niger State, Nigeria* (Doctoral Dissertation).

Ishaq, M., Ibrahim, M., Hassan, A., Saeed, M. & Lal, R. (2001). Subsoil compaction effects on crops in Punjab, Pakistan: II. Root growth and nutrient uptake of wheat and sorghum. *Soil and Tillage Research* 60 153-61.

Israelson, O. W. & Hansen, V. E. (1967). *Irrigation Principles and Practices*. 198 – 200. John Wiley, New Delhi.

Jat, H. S., Datta, A., Sharma, P. C., Kumar, V., Yadav, A. K., Choudhary, M., ... & McDonald, A. (2018). Assessing soil properties and nutrient availability under conservation agriculture practices in a reclaimed sodic soil in cereal-based systems of North-West India. *Archives of Agronomy and Soil Science*, *64*(4), 531-545.

Jia, H. F., Yao, H. R. & Tang, Y. (2015). LID-BMPs planning for urban runoff control and the case study in China. *Journal of Environmental Management*, 149: 65–76. doi: 10.1016/j. jenvman.2014.10.00

Jim, C. Y. (1998a). Physical and chemical properties of a Hong Kong roadside soil in relation to urban tree growth. *Urban Ecosystems*, 2(2–3), 171–181. doi: 10.1023/A:1009585700191

Jim, C Y. (1998c). Soil characteristics and management in an urban park in Hong Kong. Environmental Management, 22(5), 683–695. doi: 10.1007/s002679900139

Jury, W. A., Gardener, W. R. & Gardener, W. H. (1991). *Soil Physics*, 5th edn. Wiley, New York, NY.

Kayombo, B., Lal, R., Mrema, G.C. & Jensen, H.E. (1991). Characterizing compaction effects on soil properties and crop growth in southern Nigeria. *Soil and Tillage Research*, 21 325-45.

Khasraei, A., Abyaneh, H. Z., Jovzi, M., & Albaji, M. (2021). Determining the accuracy of different water infiltration models in lands under wheat and bean cultivation. *Journal of Hydrology*, *603*, 127122.

Kirby, J.M. & Kirchhoff, G. (1990). The compaction process and factors affecting soil compatibility. In: *Proceedings of Queensland Department of Primary Industries*, edited by Hunter MN, Paull CJ and Smith GD, Soil Compaction Workshop, Toowoomba, Australia 28–31.

Kohnke, N. (1968). *Soil Physics*. New York: McGraw-Hill.

Kostiakov, A. N. (1932). On the dynamics of the coefficient of water-percolation in soils and on the necessity for studying it from a dynamic point of view for purposes of amelioration. *Transactions Congress International Society for Soil Science*, 6th, Moscow, Part A: 17-21.

Kozak, J. A. & Ahuja, L. R. (2005). Scaling of infiltration and redistribution of water across soil textural classes. *Soil Science Society of America Journal*, 69: 816-827.

Kumar, S., Anderson, S. H. & Udawatta, R. P. (2012). Water infiltration influenced by agroforestry and grass buffers for a grazed pasture system. *Agroforestry Systems*, 84(3), 325–335. doi: 10.1007/s10457-011-9474-4

Kumar, V., Jain, M., Rani, V., Kumar, A. & Kumar, S. (2018). A Review of Soil Compaction-Concerns, Causes and Alleviation. *Int. J. Plant Soil Sci*, *22*, 1-9.

Larson, W.E., Eynard, A., Hadas, A. & Lipiec, J. (1994). Control and avoidance of soil compaction in practice. In: *Soil Compaction in Crop Production*, edited by Soane BD and van Ouwerkerk C (Elsevier Science) Amsterdam, 597-625.

Larson, W.E., Gupta, S.C. & Useche, R.A. (1980). Compression of agricultural soils from eight soil orders. *Soil Science Society of America Journal*, 44: 450-57.

Lasanta, T., Arnáez, J. & Nadal-Romero, E. (2019). Soil degradation, restoration and management in abandoned and afforested lands. In *Advances in Chemical Pollution, Environmental Management and Protection*, 4:71-117).

Le Van, P. & Morel-Seytoux, H. J. (1972). Effect of soil air movement and compressibility on infiltration rates. Soil Science Society of America Proceedings 36: 237-241.

Lebert, M., Burger, N. & Horn, R. (1998). Effect of dynamic and static loading on compaction of structured soils. In: *Mechanics and Related Processes in Structured Agricultural Soils*, edited by Larson WE, Blake GR, Allmaras RP, Voorhees WB and Gupta S. NATO ASI Series, Applied Science (Kluwer Academic Publisher) Dordrecht, Netherland 73-80.

Li, J., He, B. & Mei, X. (2013). Effects of different planting modes on the soil permeability of sloping farmlands in purple soil area. *Chinese Journal of Applied Ecology*, 24(3), 725–731.

Li, J., Yue, X. & Sun, K. (2015). Investigation and improvement of soil fertility of road greenbelt in Tianjin city. Urban Environment & Urban Ecology, 28(6), 17–21.

Lipiec, J. & Stepniewski, W. (1995). Effects of soil compaction and tillage systems on uptake and losses of nutrients. *Soil and Tillage Research*, 35, 37-52.

Liu, S. X. (2001). Spatial variation of soil moisture in China: geostatistical characterization. *Journal of the Meteorological Society of Japan*, 79 (1B), 555–574.

Liu, D., Chen, S. & Zhang, J. (2007). Soil infiltration characteristics under main vegetation types in Anji County of Zhejiang Province. *Chinese Journal of Applied Ecology*, 18(3), 493–498.

Liu, M., Bárdossy, A., Li, J. & Jiang, Y. (2012). Physically-based modeling of topographic effects on spatial evapotranspiration and soil moisture patterns through radiation and wind, Hydrol. Earth Syst. Sci., 16:357–373, doi:10.5194/hess-16-357-2012, 2012.

Llorens, P. & Domingo, F. (2007). Rainfall partitioning by vegetation under Mediterranean conditions. A review of studies in Europe. *Journal of Hydrology*, 335: 37-54.

Lu, S. G., Wang, H. Y. & Bai, S. Q. (2009). Heavy metal contents and magnetic susceptibility of soils along an urban-rural gradient in rapidly growing city of eastern China. Environmental Monitoring & Assessment, 155(1–4), 91–101. doi: 10.1007/s10661- 008-0420-5

Luo, Y., Zhang, J. M., Zhou, Z., Shen, Z. J., Chong, L. & Victor, C. (2021). Investigation and prediction of water infiltration process in cracked soils based on a full-scale model test. *Geoderma*, *400*, 115111.

Lv, H. L., Wang, W. J. & He, X. Y. (2016). Quantifying tree and soil carbon stocks in a temperate urban forest in Northeast China. Forests, 7(9), 200. doi: 10.3390/f7090200

Maleksaeedi, E. & Nuth, M. (2020). Evaluation of capillary water retention effects on the development of the suction stress characteristic curve. *Canadian Geotechnical Journal*, 57(10), 1439-1452.

Marsili, A., Servadio, P., Pagliai, M. & Vignozzi, N. (1998). Changes of some physical properties of a clay soil following passage of rubber and metal-tracked tractors. *Soil and Tillage Research*, 49(1), 85-99.

Mbagwu, J. S. C. (1990). Mulch and tillage effects on water transmission characteristics of an Ultisol and maize grain yield in SE. Nigeria. *Pedologie*, 40: 155-168.

Mbagwu, J. S. C. (1993). Testing the goodness of fit of selected infiltration models on soils with different land use histories. International Centre for Theoretical Physics. Trieste, Italy.

Mbagwu, J.S.C. (1994). Soil physical properties influencing the fitting parameters in Philip and Kostiakov infiltration models. International Centre for Theoretical Physics. Trieste, Italy.

Meek, B D., Rechel, E A. & Carter, L M. (1989). Changes in infiltration under alfalfa as influenced by time and wheel traffic. *Soil Science Society of America Journal*, 53(1), 238–241. doi:10.2136/sssaj1989.03615995005300010042x

Messing, I., Iwald, J., Lindgren, D., Lindgren, K., Nguyen, L. & Hai, T. S. (2005). Using pore sizes as described in soil profile descriptions to estimate infiltration rate and saturated hydraulic conductivity. *Soil Use and Management*, 21: 376-277.

Mezencev, V. J. (1948). Theory of formation of the surface runoff. *Meteorologiae Hidrologia* 3:33-40.

Milesi, C., Elvidge, C D. & Nemani, R. R. (2003). Assessing the impact of urban land development on net primary productivity in the southeastern United States. *Remote Sensing of Environment*, 86(3): 401–410. doi: 10.1016/S0034-4257(03)00081-6

Mosaddeghi, M.R., Hajabbasi, M.A., Hemmat, A. & Afyuni, M. (2000). Soil compactibility as affected by soil moisture content and farmyard manure in central Iran. *Soil and Tillage Research* 55 87-97.

Musgrave, G.W. (1955). How much of the rain enters the soil? In *USDA Water Yearbook of Agriculture.* Washington, D.C., 151-159.

Mutonyi, J., & Muturi, P. (2021). What Do Data on Dry Bulk Density (BD) And Porosity (P) Tell About The Quality of Soils in the Mumias Sugar Zone, Western Kenya?.

Natarajan, P., Weiss, P. T. & Gulliver, J. S. (2020). Characterization of Runoff Quality from Paved Low-Volume Roads and Optimization of Treatment Methods.

Naeth, M. A. (1988). *The impact of grazing on litter and hydrology in mixed prairie and fescue grassland ecosystems of Alberta*. Ph.D. Thesis. University of Alberta, Edmonton, Canada.

Naeth, M.A., Chanasyk, D.S. & Bailey, A.W. (1991). Applicability of the Kostiakov equation to mixed prairie and fescue grasslands of Alberta. *Journal of Range Management*, 44(1), 18-21.

Niemczynowicz, J. (1999). Urban hydrology and water management – present and future challenges. Urban Water, 1, 1-14.

Novotny, V. & Olem, H. (1994). *Water Quality; Prevention, Identification, and Management of Diffuse Pollution.* New York, NY.: Van Nostrand Reinhold.

NRCS. Soil Quality Institute (2000). Urban Technical Note 2, as reported by Ocean County Soil Conservation District, Forked River, NJ. 2001.

Ogbuagu, A. E. (2019). *Characterization of Aquifers in Afikpo North Local Government Area, South Eastern Nigeria* (Doctoral dissertation, Federal University of Technology, Owerri).

Ohu, J.O., Folorunso, O.A. & Ekwue, E.I. (1993). Vehicular traffic effect on physical-properties of sandy loam soil profiles in a semiarid region of Nigeria. *Soil and Tillage Research*, 28:27-35.

Pataki, D E., Carreiro, M M. & Cherrier, J. (2011). Coupling biogeochemical cycles in urban environments: ecosystem services, green solutions, and misconceptions. Frontiers in Ecology and the Environment, 9(1), 27–36. doi: 10.1890/090220

Pan, Y., Chen, B. & Xiao, Y. (2008). Heavy metal pollution status and evaluation of urban forest soils in Guangzhou. Ecology and Environment, 17(1), 210–215.

Parveen, S. (2018). Field Evaluation of Infiltration Models

Patel, M.S. & Singh, N.T. (1981). Changes in bulk density and water intake rate of a coarse textured soil in relation to different levels of compaction. *Journal of the Indian Society of Soil Science*, 29 110-2.

Pathmanathan, P., Cordeiro, J. M., & Gray, R. A. (2019). Comprehensive uncertainty quantification and sensitivity analysis for cardiac action potential models. *Frontiers in physiology*, *10*, 721.

Pitt, R., Clark, S. & K (1994). Parmer. *Protection of Groundwater from Intentional and Nonintentional Stormwater Infiltration*. U.S. Environmental Protection Agency, EPA/600/SR-94/051. PB94-165354AS, Storm and Combined Sewer Program, Cincinnati, Ohio. 187 pgs. May 1994.

Pitt, R.E. & Lantrip, J. (2000). "Infiltration through Disturbed Urban Soils." *Journal of Water Management Modeling* R206-0I. doi: 10.14796/JWMM.R206-0l.

Pitt, R., Chen, S. E. & Clark, S. E. (2008). Compaction's impacts on urban storm-water infiltration. *Journal of Irrigation and Drainage Engineering*, 134(5), 652–658. doi: 10.1061/(ASCE)0733-9437(2008)134:5(652)

Philip, J. R. (1954). An infiltration equation with physical significance. *Soil Science* 77: 153-157.

Philip, J. R. (1957a). The theory of infiltration: 1. The infiltration equation and its solution. *Soil Sci.* 83, 345–357.

Poesen, J. W. A. (1984). The influence of slope angle on infiltration rate and Hortonian overland flow. Geomorphology, 2(49), 117-131.

Pouyat, R. V., Yesilonis, I. D. & Szlavecz, K. (2008). Response of forest soil properties to urbanization gradients in three metropolitan areas. Landscape Ecology, 23(10), 1187–1203. doi: 10.1007/s10980-008-9288-6

Qi, J., Lee, S., Zhang, X., Yang, Q., McCarty, G. W. & Moglen, G. E. (2020). Effects of surface runoff and infiltration partition methods on hydrological modeling: A comparison of four schemes in two watersheds in the Northeastern US. *Journal of Hydrology*, *581*, 124415.

Quiroga, A.R., Buschiazzo, D.E. & Peinemann, N. (1999). Soil compaction is related to management practices in the semi-arid Argentine pampas. *Soil and Tillage Research*, 52: 21-28.

Radcliffe, D. E. & Simunek, J. (2018). *Soil physics with HYDRUS: Modeling and applications*. CRC press.

Rabot, E., Wiesmeier, M., Schlüter, S. & Vogel, H. J. (2018). Soil structure as an indicator of soil functions: a review. *Geoderma*, *314*, 122-137.

Radford, B.J., Bridge, B.J., Davis, R.J., McGarry, D., Pillai, U.P., Rickman, J.F., Walsh, P.A. & Yule, D.F. (2000). Changes in the properties of Vertisol and responses of wheat after compaction with harvester traffic. *Soil and Tillage Research*, 54(1), 55-70.

Raper, R.L., Reeves, D.W. & Burt, E.C. (1998). Using in-row subsoiling to minimize soil compaction caused by traffic. *Journal of Cotton Science*, 2(1), 30-35.

Rawls, W. J., Ahuja, L. R., Brakensiek, D. L. & Shirmohammadi, A. (1993). Infiltration and soil water movement. In *Handbook of Hydrology*. McGraw-Hill, Inc.

Reichert, J.M., da Silva, V.R. & Reinert, D.J. (2004). Soil moisture, penetration resistance, and least limiting water range for three soil management systems and black beans yield. *Conserving Soil and Water for Society: Sharing Solutions* ISCO 2004 - 13th International Soil Conservation Organization Conference – Brisbane, Australia.

Richards, L. A. (1931). Capillary conduction through porous mediums. *Physics* 1: 313-318.

Richard, G., Cousin, I. & Sillon, J. F. (2001). Effect of compaction on the porosity of a silty soil: influence on unsaturated hydraulic properties. *European Journal of Soil Science*, 52(1), 49–58. doi: 10.1046/j.1365-2389.2001.00357.

Rizzon, M. M., Wagner, A. C., Godoy, V. B., Moreira, E. B. & Consoli, N. C. (2021). The Effect of Heavy Tamping on Structured Residual Clay Site. *Geotechnical and Geological Engineering*, 1-10.

Römkens, M. J. M., Baumhardt, R.L., Parlange, J. Y., Whisler, F. D. & Prasad, S. N. (1985). Effect of rainfall characteristics on seal hydraulic conductance. In Callebaut et al. (eds), *Proceedings of the Syposium on the assessment of Soil Surface Sealing and Crusting.* State University of Ghent, Belgium.

Robinson, D. A., Hopmans, J. W., Filipovic, V., van der Ploeg, M., Lebron, I., Jones, S. B., ... & Tuller, M. (2019). Global environmental changes impact soil hydraulic functions through biophysical feedbacks. *Global change biology*, *25*(6), 1895-1904.

Scharwies, J. D. & Dinneny, J. R. (2019). Water transport, perception, and response in plants. *Journal of plant research*, *132*(3), 311-324.

Sihag, P. & Singh, B. (2018). Field evaluation of infiltration models. *Техногенно-екологічна безпека*, (4), 3-12.

Sohn, W., Brody, S. D., Kim, J. H. & Li, M. H. (2020). How effective are drainage systems in mitigating flood losses?. *Cities*, *107*, 102917.

Shrestha, P., Hurley, S. E. & Wemple, B. C. (2018). Effects of different soil media, vegetation, and hydrologic treatments on nutrient and sediment removal in roadside bioretention systems. *Ecological Engineering*, *112*, 116-131.

Sahraei, S., Asadzadeh, M. & Unduche, F. (2020). Signature-based multi-modelling and multi-objective calibration of hydrologic models: Application in flood forecasting for Canadian Prairies. *Journal of Hydrology*, 588(12), 50-95.

Sprenger, M., Stumpp, C., Weiler, M., Aeschbach, W., Allen, S. T., Benettin, P., ... & Werner, C. (2019). The demographics of water: A review of water ages in the critical zone. *Reviews of Geophysics*, 57(3), 800-834.

Sileshi, R. K., Pitt, R. E. & Clark, S. E. (2017). Impacts of Soil Media Characteristics on Stormwater Biofiltration System Performance. *International Advanced Research Journal in Science, Engineering and Technology (IARJSET), ISO*, 3297, 2007.

Sivarajan, S., Maharlooei, M., Bajwa, S. G. & Nowatzki, J. (2018). Impact of soil compaction due to wheel traffic on corn and soybean growth, development and yield. *Soil and Tillage Research*, 175, 234-243.

Shah, A. N., Tanveer, M., Shahzad, B., Yang, G., Fahad, S., Ali, S., ... & Souliyanonh, B. (2017). Soil compaction effects on soil health and cropproductivity: an overview. *Environmental Science and Pollution Research*, *24*(11), 10056-10067.

Schwen, A., Ramirez, G.H., Smith, E.J., Sinton, S.M., Carrick, S., Clothier, B.E, Buchan, G.D. & Loiskandl, W. (2011). Hydraulic properties and the water-conducting porosity as affected by subsurface compaction using tension infiltrometers. *Soil Science Society of America Journal*, 75(8), 22-31.

Semadeni-Davies, A., Hernebring, C. & Svensson, G. (2008). The impacts of climate change and urbanisation on drainage in Helsingborg, Sweden: Combined sewer system. Journal of Hydrology, 350, 100–113.

Sharma, P.K. & Bhagat, R.M. (1993). Puddling and compaction effects on water permeability of texturally different soils. *Journal of the Indian Society of Soil Science*, 41:1-6.

Sharma, P.K. & De Datta, S.K. (1986). Physical properties and processes of puddle rice soils. *Advances in Soil Science*, 5(1), 39-78.

Shaw, R. K., Wilson, M. A. & Reinhardt, L. (2010). Geochemistry of artifactual coarse fragment types from selected New York City soils. In: 19th World Congress of Soil Science. Soil Solutions for a Changing World. Brisbane, Australia: DVD.

Sidhu, S.S. (1980). *Water retention, transmission and other physical properties of soils under paddy in Punjab*. M.Sc. Thesis, Punjab Agricultural University, Ludhiana.

Singh M (1986). *Effect of traffic sole density on soil-water relations and water uptake under different soil moisture regimes*. Ph.D Dissertation, Punjab Agricultural University, Ludhiana.

Singh NT, Patel MS, Singh, R. & Vig, A.C. (1980). Effect of soil compaction on yield and water use efficiency of rice in a highly permeable soil. *Agronomy Journal* 72 499-502.

Singh, J. (1961). Note on measurement of puddling. Paper presented at Agricultural Implement Seminar at Bombay, ICAR, New Delhi.

Silva, V,R., Reinert, D.J. & Reichert, J.M. (2000). Soil strength as affected by combine wheel traffic and two soil tillage systems. *Ciencia Rural* 30 795-801.

Skaggs, R. W. & Khaleel, R. (1982). Chapter 4: Infiltration. In *Hydrology of Small Watersheds*. St Joseph, Mich.: ASAE.

Smiles, D. E. & Knight, J. H. (1976). A note on the use of the Philip infiltration equation. *Australian Journal of Soil Research,* 14:103-108.

Sullivan, M., Warwick, J. J. & Tyler, S. W. (1996). Quantifying and delineating spatial variations of surface infiltration in a small watershed.

Sur, H.S. & Singh, N.T. (1972). Morphological and physical characteristics of soils of the pilot project, Patiala. *Journal Research Punjab Agricultural University*, 9:586-97.

Sur, H.S., Prihar, S.S. & Jalota, S.K. (1980). Effect of rice-wheat and maize-wheat rotation on water transmission and wheat root development in a sandy loam soil of Punjab, India. *Soil and Tillage Research*, 1(3), 61-71.

Tang, B., Jiao, J., Yan, F. & Li, H. (2019). Variations in soil infiltration capacity after vegetation restoration in the hilly and gully regions of the Loess Plateau, China. *Journal of Soils and Sediments*, 19(3), 1456-1466.

Talsma, T. (1969). *In situ* measurement of sorptivity. *Australian Journal of Soil Research*, 7: 269-276

Tarawally, M.A., Medina, H., Frómeta, M.E. & Itza, A. (2004). Field compaction at different soil-water status: effects on pore size distribution and soil water characteristics of a Rhodic Ferralsol in Western Cuba. *Soil and Tillage Research,* 76 95-103.

Tisdall, J.M. & Adem, H.H. (1986). Effect of water content of soil and tillage on size-distribution of aggregates and infiltration. *Australian Journal Experimental Agriculture,* 26 193-95.

Turner, E. R. (2006). *Comparison of infiltration equations and their field validation with rainfall simulation* (Doctoral dissertation).

Tullberg, J.N. (1990). Why control field traffic. In: *Proceeding Queensland Department of Primary Industries, Soil Compaction Workshop,* edited by Hunter MN, Paull CJ and Smith GD, Toowoomba, Australia 28 13-25.

United Nations, (2012). World population prospects: The 2011 version. New York: United Nations Department of Economic and Social Affairs, Population Division

Varley, L., Rutherford, M. E., Zhang, L., & Pellegrino, A. (2020). The Mechanical Response of Wet Volcanic Sand to Impact Loading, Effects of Water Content and Initial Compaction. *Journal of Dynamic Behavior of Materials*, *6*(3), 358-372.

Venter, C., Mahendra, A. & Hidalgo, D. (2019). From mobility to access for all: Expanding urban transportation choices in the Global South. *World Resources Institute, Washington, DC*, 1-48.

Vereecken, H., Weihermüller, L., Assouline, S., Šimůnek, J., Verhoef, A., Herbst, M., ... & Xue, Y. (2019). Infiltration from the pedon to global grid scales: An overview and outlook for land surface modeling. *Vadose Zone Journal*, *18*(1), 1-53.

Verbist, K., Cornelis, W.M., Schiettecatte, W., Oltenfreiter, G., Van Meirvenne, M. & Gabriels, D. (2007). The influence of a compacted plow sole on saturation excess runoff. *Soil and Tillage Research* 96 292-302.

Wang, M., He, D., Shen, F., Huang, J., Zhang, R., Liu, W., ... & Zhou, Q. (2019). Effects of soil compaction on plant growth, nutrient absorption, and root respiration in soybean seedlings. *Environmental Science and Pollution Research*, *26*(22), 22835-22845.

Walker, W. (1998). SIRMOD - Surface Irrigation Modeling Software. Utah State University.

Wangeman, S. G., Kohl, R. A. & Molumeli, P. A. (2000). Infiltration and percolation influenced by antecedent soil water content and air entrapment. *American Society of Agricultural Engineers*, 43(6), 1517-1523.

Wei Junling, Jin Youqian, Gao Hongjian. (2012). Investigation on soil water infiltration in different urban green lands in Hefei City. *Chinese Agricultural Science Bulletin*, 28(25), 302–307.

Wheater, H. & Evans, E. (2009). Land use, water management and future flood risk. Land Use Policy, 26S, S251–S264.

Whisler, F.D. & Bouwer, H. (1970). Comparison of methods for calculating vertical drainage and infiltration for soils. *Journal of Hydrology*, 10(1), 1-19.

White, I. & Perroux, K. M. (1987). Use of sorptivity to determine field hydraulic properties. *Soil Science Society of America Journal*, 51:1093-1101.

White, M.D. & Greerbb, K.A. (2006). The effects of watershed urbanization on the stream hydrology and riparian vegetation of Los Penasquitos Creek, California, Landscape and Urban Planning. 74, 125–138.

Winzig, G. (2000). The concept of storm water infiltration. In: *First International Conference on Soils of Urban, Industrial, Traffic and Mining Areas*. Essen: Essen University Press, 427–433.

Willeke, G.E. (1966). Time in Urban Hydrology. *Journal of the Hydraulics Division Proceedings of the American Society of Civil Engineers.* pp. 13-29. January 1966.

Wu, G. L., Yang, Z. & Cui, Z. (2016). Mixed artificial grasslands with more roots improved mine soil infiltration capacity. *Journal of Hydrology*, 535: 54–60. doi: 10.1016/j.jhydrol. 2016.01.059

Xiao, Q. & McPherson, W.G. (2003). Rainfall interception by Santa Monica's municipal urban forest. Urban Ecosystems, 6, 291-302.

Xu, C. Y. 2003. Approximate infiltration models. Section 5.3 In Hydrologic Models. Uppsala University Department of Earth, Air and Water Sciences. Uppsala, Sweden.

Yang, J. & Zhang, G. (2008). Loss of soil water capacity in urban areas and it's impacts on environment. *Soils*, 40(6):992–996. (in Chinese)

Yang, J. L. & Zhang, G. L. (2011). Water infiltration in urban soils and its effects on the quantity and quality of runoff. *Journal of Soils and Sediments*, 11(5): 751–761. doi: 10.1007/s11368-011-0356-1

Yang, M., Zhang, Y. & Pan, X. (2020). Improving the Horton infiltration equation by considering soil moisture variation. *Journal of Hydrology*, *586*, 124864.

Yao, L., Chen, L. D. & Wei, W. (2015). Potential reduction in urban runoff by green spaces in Beijing: a scenario analysis. Urban Forestry & Urban Greening, 14(2): 300–308. doi: 10.1016/j. ufug.2015.02.014

Ying, C., Youpeng, X. & Yixing, Y. (2009). Impacts of land use change scenarios on storm-runoff generation in Xitiaoxi basin, China, Quaternary International, doi: 10.1016/j.quaint.2008.12.014

Zhai, C., Wang, W. J. & He, X. Y. (2017). Urbanization drives SOC accumulation, its temperature stability and turnover in forests, Northeastern China. *Forests*, 8(4): 130. doi: 10.3390/f8040130

Zhang, M. K., Wang, M. Q. & Liu, X. M. (2003). Characterization of soil quality under vegetable production along an urban-rural gradient. Pedosphere, 13(2): 173–180

Zhang, X.Y., Cruse, R.M., Sui, Y.Y. & Jhao, Z. (2006). Soil compaction induced by small tractor traffic in Northeast China. *Soil Science Society of America Journal* 70 613-19.

Zhang, B, Xie, G. D. & Li, N. (2015). Effect of urban green space changes on the role of rainwater runoff reduction in Beijing, China. Landscape and Urban Planning, 140: 8–16. doi: 10. 1016/j.landurbplan.2015.03.014

Zhang, J, Lei, T. W. & Qu, L. Q. (2017). Method to measure soil matrix infiltration in forest soil. *Journal of Hydrology*, 552:241–248. doi: 10.1016/j.jhydrol.2017.06.032

Zhao, Y. G., Zhang, G. L. & Zepp, H. (2007). Establishing a spatial grouping base for surface soil properties along urban-rural gradient—A case study in Nanjing, China. Catena, 69(1): 74–81. doi: 10.1016/j.catena.2006.04.017

Zhao, Z. X. & Guo, H. C. (2010). Effects of urbanization on the quantity changes of microbes in urban-to-rural gradient forest soil. Agricultural Science & Technology, 11(3), 118–122.

Zipper, S. C., Soylu, M. E., Kucharik, C. J. & Loheide, S. P. (2017). Quantifying indirect groundwater-mediated effects of urbanization on agroecosystem productivity using MODFLOW-AgroIBIS (MAGI), a complete critical zone model. *Ecological Modelling*, 359, 201-219.